Open File 219

GEOLOGY OF THE NORTHEASTERN GALLINAS MOUNTAINS

SOCORRO COUNTY, NEW MEXICO

by

Lee Allan Brouillard

Submitted in Partial Fulfillment
of the Requirements for the Degree of
Master of Science in Geology

New Mexico Institute of Mining and Technology
Socorro, New Mexico
December, 1984

TABLE OF CONTENTS

PLATES

TABLES

FIGURES

ABSTRACT

Within the area of the northeastern Gallinas Mountains, deposition of lacustrine sediments of the Baca Formation was followed by a rapid influx of dacitic to andesitic volcaniclastic sediments in latest Eocene- early Oligocene time. The lower portion of the Dog Springs Member of the Spears Formation records subaqueous grain-flow deposition into the shallow Baca Lake. This was followed by an inundation of debris flows which displaced water and led to the demise of the Baca Lake. Exotic blocks of Paleozoic limestone, Permian Abo Formation, and monolithologic volcanic breccias were rafted into the area by debris flows.

Continuous basin sedimentation was accompanied by intermittent slumping and development of disturbed bedding on a north- to northeast-oriented depositional slope. Slumping occurring on a large scale is indicated by the presence of extensive detachment surfaces, folds with amplitudes of 50-60 m, and cutting out by slump faulting of thick sections of the lower portion of the Dog Springs Member. Burial diagenesis has resulted in the development of calcite, phyllosilicates, hematite, chlorite, silica, heulandite, and celadonite within volcaniclastic rocks of

the Dog Springs Member.

Debris-flow processes, characterizing most of the Dog Springs Member, were abruptly replaced by fluvial processes and development of braided streams during deposition of the Chavez Canyon Member of the Spears. Emplacement of the Rock House Canyon Tuff briefly interrupted volcaniclastic sedimentation. Development of cauldron systems and emplacement of ash-flow tuff sheets eventually resulted in the closing off of source areas for Spears sediments. Following emplacement of the Hells Mesa Tuff (about 32 m.y.B.P.), a 3-m.y. hiatus occurred prior to deposition of the La Jencia and Vicks Peak Tuffs. An extensive surface of erosion, having considerable relief, developed on the Hells Mesa during this time.

Uplift of the Colorado Plateau in early Miocene time resulted in the creation of a monoclinal flexure along its southeast margin. A reversal from a north to northeast depositional slope to a south-southwest tectonic dip occurred in the area. The most northerly deposited portion of the Spears volcaniclastic apron was stripped and redeposited to the south as the Plateau rose.

Extensional tectonics, associated with the opening of the Rio Grande rift to the east, caused the development of high-angle normal faults and fractures in the northeastern Gallinas Mountains. These zones of weakness have acted as

pathways for the intrusion of late Oligocene and Pliocene dikes.

INTRODUCTION

Purpose of the Investigation

The objectives of this study are to determine the stratigraphic relationships, structural trends, and distribution of rock units within the northeastern Gallinas Mountains. This thesis represents part of a continuing mapping project of the northeastern Mogollon-Datil volcanic field being undertaken by the New Mexico Bureau of Mines and Mineral Resources.

A detailed geologic investigation of this area is important for the following reasons:

1. The study of the area will extend stratigraphic relationships and correlations between geologic units in the Crosby, Datil, Gallinas, Bear, San Mateo, and Magdalena Mountains.

2. Study of the Dog Springs Member of the Spears Formation will aid in further understanding the character of initial Tertiary volcanic and sedimentary processes that occurred in the area.

3. Analysis of structural trends will aid in the interpretation of the regional tectonic history.

Methods of Investigation

Detailed geologic mapping was done at scale of 1:24,000 using portions of the United States Geologic Survey's Indian Mesa and Table Mountain 7.5-minute topographic quadrangles as a base map. United States Forest Service color and aerial photographs of the F16-C1B series, 1974-1975, at a scale of approximately 1:17,000, were used as an aid in following structural trends and delineating rock units. Field work was conducted during the summer and fall of 1982 and spring of 1983.

Fifty-six samples were used in petrographic analyses. Modal analyses were made using a Nikon Labophot-pol microscope and a Swift automatic point counter. Thin sections were point counted using the line method described by Galehouse (1971). The number of points chosen for counting was based on a chart of reliability of modal analysis constructed by Van der Plas and Tobi (1965). Selected thin sections were stained with sodium cobaltinitrate to aid in the identification of sanidine and potassium metasomatism. Etch times were increased to 40 seconds from the recommended 1.5 seconds indicated in the method used by Wilson and Sedora (1979). Anorthite content of plagioclase was determined following the Michel-Levy statistical method as outlined by Heinrich (1965, p.360).

Ten representative samples of clasts from the middle and upper portion of the Dog Springs Member were selected for analysis of major-element composition. Samples were analyzed using standard procedures on an automated Rigaku 3064 x-ray fluorescence spectrometer at the New Mexico Tech x-ray fluorescence laboratory.

Classification of sediment gravity-flows is after that used by Middleton and Hampton (1976). Terminology used for stratification and cross-stratification is after Mckee and Weir (1953). Rock colors were determined using the rock color chart published by the Geological Society of America.

Location and accessibility

The study area is located approximately 31 km northwest of Magdalena, New Mexico (fig.1). It lies on the northeastern margin of the Mogollon-Datil volcanic field, just south of the physiographic margin of the Colorado Plateau. The area mapped during the study encompasses most of the northeastern Gallinas Mountains. The map area covers approximately 104 km2 between latitudes 34°17' 30'' and 34° 24' N, and longitudes 107°37' 30'' and 107°30' W. The area is privately owned and permission for access is required. The study area can be entered from the west and southwest through the HH Ranch (J. Taylor, owner) via the North Lake Road. Access from the north and northeast is by New Mexico

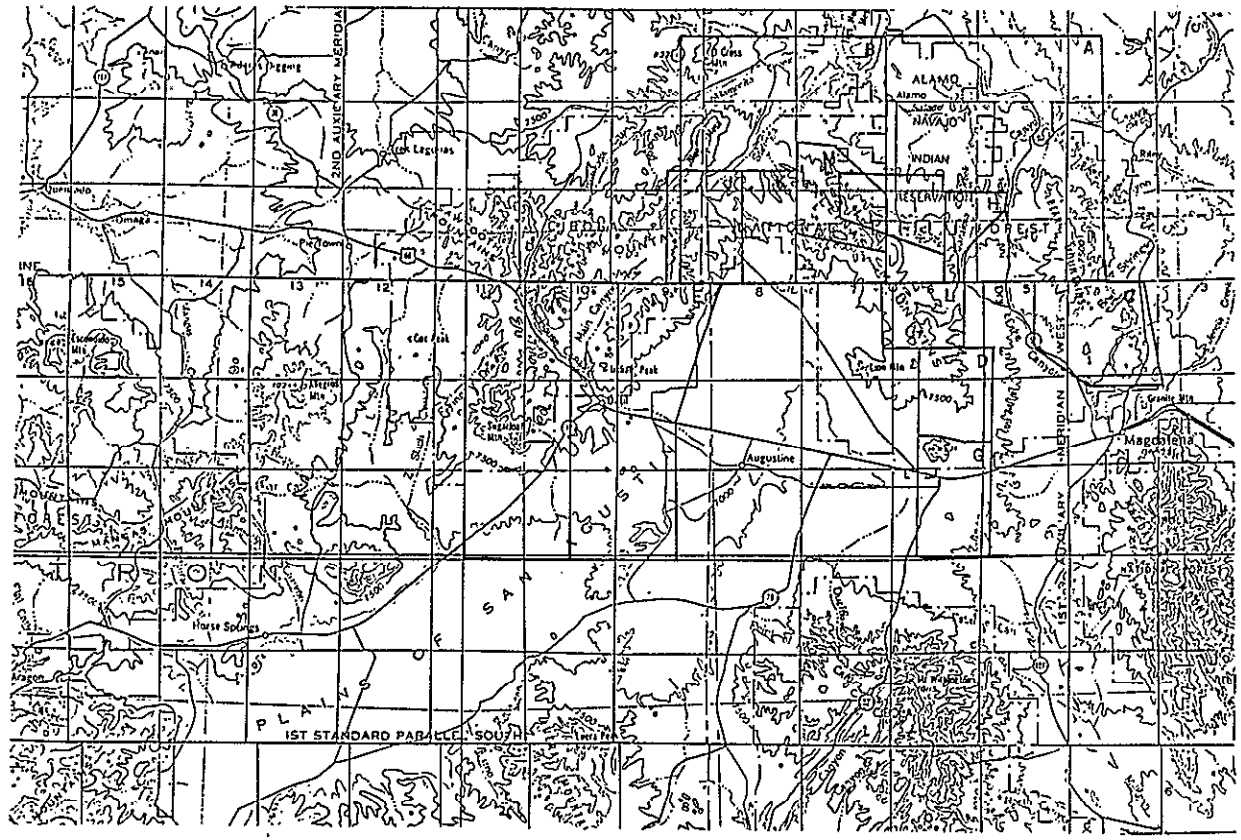

Figure 1. Location map of study area and previous studies in the surrounding region.

A) Tonking (1957)
B) Givens (1957)
C) Brown (1972)
D) Chamberlin (1974)
E) Lopez (1975)
F) Bornhorst (1976)
G) Wilkinson (1976)
H) Mayerson (1978)
I) Cather (1980)
J) Harrison (1980)
K) Coffin (1981)
L) Laroche (1981)
M) This Study

State Highway 52 and a light-duty road on the Burns-Lindsay (Tom Burns, owner) and B. Henderson ranches. A portion of the property just east and southeast of the map area is part of the Alamo Navajo Indian Reservation. Numerous ranch roads provide partial access to areas at lower elevations. Areas of higher elevation generally require access by foot. A four-wheel drive or high-clearance vehicle is needed for roads within the map area, particularly during wet weather.

Previous studies

The earliest recorded geologic investigation of the Gallinas Mountains was done by Herrick (1900) as part of a reconnaissanace study on the geology of western Socorro and Valencia counties. He reported the Datil and Gallinas Mountains as being composed of trachyte and rhyolite intrusives.

Winchester (1920) described a type section for the Datil Formation at the north end of the Bear Mountains. He included the entire Tertiary sequence of tuffs, rhyolites, conglomerates and sandstones. Wilpolt and others (1946) separated the lower 208 meters of redbeds and renamed them the Baca Formation. Tonking (1957) mapped and described the geology within the Peurtecito 15-minute quadrangle. He expanded the Datil Formation by including 48 m of vitric and welded rhyolite tuff and 366 m of basalt and basaltic

andesite lava flows present above Winchester's section. He then divided the Datil Formation into the Spears, Hells Mesa, and La Jara Peak Members. Givens (1957), working in the adjacent Dog Springs 15-minute quadrangle, extended Tonking's Spears and Hells Mesa Members into the Gallinas and eastern Datil Mountains. He subdivided the Hells Mesa Member into 7 mappable units.

Willard (1959) reported on the Tertiary stratigraphy of northern Catron County. He divided the Datil Formation into 4 distinct facies consisting of andesite, rhyolite sedimentary, and latite facies. He also recognized the regional occurrence of post-Datil basalts, correlating the Mangas Basalt to the La Jara Peak Member of the Datil Formation. Weber (1963) separated the La Jara Peak Member from the Datil Formation. Later Weber (1971) elevated the Datil Formation to group status and Chapin (1971) raised the La Jara Peak, Hells Mesa, and Spears members to formational status.

A number of thesis studies have described the local characteristics of the volcanic rocks in the region surrounding this study area (fig.1). Brown (1972) conducted a detailed study of the stratigraphy and petrology of the southern Bear Mountains. He divided the Spears Formation into upper and lower members and the Hells Mesa Formation into the tuff of Goat Springs, upper and lower tuff of Bear

Springs, and tuff of Allen Well. To the south of the study area investigations have been completed by Chamberlin (1974) in the Council Rock area, Wilkinson (1976) in the Tres Montosas-Cat Mountain area, and Laroche (1981) in the Gallinas Peak area. To the west and southwest, detailed investigations on the Tertiary geology have been performed by Coffin (1981) in the northwest Gallinas Mountains, Harrison (1980) in the northeast Datil Mountains, and Lopez (1975) and Bornhorst (1976) in the Datil area.

Osburn and Chapin (1983) have recently tied together the work of previous investigators and proposed formal nomenclature to be used for Cenozoic rocks present in the northeastern Mogollon-Datil volcanic field.

Acknowledgments

I would like to thank the many people who contributed to the completion of this thesis. Appreciation is extended to Dr. Charles Chapin who suggested the project and served as principal advisor during the course of the study; and to the New Mexico Bureau of Mines and Mineral Resources for use of a field vehicle and financial support for this study. I am grateful for the use of facilities and general friendliness of the residents of North Lake on J. Taylor's ranch during my time in the area. A special thank-you is given to Danny Bobrow and Bob Osburn for geologic

discussions and aid in many aspects of this project. Dr. Dave Johnson provided helpful discussions and aided in the taking of photomicrographs. Drafting was accomplished with the help of James Brannan. Additional thanks go to Dr. Clay T. Smith and Dr. Philip Kyle who served on the thesis committee and reviewed the manuscript. Heart-felt gratitude is given to my wife Elaine for moral support and encouragement during the completion of this thesis.

STRATIGRAPHY AND PETROLOGY

Crevasse Canyon Formation

Late Cretaceous rocks underlie the Eocene Baca Formation and crop out approximately 1.9 km to the north and 0.6 km to the northeast of the study area. Tonking (1957) first correlated these rocks with the Crevasse Canyon Formation (Allen and Balk, 1954) exposed on the west side of the San Jaun Basin. Subsequent workers in the area have referred to these rocks in various ways. Cather (1980) and Robinson (1981) followed Tonking's usage whereas Jackson (1979), Mayerson (1979) and Massingill (1979) assigned these rocks to the Mesa Verde Formation. Recent work by Hook and others (1983) have clarified nomenclature and stratigraphic problems associated with Upper Cretaceous rocks in west-central New Mexico. Their study recommends that the Cretaceous rocks above the Gallup Sandstone be referred to as the Crevasse Canyon Formation.

The Crevasse Canyon Formation consists of a sequence of yellowish-gray, fine- to medium-grained sandstones, medium-gray to black carbonaceous shales, and a few thin coal beds (Tonking, 1957; Cather,1980). This unit forms a portion of a wedge of coastal plain and littoral sediments which prograded northeastward as an epicontinental sea

withdrew from west-central New Mexico during late Turonian-early Coniacian time (Hook, 1983; Johansen, 1983)

Baca Formation

The Baca Formation overlies the Crevasse Canyon Formation and underlies the Spears Formation. It is present in noncontinuous exposures along the north and northeastern portion of the study area.

The Baca was first defined by Wilpolt and others (1946) for exposures located approximately 22.4 km to the east of the study area in the upper part of Baca Canyon on the eastern flank of the Bear Mountains. Scattered outcrops of the Baca form a west-trending belt from near Socorro, New Mexico to west-central Arizona. The local and regional characteristics of the Baca have been studied by many workers (see Cather, 1980, table 1). Geologic mapping and sedimentologic studies by Potter (1970), Snyder (1971), Johnson (1978), Massingill (1979), Cather (1980, 1983), and Cather and Johnson (1984) have been carried out on exposures of the Baca adjacent to the study area. Fossil mammals from the Baca Formation in west-central New Mexico tentatively indicate a Duchesnean (late Eocene) age (Lucas, 1983).

Within the study area, the upper Baca Formation consists of nearly equal amounts of intercalated sandstones and mudstones. Cather (1980, 1983) refers to this upper portion of the Baca as the upper red unit. Strata composing the unit are interpreted as indicating the presence of a large shallow-water lacustrine system. This lake formed along the eastern margin of the Baca basin (fig.2).

Exposures of the Baca along the Baca-Spears contact in the study area show lateral variations in lithology. An outcrop of the Baca in section 12, R.7W., T.1N., lying below the lower and middle Dog Springs map units, consists of coarsening upward sequences composed of mudstone and channel-shaped coarse- to medium-grained sandstone. Sandstones have medium-scale, trough-shaped cross-stratification and planar bedding. Following along the contact approximately 0.6 km to the northwest (section 2, R.7W., T.1N.), a vertical sequence of laterally persistent mudstones is present. Such lateral variations in lithology in the upper Baca are also present along this contact from the northwest corner of the study area to Dog Springs Canyon, appoximately 4 km to the northwest.

It has been well documented (Cather 1980, 1983; Cather and Johnson, 1984) that the coarsening-upward sequences, consisting of mudstone grading upward to sandstone, represent the delta plain portion of a fan delta prograding

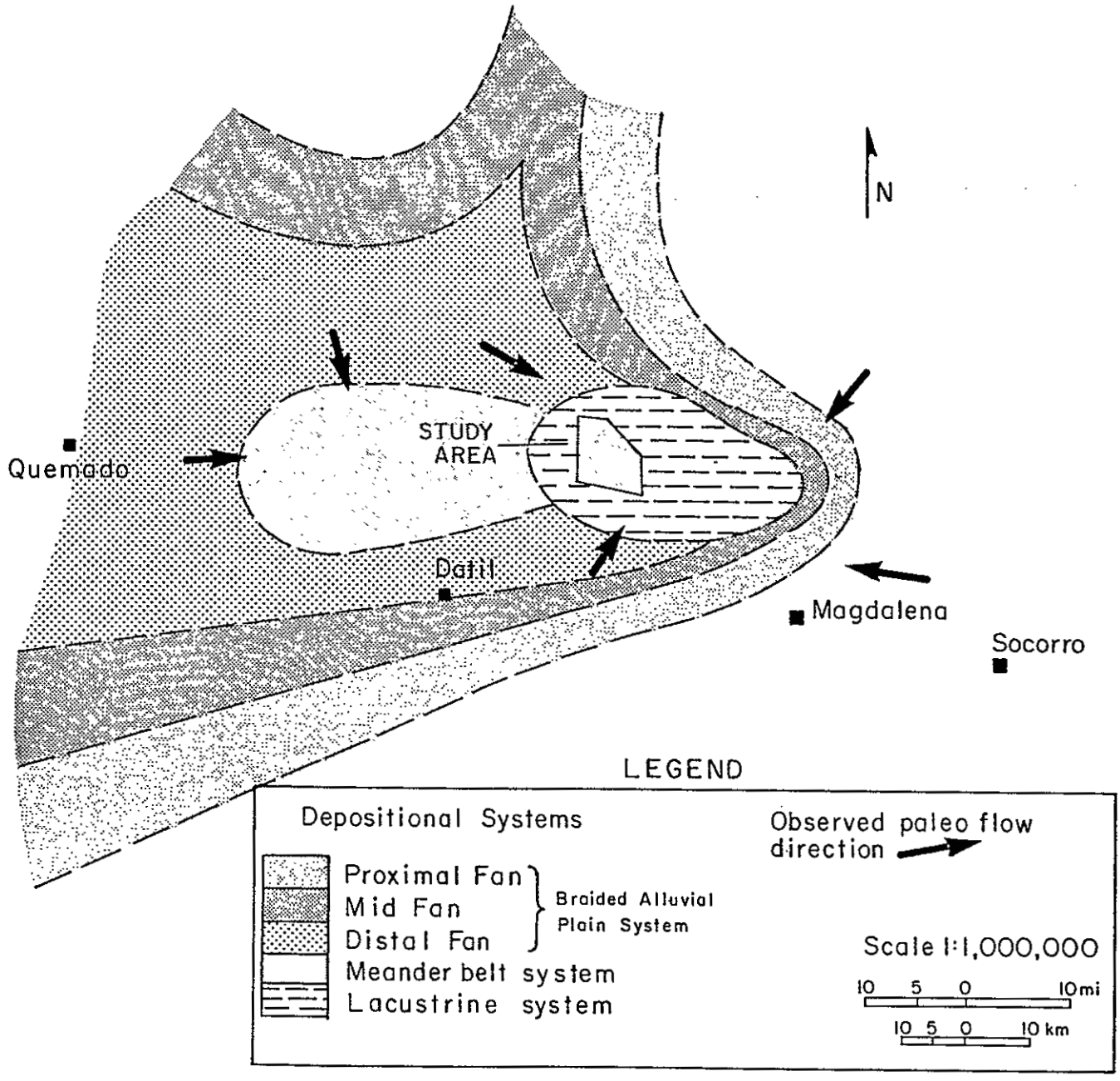

Figure 2. Location of study area with respect to the depositional systems found within the Baca basin during early Baca time (high lake stand) (After Cather, 1983).

into a shallow-water lake. Traverses along the Spears-Baca contact in the study area and to the northwest further indicate that individual fan-delta lobes surrounded by lacustrine sediments may be discerned.

Datil Group

All rocks in the study area above the Baca Formation and below the Hells Mesa Tuff are collectively referred to as the Datil Group. This follows the redefinition of the Datil Group for the northeastern Mogollon-Datil volcanic field recently proposed by Osburn and Chapin (1983).

Winchester (1920) originally proposed the name "Datil Formation" for an approximately 615-m-thick sequence of Tertiary volcanic and non-volcanic rocks exposed in the Datil, Gallinas and Bear Mountains. The formation was named for the Datil Mountains, but the type section was measured at the north end of the Bear Mountains. Wilpolt and others (1946) removed the lower 298 m of non-volcanic strata from Winchester's "Datil Formation" and named them the Baca Formation. Tonking (1957) later subdivided the Datil Formation into three members. In ascending order they consisted of: the Spears member, comprised of quartz latite tuffs and volcaniclastic rocks; the Hells Mesa member, composed of vitric rhyolite tuffs; and the La Jara Peak

member, made up of basalt and basaltic andesite flows. Willard (1959) later excluded the upper mafic lava flows of Tonking's Datil Formation. Weber (1971) raised the Datil to Group status, retaining the Spears and Hells Mesa members as defined by Tonking (1957). Difficulties arose in correlating volcanic rocks in the surrounding area with Weber's Datil Group. It became apparent as detailed mapping progressed in the region that a number of ash-flow sheets from several different vent areas were present in the stratigraphic interval defined as the Datil Group by Weber (Osburn and Chapin, 1983).

The Datil Group as redefined by Osburn and Chapin (1983) encompasses the many local variations that occur in the unit. Throughout the northeastern Mogollon-Datil volcanic field one finds a varying sequence of interbedded volcaniclastic rocks, ash-flow sheets, and lavas. Chemically and mineralogically, rocks of the Datil Group are similar in that they range from andesitic to low-silica rhyolite in composition and generally lack phenocrystic quartz (Osburn and Chapin, 1983).

Datil rocks record the earliest occurrence of Tertiary volcanism in the Mogollon-Datil volcanic field. The age of these rocks is bracketed between approximately 39 and 32 m.y. based on K-Ar, 40Ar/39Ar, and fisson-track dates from rocks in the Spears Formation and the overlying Hells Mesa

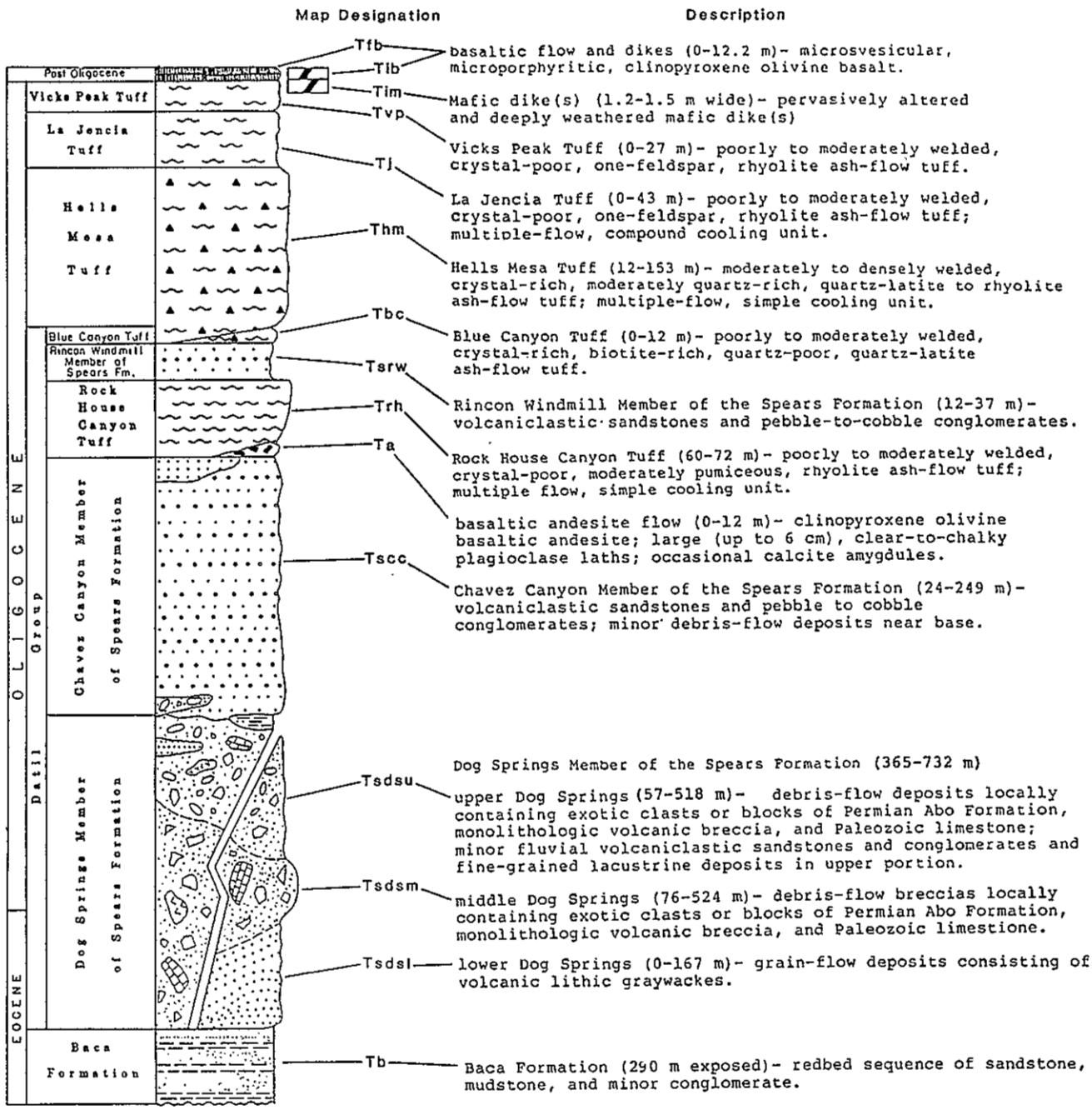

Figure 3. Generalized stratigraphic column for the northeastern Gallinas Mountains, Socorro County, New Mexico.

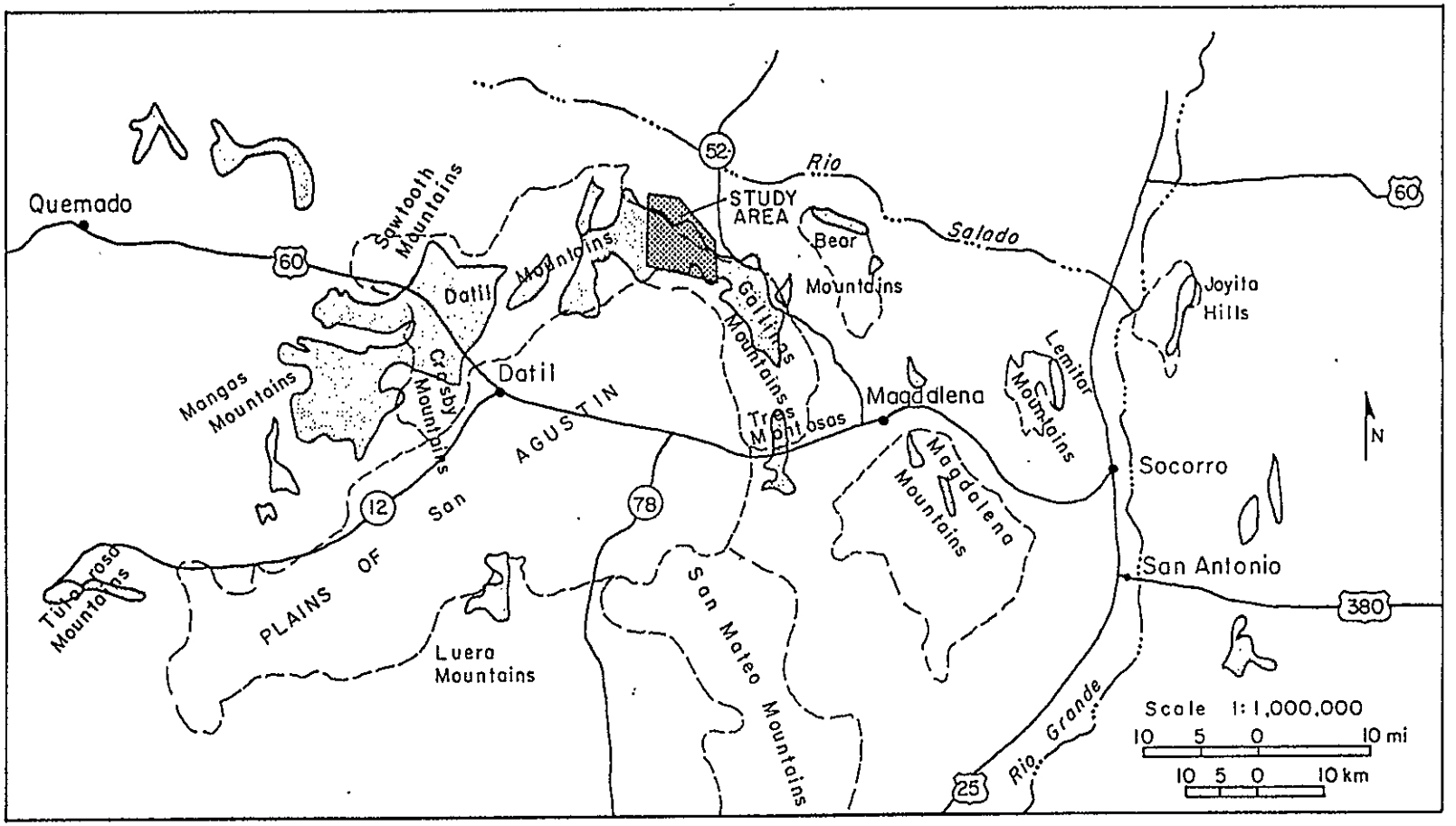

Figure 4. Index map of locations of the Spears Formation and equivalent units exposed in the region surrounding the study area. Base map is from the Topographic Map of New Mexico (1983). Geology from the New Mexico Geologic Highway Map (1982).

Tuff (Osburn and Chapin, 1983; Laura Kedzie, in prep.).

In the study area, the Datil Group is composed, in ascending order, of Dog Springs Member of the Spears Formation, Chavez Canyon Member of the Spears Formation, Rock House Canyon Tuff, Rincon Windmill Member of the Spears Formation, and Blue Canyon Tuff (fig.3).

Spears Formation

The Spears member of the Datil Group was raised to formational status by Chapin (1971). Brown (1972) divided the Spears into upper and lower members, separated by the tuff of Nipple Mountain (Rock House Canyon Tuff). Osburn and Chapin (1983) formally divided volcaniclastic rocks of the Spears Formation present in the Datil and western Gallinas Mountains into the Dog Springs, Chavez Canyon and Rincon Windmill members. Mapping performed during the present study has extended these units into the northeastern Gallinas Mountains.

The Spears Formation represents the deposition of a large sedimentary apron around the northeastern margin of the Mogollon-Datil volcanic field during latest Eocene and early Oligocene time. The unit is exposed throughout the region surrounding the study area along the margins of tilted fault-block mountains (fig.4). Numerous geologic

studies have been carried out in the region which describe the local character of the Spears (Table 1). Recently, a study has been undertaken by Steve Cather (University of Texas at Austin), in cooperation with the New Mexico Bureau of Mines and Mineral Resources, which will detail the regional sedimentologic, petrographic, and geochemical characterisics of the Spears Formation.

Dog Springs Member

Within the study area the lower 365 to 732 m of the Spears Formation is composed of: grain-flow deposits, debris-flow deposits which locally contain exotic clasts and/or blocks of Permian Abo Formation, Paleozoic limestone and monolithologic volcanic breccias; and minor occurrences of sandstone, conglomerate and mudstone. These rocks are referred to as the Dog Springs Member of the Spears (Osburn and Chapin, 1983) and occur above the Baca Formation and below the Chavez Canyon Member of the Spears. The type locality of the unit is situated along Dog Springs Canyon (S 1/2, T.2N., R.8W., and north edge of T.1N., R.8W., unsurveyed D Cross Mountain and Dog Springs quandrangles), which is located approximately 3.8 km west of the northwest border of the area mapped for this study. Within the study area the Dog Springs Member has been divided into lower, middle and upper map units.

Table 1. Studies dealing with the Spears Formation and equivalent units in the region surrounding the study area.

Location	Author
Datil area	Lopez, 1975 Bornhorst, 1976 Lopez and Bornhorst, 1979
Northern Datil Mountains	Givens, 1956 Harrison, 1980 Robinson, 1981
Northern and central Gallinas Mountains	Tonking, 1957 Givens, 1957 Coffin, 1981 Laroche, 1981 This Study
Southern Gallinas Mountains	Chamberlin, 1974 Wilkinson, 1976
Bear Mountains	Tonking, 1957 Brown, 1972 Massingill, 1979 Mayerson, 1979
Magdalena Mountains	Blakestad, 1978 Allen, 1979 Krewedl, 1974
Lemitar Mountains	Chamberlin, 1980
Joyita Hills	Spradlin, 1976
Tularosa and southern Mangas Mountains	Stearns, 1962

Lower Dog Springs map unit

The lower Dog Springs map unit consists of plane-bedded coarse- to medium-grained volcaniclastic sandstones with occasional thin, discontinuous, lens-shaped clay drapes. The unit is best exposed in the Cottonwood Well area (sections 28, 32 and 33, T.2N., R.7W.). Where a depositional base of the unit is exposed, it conformably overlies the Baca Formation. The contact between the Baca and the lower Dog Springs is sharply defined by the first appearance of volcaniclastic sandstones. Very thick to thin, plane-bedded sandstones of the Baca are overlain by volcanic sandstones with similar bedding characteristics. The contact is also marked by a color change from red, yellow or gray sandstones or red mudstones of the Baca to yellowish or pinkish-gray volcaniclastic sandstones. Local relief of tens of meters occurs along the Baca-lower Dog Springs contact because of Baca depositional topography. Deposition of fan-delta lobes of the Baca Formation has resulted in elevated areas on it's upper surface.

Strike directions within the lower Dog Springs are variable, and dip of bedding ranges from 2 degrees to vertical, or overturned on asymmetric folds. In general, bedding is more disturbed near the top of the unit where it is in contact with the overlying middle Dog Springs map unit

along an extensive surface of detachment. The lower-middle Dog Springs contact is very irregular because of the effects of post-depositional soft-sediment deformation. In several places the contact shows considerable relief were large portions of the lower Dog Springs have been removed by slump emplacement of the middle Dog Springs (see section on deformational structures related to slumping). A detachment surface near or at the base of the lower Dog Springs is also present at some locations. Southeast of Pinto Tank (sec. 12, T.1N., R.7W.) and east of Cottonwood Well (SW 1/4 sec. 35, T.2N., R.7W.), folded and thrusted bedding is present within a several meter thick zone at the base of the lower Dog Springs.

Approximately 2.4 km west-northwest of the old Baca Homestead (SW 1/4 sec. 28, T.2N., R.7W.) the lower Dog Springs is thickest, and from cross-sectional constructions is estimated to consist of approximately 167 m of strata. Soft-sediment deformation, such as folding and thrusting of strata, have increased the unit's thickness. To the northwest it is truncated by bounding faults of a major down-to-the-basin slump.

Bedding within the unit is characterized by sharply bounded planar beds that are internally massive but sometimes contain diffuse parallel laminations (fig.5). At many locations beds are intensely bioturbated. Burrow casts

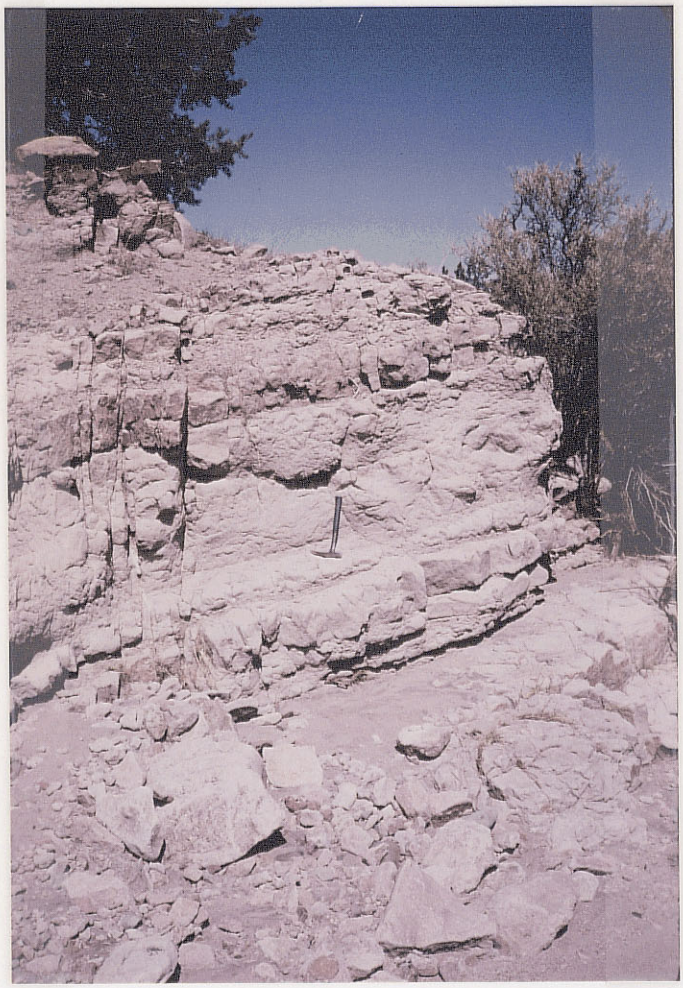

Figure 5. Photograph of grain-flow deposits comprising the lower Dog Springs map unit. Note flat, sharply defined, internally structureless, planar beds. East-facing exposure located along dry-wash running through NW 1/4 sec. 28, R.7W., T.2N.

OFR 219 #32

and molds approximately 0.5-1.0 cm in width and several centimeters in length are common. Normal grading from very coarse- to medium- or fine-grained sand occurs over an interval of 12-15 cm in some beds. Bedding thickness varies considerably within the unit, often having thinning-upward sequences. Beds 2-4 m thick at the base of a sequence grade upward to beds as thin as 2-3 cm. Many of the beds contain veinlets of mud-sized material branching laterally or in an upward direction. These veinlets are thought to have been injected as the result of excessive pore-water present during deposition of the sediment. Compaction of the sediment caused dewatering and entrainment of mud-sized material that was carried upward with the escaping fluids. Internally massive planar beds, containing escape structures similar to those observed in the lower portion or the Dog Springs Member, have been described by Middleton and Hampton (1976) and Stauffer (1967) in deposits resulting from fluidized or grain-flow deposition.

Lens-shaped accumulations consisting of mud drapes several centimeters in thickness, interbedded with medium- to coarse-grained sandstone containing mudstone rip-up clasts, are scattered throughout the plane-bedded sandstones. These lens-shaped mudstone bodies range in thickness from approximately 2 to 10 cm and vary in lateral extent from about 3 to 6 m. Load casts occur in some mudstone lenses where the overlying sand protrudes down into

the mudstone. Clastic dikes consisting of mud to sand-sized material are common within the unit. The internally massive sandstone beds containing mudstone rip-up clasts that are present in the lower Dog Springs, are similar in character to supposed grain-flow deposits described by Stauffer (1967) in Tertiary rocks found in California.

Based on criteria defined by Folk (1974), sandstones composing the lower Dog Springs are texturally immature. They can be classified as lithic graywackes (Pettijohn and others, 1973; figure 5f-3, p. 158) or, more specifically, volcanic lithic graywackes. The sandstones are typically medium to coarse grained, very poorly sorted, and contain angular to subangular grains. Seven grab samples were collected from localities scattered throughout the unit. Three samples were selected as representative of the unit and used for point-count analysis (Table 2). These sandstones consist of approximately 70 percent detrital grains, 29 percent matrix and 1 percent pore space. Of the detrital fraction, about 27 percent of the rock is composed of volcanic rock fragments.

Volcanic rock fragments consist of angular to subangular, subelongate (Folk, 1974) lithic pieces which average approximately 0.4 mm in their long dimension. The largest lithic fragment observed in thin section had a dimension of 3.0 X 2.5 mm. Lithic fragments consist

Table 2. Modal analyses of sandstones from the lower portion of the Dog Springs Member (Tsdsl).

	1	2	3	Average
Matrix*	32.3	24.8	29.8	29.0
Volcanic rock fragments	30.0	15.2	36.8	27.3
Plagioclase (An content)	26.5 (32)	44.8 (36)	24.3 (34)	31.9 (34)
Hornblende	8.1	12.9	5.9	8.9
Opaque oxides	1.1	1.5	0.8	1.1
Biotite	0.3	0.8	0.1	0.4
Clinopyroxenes	0.2	---	---	Tr
Pores	1.6	---	2.2	1.3
Total	100.1	100.0	99.9	100.0
Points counted†	631	612	625	

Tr Trace (less than 0.1 percent).

* Matrix consists of material less than 0.02 mm in size.

† A 1 mm x 1 mm grid spacing covering the entire slide was used in point counting. Recorded values represent the number frequency (Galehouse, 1971) of species counted.

predominantly of volcanic groundmass material or phenocrysts of plagioclase mantled by a thin rim of groundmass. Microphenocrysts of hornblende, opaque oxides and biotite are also present in some rock fragments.

A variety of groundmass textures are present within the rock fragments. Groundmass material has a cryptocrystalline to seriate texture. Plagioclase microlites predominate in the groundmass and sometimes have a pilotaxitic habit. Occasionally glass and/or potassium feldspar is present in the groundmass and hyalopilitic or orthophyric textures occur.

The remainder of the detrital constituents consist of crystal grains derived from the breakdown of volcanic lithic fragments during transport. In decreasing order of abundance they consist of plagioclase, hornblende, opaque oxides, biotite and clinopyroxene. Plagioclase grains are subangular to angular and elongate. They average 0.25 mm in their largest dimension but occasional grains are present as large as 1.5 mm. Plagioclase occurs in a variety of twin types. Albite twinning is predominant with lesser combinations of albite twinning with carlsbad twins, zoned crystals, and pericline twinning. Plagioclase has an Anorthite (An) content of approximately 34 (average of 3 maximum values obtained from 30 grains in 3 thin sections, Michel-Levy method). Hornblende and biotite grains are

angular to subangular with very elongate shapes. Both average 0.25 mm in their longest dimension. Subangular to angular, equant opaque oxides are scattered throughout. These opaques range from 0.05 mm in diameter to a cryptocrystalline dust found in the matrix. Clinopyroxene grains are occasionally present.

Interstitial constituents consist of cement and matrix. Cement and detrital material composing the matrix are intimately associated and total approximately 29 percent of the rock. Material less than 0.02 mm in size was considered as belonging to the matrix. The matrix consists mainly of a mixture of broken lithic groundmass, plagioclase microlites, opaque oxides, biotite, hornblende and recrystallized detrital material. Framework grains grade almost imperceptably into the surrounding clay- to silt-sized paste. Boundaries between rock fragments and matrix are often vague but are generally discernable because of the slightly darker color of the matrix in plane polarized light (fig.6). This tan to reddish color is the result of the presence of a dissemination of finely pulverized magnetite that has been altered to limonite and/or hematite. Recrystallized detrital material or orthomatrix (Dickinson, 1970) is indicated by the presence of relict clastic textures and inhomogeneity of its composition contrasting with the homogeneity of phyllosilicate cements present. Differentiating clay cements from recrystallized detrital

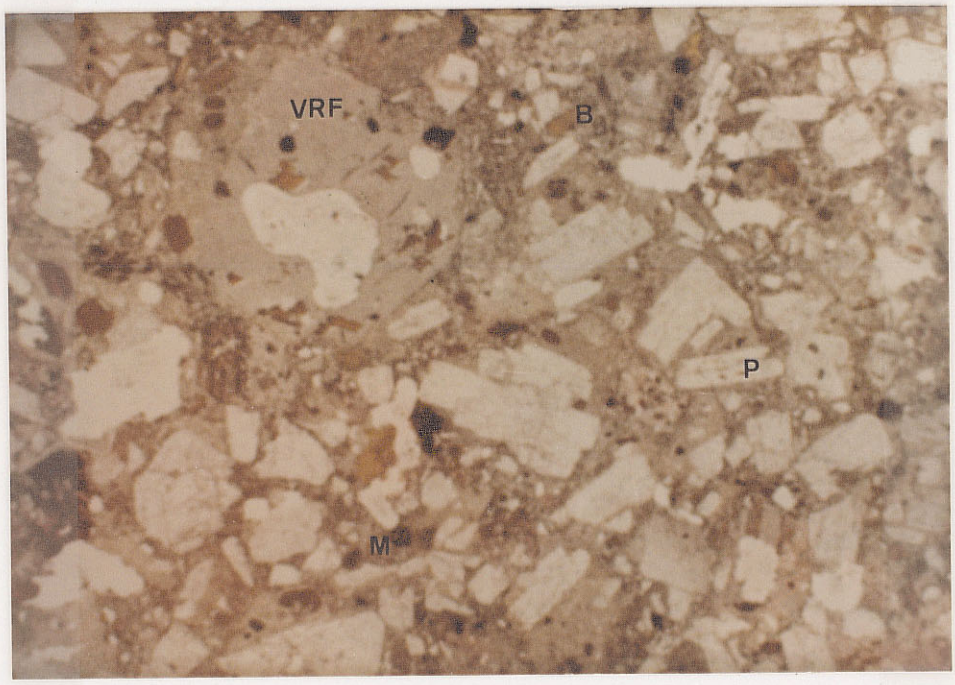

Figure 6. Photomicrograph of volcanic lithic graywacke from the lower Dog Springs map unit. Detrital volcanic rock fragments (VRF) contrast with the slightly darker color of the matrix (M). Mineral grains are plagioclase (P) and biotite (B). Photo taken in plane-polarized light. Field of view between points A and B = 6.5 mm.

OFR 219 #38

material is not always possible. Both constiutuents act as a portion of the material binding the rock and therefore are lumped together (Table 2).

These texturally immature (Folk, 1974) sandstones possess very low porosities. Microscopically observed pore space varied from none discernable to about 2 percent. The variety of void space present has been referred to by Scholle (1979, p. 170) as a primary interparticle porosity. Original porosity was higher, but during diagenesis nearly all of the primary void space was filled by silica, zeolites, chlorite or calcite.

The textural characteristics of these rocks suggest deposition as subaqueous sediment gravity flows. Most graywackes in the geologic record are found within marine depositional settings, predominantly as turbidites in flysch deposits (Pettijohn and others, 1973). Sediments comprising the lower Dog Springs were probably not deposited in deep water, as are flysch deposits, but rather represent sedimentation in a shallow-water environment. Brenchly (1969) describes a group of graywackes of Ordovician age from north Wales interpreted as being deposited in a shallow-water deltaic setting. These deposits are similar to lower Dog Springs strata in that both contain massive beds displaying a faint parallel lamination and sometimes contain mud clasts.

Lower Dog Springs strata most closely resemble Tertiary grain-flow deposits present in the Santa Ynez Mountains in southern California described by Stauffer (1967). These deposits are characterized by thick, ungraded, sharply bounded beds, commonly massive except for diffuse flat laminations. Beds occasionally contain irregularly shaped plastically deformed lutite clasts. These characteristics, along with the lack of traction-current features, suggest grain-flow deposition.

The graywacke texture and grain-flow sedimentologic characteristics of strata composing the lower Dog Springs map unit strongly suggest subaqueous deposition of these sediments. This indicates that the Baca lake continued to be present within the study area at least through lower Dog Springs deposition.

Middle Dog Springs map unit

The middle Dog Springs map unit is present as a wide belt of exposures extending from the northwest corner of the map area to the southeast. The unit is thickest in the central portion of the study area, with a maximum estimated thickness based on cross-sectional construction of 524 m. Along the eastern margin of the map area it thins to approximately 76 m.

The middle Dog Springs is composed of a sequence of stacked and contorted volcanic debris-flow deposits. It has been mapped by Coffin (1981) as the lower member of the Dog Springs volcanic complex and mapped by Harrison (1980) as undifferentiated Dog Springs volcanic complex. In the Datil area, rocks similar to those composing this unit have been mapped and described by Lopez and Bornhorst (1979) as part of the Spears Formation. Robinson (1981) noted the presence of the unit along the northern front of the Gallinas Mountains. This thick sequence of debris-flow deposits seems to be areally restricted to the northern and central portions of the Gallinas and Datil Mountains. Studies further west, south, or east, do not note rocks of similar characteristics at the same stratigraphic level.

Within the study area this unit overlies the lower Dog Springs along an extensive surface of detachment. Emplacement of the middle Dog Springs into the area occurred as large slump deposits (see section on deformational structures related to slumping). Where the lower Dog Springs is very thin, contorted lower Dog Springs lithologies occur over vertical intervals of several meters below the middle Dog Springs. This zone of deformed bedding gives the appearance of an angular unconformity between the Dog Springs and underlying Baca Formation.

The middle Dog Springs is composed predominantly of dacitic to andesitic debris-flow breccias with minor localized accumulations of fluvial deposits. Clasts composing the breccias are light gray (N7) in color when fresh and weather to pale blue green (5 BG 7/2), grayish yellow green (5 GY 7/2), light brownish gray (5 YR 6/1), pale green (10 G 6/2) or white, depending on the type and degree of alteration affecting the clasts. From a distance, weathered exposures of debris-flow breccias appear light gray to light brownish gray.

Debris-flow breccias comprising the middle Dog Springs are more resistant to weathering than the underlying lower Dog Springs or Baca Formation and the overlying upper Dog Springs. An accumulation of resistant debris-flow breccias forms the lower portion of the prominent escarpment along the northeast front of the Gallinas Mountains (fig.7). Erosion along vertical joint surfaces present in the most resistant deposits has resulted in the development of spires, fins and other hoodoo-like shapes. These debris-flow breccias are thoroughly indurated and weather to cobble-sized material with clast and matrix having equal resistance. Stacked sequences of individual flows are discernable in some exposures (fig.8). Separate debris flow events and resulting individual deposits are distinguishable by a variety of physical characteristics. Individual flows can be distinguished from one another by differences in the

Figure 7. Photograph showing the outcrop character of middle Dog Springs debris-flow breccias along the northeast front of the Gallinas Mountains. Weathering along joint surfaces has resulted in the development of fins and spires. Outcrop of resistant sandstones within fan-delta lobe at top of the Baca Formation located above arrows. Location of detachment surface occurring near Baca-Dog Springs Member contact indicated by dashed line.

Figure 8. Photograph of sequence of stacked debris-flow deposits present in the middle Dog Springs map unit. Boundaries between individual flows are marked by weathering along bedding-plane surfaces. Exposed sequence is approximately 85 m thick. East-facing exposure, NW 1/4, SW 1/4 sec. 12, R.7W., T.1N.

OFR 219 #44

size, color, and composition of included clasts; the matrix composition, color, and its percentage of the flow; and overall color and degree of induration. In some cases individual flows can easily be distinguished from overlying or underlying flows because of concentrations of non-volcanic clasts present within them. Debris-flow deposits are very poorly sorted with a clast size averaging about 5-6 cm in diameter but occasionally containing boulder-sized material. Deposits which are composed exclusively of grains no larger than coarse sand are also present. Reverse and normal graded beds are present over vertical intervals of approximately 15 cm or less in some deposits. Most of the debris-flow breccias within this map unit have an estimated matrix percentage of at least 40 to 50 percent of the rock. Individual debris-flow deposits range in thickness from a meter or less up to approximately 20 m, with an average thickness of about 10 m.

Debris-flow deposits are internally massive and have a random fabric. Deposits are poorly sorted with clasts of various sizes supported by the finer-grained matrix. The presence of occasional clasts which have their long axes in a near-vertical position attests to the fact that the matrix is supporting them. The base of an individual flow is often defined by a gently undulating surface, which in many cases weathers out to form an overhanging ledge. Examination of exposed bedding-plane surfaces on a number of flows showed

no evidence of current produced sole markings. It has been noted by several investigators (Enos, 1977; Middleton and Hampton, 1976) that debris flows typically do not abrade underlying beds. Absence of scour marks suggests lack of turbulence within the flow or at least failure of turbulence to penetrate a laminar boundary layer present at the base of a flow (Enos, 1977). Johnson (1970, p. 442), Enos (1977), and Hampton (1972, p.749) infer from fabric studies that peripheral regions within debris flows move in a laminar manner. Both Johnson and Enos concluded from field and laboratory studies that a rigid plug of material is rafted on top of debris that is in laminar flow. Deposition from debris flows occurs when the driving stress of gravity decreases below the strength of debris and the entire mass is essentially frozen in place. Parallel striation marks were observed at the base of two flows in the study area. Such striations may be slide marks that are the result of rigid-block sliding. This mechanism (Middleton and Hampton, 1976) involves tensile separation of a debris flow when the channel is smooth and wet. Blocks produced by separation slide along rigidly ahead of the main flow. An alternative interpretation is that these striae were formed slightly after deposition, during movement that occurred during slumping. Details on slump features are discussed in the section on deformational structures.

Deposits composing the middle Dog Springs vary in composition from monolithologic to heterolithologic. Heterolithologic debris-flow breccias consist of variously textured dacitic to andesitic clasts and admixed non-volcanic material (fig.9). The percentage of matrix within these deposits ranges from approximately 40 to 70 percent. Non-volcanic clasts consist of red mudstones, siltstones and sandstones, and gray limestones (fig.10). Non-volcanic foreign clastic material ranges in size from sand to boulders, but generally is pebble to cobble size. Limestone clasts range from sand-size to blocks tens of meters thick and hundreds of meters in diameter.

Monolithologic breccias are composed of dacitic to andesitic angular to subrounded clasts set in a matrix of pulverized clast components (fig.11). The percentage of matrix within these deposits is much lower than within heterolithologic deposits, and generally consists of approximately 30 percent of the rock. Maximum clast size in these breccias is about 30 to 40 cm. Grain size ranges down to clay-sized material in the matrix. The larger clasts often grade from their periphery into smaller sized constituents. Such texural relations are indicative of both alloclastic and autoclastic breccias (Parsons, 1969).

Figure 9. Photograph of heterolithic debris-flow breccia present in the middle Dog Springs map unit. Note angular red sandstone clasts derived from the Abo Formation. Dacite clasts in exposure have weathered to a light gray or chalky white. Exposure is located on west side of canyon, SW 1/4, NW 1/4 sec. 30 R.7W., T.2N.

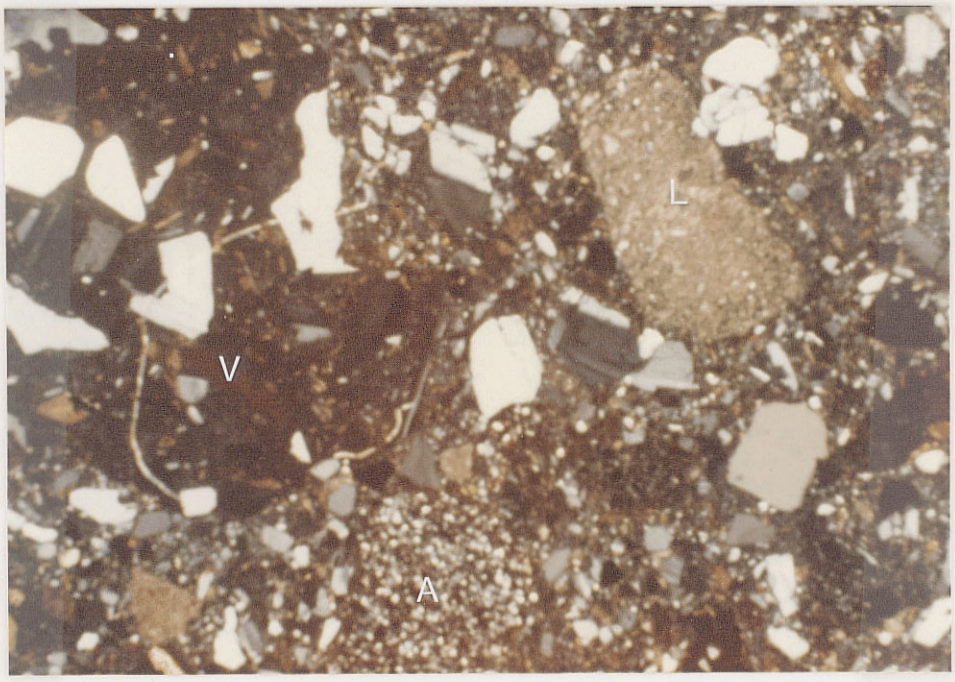

Figure 10. Photomicrograph of matrix of heterolithic debris-flow breccia. (A) Abo clast, (L) Paleozoic limestone clast, (V) volcanic rock fragment. Photo taken in cross-polarized light. Field of view between points A and = 6.5 mm.

OFR 219 #49

A B

Figure 11. Photographs of dacitic to andesitic monolithologic breccias present in the middle Dog Springs map unit. Note abundance of clasts versus matrix. Clasts are set in a matrix of pulverized clast components.
A) Exotic volcanic breccia block exposed along west wall of canyon NE 1/4, SW 1/4 sec. 29, R.7W., T.2N. Sheet jointing runs diagonally from lower right to upper left in photo.
B) Exotic breccia block or flow breccia (?) exposed near top of hill on west side of canyon NW 1/4, SE 1/4 sec. 30, R.7W., T.2N.

Volcanic clasts composing monolithologic breccias and those found in heterolithologic debris-flow breccias are of the same composition. Petrographically, these rocks can be classified as dacitic to andesitic based on textural characteristics and phenocryst composition as defined by Williams and others (1954) (Table 3). Ferromagnesian phenocrysts present within the clasts consist predominantly of hornblende and biotite. Clasts containing clinopyroxenes are less abundant. Major element analysis of selected representative clasts show weight percent silica ranging from 58.10 to 64.66 (Table 4). Chemically the rocks fall within the high-potassium andesite to dacite fields as defined by Ewart (1982) (fig.12).

In hand sample unweathered volcanic clasts are light in color, generally very light gray (1N8) to light brownish gray (5YR 6/1). Dacitic rocks are commonly porphyritc, with megaphenocrysts of clear- to milky-white plagioclase and black hornblende crystals, contrasting with the drab-colored fine-grained groundmass.

The clasts have a variety of igneous textures. Porphyritic, microporphyritic, and seriate texures are common. Seriate-textured rocks often have a pilotaxitic or hyalopilitic groundmass. The microphenocrysts and microlites of plagioclase in these rocks are disposed in a subparallel manner suggesting solidification of the magma

Table 3. Modal analyses of clasts from the middle portion of the Dog Springs Member (Tsdsm).

Sample*	BIMC 7	BIMC 9	BIMC 10
Groundmass	81.2	47.2	43.5
Plagioclase (An content)	9.6 (37)	34.0 (26)	38.7 (29)
Hornblende	----	10.5	5.0
Biotite	----	3.3	4.3
Sanidine	----	1.0	1.2
Opaque oxides	5.3	1.0	1.8
Clinopyroxenes	1.7	----	----
Quartz	----	0.2	0.2
Secondary silica	----	0.7	0.7
Secondary calcite	2.2	0.3	2.2
Vesicles	----	1.8	2.5
Total	100.0	100.0	100.1
Points counted†	591	600	600

* See Table 4 for major element analyses of these samples.

† A 1 mm x 1 mm grid spacing covering the entire slide was used in point counting. Recorded values represent the number frequency (Galehouse, 1971) of species counted.

Table 4. Major-element analyses of clasts from the middle portion of the Dog Springs Member (Tsdsm).

BIMC	7	8	9	10
SiO_2	58.10	63.66	64.66	64.62
TiO_2	0.79	0.41	0.45	0.54
Al_2O_3	18.00	15.21	16.73	16.62
Fe_2O_3*	6.67	3.75	3.95	4.32
MnO	0.06	0.08	0.06	0.06
MgO	2.69	1.23	2.20	1.31
CaO	5.49	6.09	3.63	4.25
Na_2O	4.77	4.25	4.67	5.14
K_2O	2.67	3.20	3.13	2.72
P_2O_5	0.30	0.20	0.20	0.27
LOI†	1.24	2.27	0.50	0.64
Total	100.78	100.34	100.18	100.49

* Total iron calculated as Fe203. Weight percent for individual oxides are the average value obtained from two separate analyses.

† LOI = Loss on ignition.

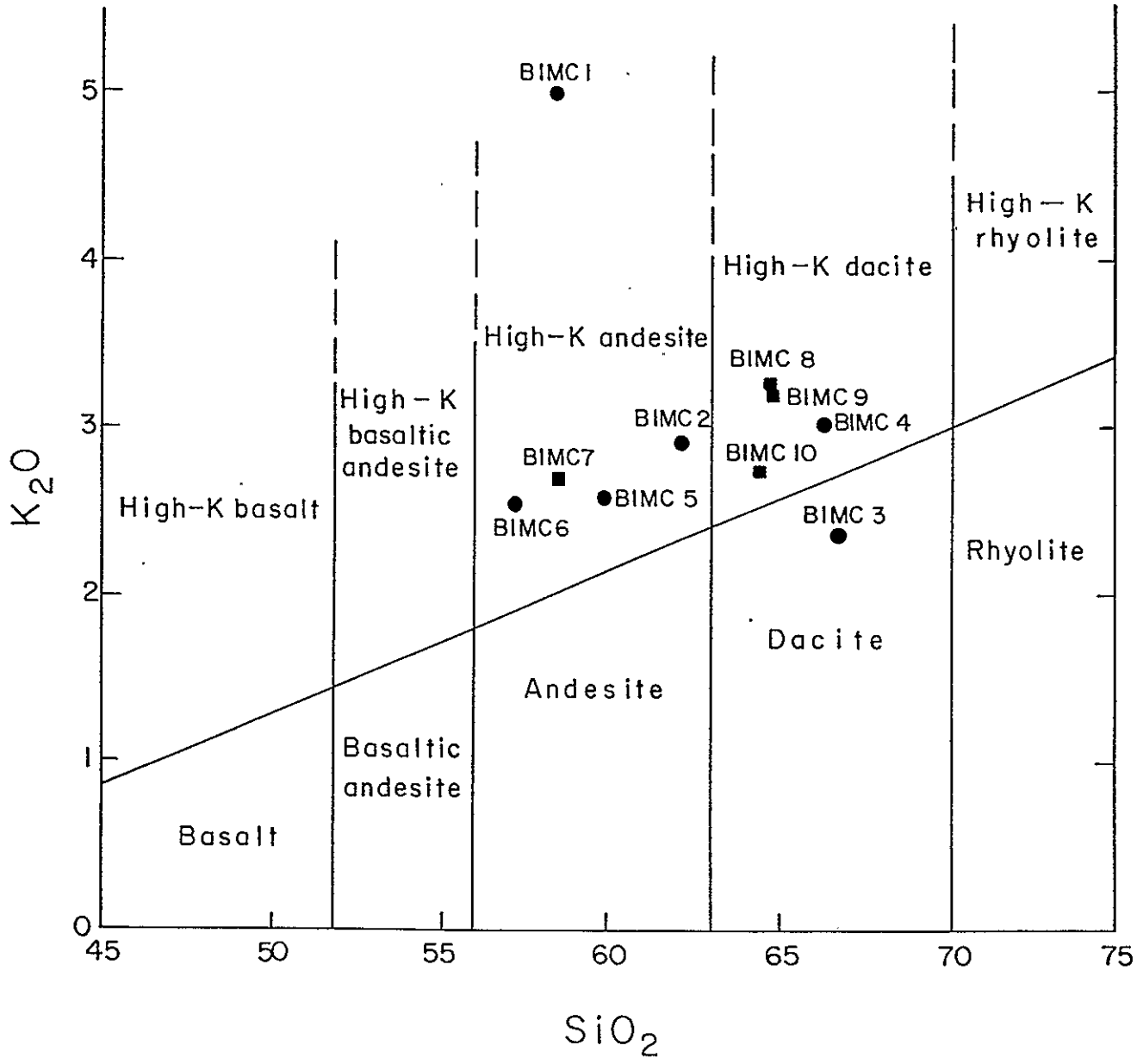

Figure 12. K20 plotted against SiO2 from major-element analyses of clasts from the Dog Springs Member. K20 and SiO2 have been recalculated on a volatile-free basis. Circles are for clasts from the upper Dog Springs (Tsdsu), squares are for clasts from the middle Dog Springs (Tsdsm). Graph modified from Ewart (1982).

during flow (fig.13).

Porphyritic dacites characteristically have a microcrystalline- to cryptocrystalline felsitic groundmass composed mainly of a mosaic of anhedral crystals of quartz and potassium feldspar with lesser plagioclase and glass. In decreasing order of abundance, phenocrysts consist of plagioclase, hornblende, biotite, opaque oxides, sanidine and quartz. Plagioclase phenocrysts in these dacites occurs as euhedral to subhedral single crystals or glomeroporphyritc patchwork-like accumulations which have maximum diameters up to 6 mm. Plagioclase crystals are commonly zoned and have combined albite, pericline and carlsbad twinning. Normal, oscillatory and reversed zoned crystals are present. A maximum An content of 37 was determined for the plagioclase (30 grains from 3 thin sections, Michel-Levy method). In some instances plagioclase megacrysts contain inclusions of euhedral crystals of hornblende or biotite (fig.14). Euhedral to subhedral phenocrysts of hornblende average 0.5 mm in size with maximum diameters of up to 2 mm. The hornblende shows a marked pleochroism of yellow brown to deep reddish-brown. Some crystals are zoned or have carlsbad or lamellar twins. The hornblende occurs both as single crystals and as glomeropophyritic clusters. Biotite laths average 0.5 mm and occasionally reach 2 mm in their long dimension. Pleochroism from light green to dark reddish brown is

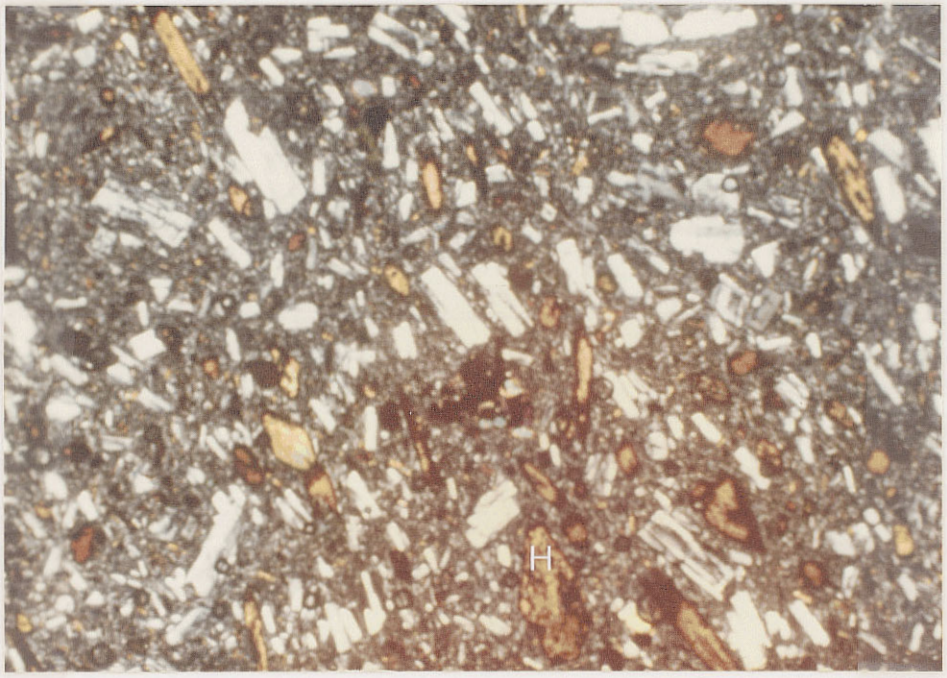

Figure 13. Photomicrograph of volcanic clast with trachytic texture from the middle Dog Springs map unit. Note abundance of Oxyhornblende (H). Subparallel alignment of phenocrysts suggests the rock solidified during flow. Photo taken in cross-polarized light. Field of view between points A and B = 6.5 mm.

#56

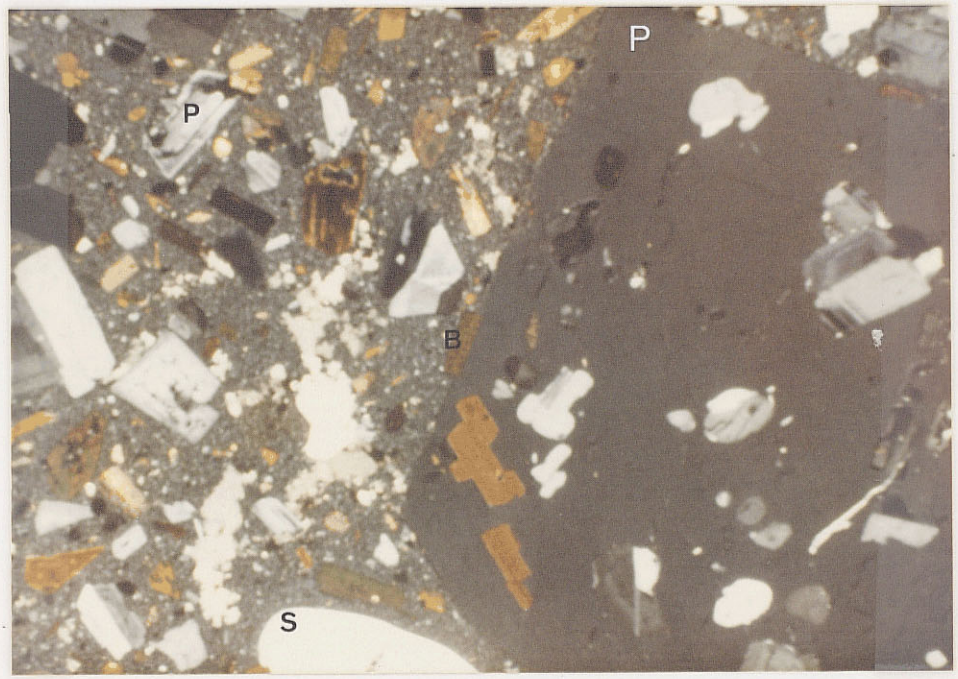

Figure 14. Photomicrograph of a typical porphyritic dacite clast from the middle Dog Springs map unit. (S) sanidine, (H) hornblende, (B) biotite, (P) plagioclase. Note biotite is present as phenocrysts and as euhedral inclusions in plagioclase megacryst. Photo taken in cross-polarized light. Field of view between points A and B = 1.3 mm.

common. Occasional single anhedral phenocrysts of quartz are present, typically having smooth rounded edges which are often embayed by the groundmass. Quartz ranges in size from 1 mm in diameter down to cryptocrystalline groundmass. It also occurs in minor amounts as a deuteric or diagenetic void-filling mineral. Sanidine is present as anhedral phenocrysts approximately 0.5 mm in size and as microcrystalline to cryptocrystalline crystals in the groundmass. Phenocrysts margins are smooth and often embayed. Opaque oxides are mostly confined to the groundmass.

Clinopyroxene-bearing clasts are less abundant than hornblende-biotite clasts within the middle Dog Springs. When present, they generally have seriate or trachytic textures. Clinopyroxenes are present either as the only ferromagnesian mineral in the clast, or in subordinate amounts when hornblende is present. Euhedral to subhedral phenocrysts of clinopyroxene as large as 4 mm are present in some clasts, and are in many instances glomeroporphyritic. Phenocrysts grade in size down to the groundmass and may be totally replaced by opaque oxides.

The matrix material present in heterolithologic debris-flow breccias, and in monolithologic breccias, consists of finely comminuted fragments derived from the clasts. The matrix is often clouded by hematitic staining

caused by the breakdown of magnetite and ferromagnesian mineral components. Secondary minerals are commonly associated with the primary matrix constituents. Calcite, chlorite, phyllosilicates, silica, sericite, and hematite, are present as replacement products and as cementing agents. Very low porosity (e.g. 1-2 percent) is present within the debris-flow breccias because of filling of void space by secondary minerals. No pyroclastic material (e.g. shards or pumice) was observed as clasts or within the matrix of any of the debris flows sampled within the middle portion of the Dog Springs Member.

Upper Dog Springs map unit

The main exposures of the upper Dog Springs map unit are present along a northwest-trending band within the southern half of the map area. An anomalously thin exposure of the unit is present north of the Thompson Canyon fault, along the northwest margin of the map area. South of the Thompson Canyon fault the unit ranges in thickness from approximately 144 m to 518 m, in general thickening to the southeast.

The upper Dog Springs is gradational with the underlying middle Dog Springs. The contact between the units was placed where the sequence of light-colored,

porphyritic dacitic clast-dominated debris-flow breccias of the middle Dog Springs grade into a sequence of debris flow deposits containing dark, rounded, aphanitic volcanic clasts and subordinate, interbedded fluvial deposits. This map unit is equivalent to the upper member of the Dog Springs volcanic complex as mapped and described by Coffin (1981) to the west. The upper Dog Springs is overlain by the Chavez Canyon Member of the Spears. In most places in the study area where the contact between the two units is exposed, it is marked by a angular unconformity. Chaotically bedded debris-flow deposits of the upper Dog Springs are in sharp angular discordance with overlying sandstones, conglomerates, and occasional debris-flow deposits present at the base of the Chavez Canyon Member. Deposits composing the Chavez Canyon Member are concordant with the regional tectonic strike and dip of bedding. A conformable contact is sometimes present between the two units in small, isolated areas, where laminated- to thin-bedded claystone, siltstone, mudstone and sandstone comprising the mudstone facies of the upper Dog Springs occur.

Deposits comprising the upper Dog Springs weather to subdued, rubble-covered, rounded hills, in contrast to the more resistant weathering character of middle Dog Springs debris-flow breccias. Also, the weathering character of many of the debris-flow clasts present in the upper unit is different. Rounded pebble-, cobble- and boulder-sized

clasts weather preferentially out of the less resistant matrix, in contrast with the homogeneous weathering of clast and matrix of middle Dog Springs debris-flow breccias. The bedding thicknesses of upper Dog Springs debris-flow deposits are less than those noted in the middle Dog Springs. Debris-flow deposits comprising the upper Dog Springs map unit range in thickness from about 1 m to 10 m, with an average thickness of approximately 3 m. Debris-flow breccias similar to those comprising most of the middle Dog Springs are present in the upper Dog Springs, but are neither as thick nor as volumetrically prominent as in the middle Dog Springs. Within the upper part of the upper Dog Springs Menber, laterally discontinuous exposures consisting of clast-supported volcanic conglomerates and volcaniclastic sandstones are present. These fluvial deposits are interbedded with debris flows, or are present as discrete vertical sequences.

Exotic blocks consisting of limestone and volcanic breccias, pebble- to boulder-sized red mudstone, siltstone, and sandstone, along with occasional granite and amphibolite clasts, are present in some debris-flow deposits. The size of exotic limestone and volcanic breccia blocks are smaller than those noted within middle Dog Springs deposits.

Dark, subrounded to rounded, aphanitic volcanic clasts are a prominent feature within upper Dog Springs debris-flow deposits, particularly within the upper half of the unit (fig.15). Fresh surfaces of the clasts are medium light gray (N6), greenish gray (5 GY 6/1) and light brownish gray (10 R 2/2). The clasts show little alteration in hand sample but often contain abundant microscopic alteration products. These dark clasts contrast with the lighter colored, coarser grained, porphyritic hornblende biotite dacite clasts also present in the deposits. In the upper portion of the upper Dog Springs map unit, hornblende biotite dacite clasts generally comprise less than 30 percent of the total clast types present, and often occur in an intensely weathered condition.

Chemical analysis of selected representative dark, aphanitic clasts show silica contents ranging from 56.62 to 66.43 weight percent (Table 5). These clasts can be classified on a chemical basis (Ewart, 1982) as high potassium andesites and dacites (fig.12).

Petrographically the clasts are composed of crystals indicative of andesitic to dacitic (Williams and others, 1954) rocks. Plagioclase phenocrysts are most abundant. Oxyhornblende and clinopyroxene are the predominant ferromagnesian phenocrysts. Opaque oxides and a occasional sanidine phenocryst are also present (Table 6). Volcanic

Figure 15. Photograph of upper Dog Springs debris-flow deposit. Subrounded to rounded, dark, aphanitic volcanic clasts are prominent within the upper part of the upper Dog Springs map unit. Note contrast in weathering character of this deposit with middle Dog Springs deposits (fig. 9). East-facing exposure at end of canyon directly south of old Baca Homestead. Hammer at lower left for scale.

OFR 219 #63

Table 5. Major-element analyses of clasts from the upper portion of the Dog Springs Member (Tsdsu).

BIMC	1	2	3	4	5	6
SiO_2	58.24	61.22	66.43	66.33	59.32	56.62
TiO_2	0.67	0.49	0.52	0.52	0.79	0.92
Al_2O_3	17.45	16.48	14.80	15.48	17.16	17.12
Fe_2O_3*	6.03	4.84	4.81	4.20	6.53	7.42
MnO	0.11	0.06	0.06	0.03	0.08	0.09
MgO	2.31	1.73	1.86	0.75	1.73	2.58
CaO	5.45	6.14	4.83	3.94	5.78	7.55
Na_2O	4.12	4.21	3.92	3.78	4.25	3.87
K_2O	4.99	2.84	2.30	3.08	2.52	2.51
P_2O_5	0.28	0.21	0.23	0.24	0.32	0.32
LOI†	1.13	1.86	0.86	1.28	1.52	1.72
Total	100.78	100.08	100.62	99.63	100.00	100.76

* Total iron calculated as Fe203. Weight percent for individual oxides are the average value obtained from two separate analyses.

† LOI = Loss on ignition.

Table 6. Modal analyses of clasts from the upper portion of the Dog Springs Member (Tsdsu).

Sample*	BIMC 1	BIMC 3
Groundmass	69.0	70.5
Plagioclase (An content)	18.3 (39)	18.9 (41)
Clinopyroxenes	6.4	0.7
Hornblende	2.7	7.5
Opaque oxides	3.5	1.8
Sanidine	0.2	---
Secondary chlorite	---	0.7
Total	100.1	100.1
Points counted†	597	600

* See Table 5 for major element analyses of these samples.

† A 1 mm x 1 mm grid spacing covering the entire slide was used in point counting. Recorded values represent the number frequency (Galehouse, 1971) of species counted.

clasts containing ferromagnesian phenocrysts of oxyhornblende, or oxyhornblende and biotite, or clinopyroxene and biotite, are occasionally found in the upper half of the upper Dog Springs, but are more abundant in the lower part of the unit.

Clasts containing ferromagnesian phenocrysts of oxyhornblende and clinopyroxene have porphyritic to microporphyritic, seriate, and trachytic textures (fig.16). Within these rocks, most plagioclase phenocrysts occur as unaltered, euhedral to subhedral crystals which average 0.6 mm in their largest dimension, but occasionally attain 1.75 mm in length. Zoned crystals with combined pericline, albite and carlsbad twins are common. Normal, reverse and oscillatory zoning is present, with some zones marked by inclusions of fine, opaque oxides. Sieve textures occur in some crystals. Plagioclase has a compostion of An 41 (maximum value from 20 grains in 2 thin sections, Michel-Levy method).

Oxyhornblende phenocrysts have corroded opaque margins composed of numerous inclusions of opaque oxides. In some cases magnetite and/or hematite completely mask the hornblende leaving only a relict amphiblole shape. Replacement by, or inclusions of, clinopyroxene are found in some oxyhornblende crystals. Zoned crystals of oxyhornblende occasionally occur. Oxyhornblende is the

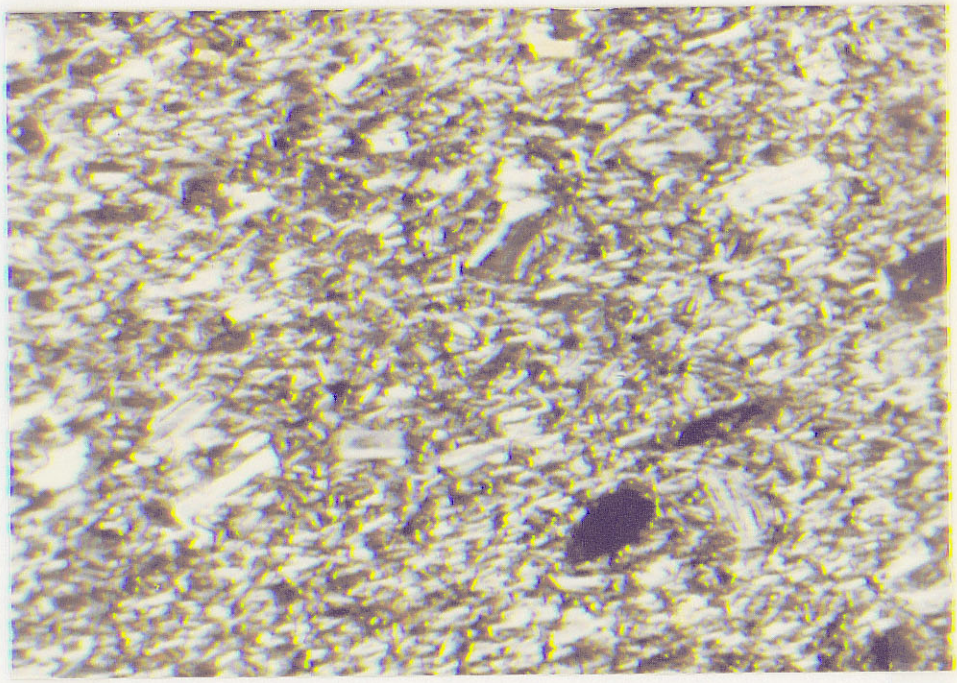

A B

Figure 16. Photomicrograph of typical dacite clast with trachytic texture from the upper Dog Springs map unit. Microlites of feldspar are disposed in a subparallel manner with interstitual magnetite, hornblende, and clinopyroxene. Opaque grains are hornblende replaced by opaque oxides. Photo taken in cross-polarized light. Field of view between points A and B = 6.5 mm.

largest phenocryst present in the rock, averaging 0.4 mm in size but reaching lengths of 2-3 mm. Crystals have a marked pleochroism from yellow green to a dark reddish brown. Clinopyroxene phenocrysts occur as euhedral to anhedral single crystals and glomeroporphyritic accumulations. Crystals average 0.2 mm in size, with some up to 0.4 mm in length. Sanidine is rare, but when present, occurs as single anhedral crystals with resorbed margins. Opaque oxides are ubiquitous, but are mainly concentrated within the groundmass. They also occur as a replacement or included mineral in oxyhornblende.

The groundmass most often has a pilotaxitic texture composed of plagioclase and clinopyroxene microlites with interstitual cryptofelsite and opaque oxides. Alteration of the groundmass and phenocrysts by chlorite, calcite, silica and celadonite is common.

Monolithologic exotic volcanic breccia blocks and boulders are present within the upper Dog Springs. They differ from debris-flow breccias in that they consist predominantly of angular clasts and lesser matrix. Exotic volcanic breccia blocks consist mainly of hornblende clinopyroxene dacitic to andesitic material. Clasts grade from their peripheries into a matrix which makes up approximately 30 percent or less of the rock.

Upper Dog Springs mudstone facies

The mudstone facies of the upper Dog Springs map unit occurs as discontinuous exposures at or near the top of the Dog Springs Member. The lateral extent of exposures is always less than 122 m, with vertical thicknesses never exceeding 18 m. Outcrops of these rocks are typically pale yellowish-brown when weathered and pale reddish-brown when fresh. Deposits comprising the mudstone facies are discordant with underlying debris-flow deposits. At one exposure, located at the end of the Canyon running directly south of the Baca Homestead, this angular discordance is well exposed (fig.17). Fine-grained constituents comprising the mudstone facies are surrounded or cradled between debris-flow deposits. Laterally, this facies abuts against debris-flow deposits in a near vertical contact. In some cases, the mudstone facies grades upward into fluvial deposits of the Chavez Canyon Member. In other areas, the mudstone deposits dip in a chaotic manner in association with the deformation noted throughout the Dog Springs Member. To the west, Coffin (1981) has mapped and described this same rock unit, referring to it as the lacustrine rocks of middle Canyon. In his study area, he suggested the exposures represented the deposits of a large lake or a series of small ponds occurring at about the same stratigraphic level. Mapping and sedimentologic analyses

Matrix material in both monolithologic exotic volcanic breccia blocks and debris-flow deposits consists of finely comminuted clast constituents. Lithic fragments, crystals, and mud-sized material comprise the matrix. No pyroclastic material (e.g. shards or pumice) was observed as clasts or as constituents of the matrix in any of the deposits sampled from the upper Dog Springs. Matrix components are bound together by a variety of secondary minerals. Calcite, hematite or limonite, silica, and clay minerals are often found together as replacement products and cementing agents within the matrix.

Upper Dog Springs sandstone facies

Fluvially deposited volcaniclastic sandstone and conglomerate sequences are interbedded with debris-flow deposits within the upper Dog Springs. Such deposits are generally thin and discontinuous but have been mapped where sufficient exposures are present. Sandstones are medium to coarse grained and are present in thin to thick, plane-bedded sets, and 15-20 cm thick, small-scale cross-stratified planar sets. Plane-bedded pebble to cobble conglomeratic beds occur in thin- to thick-bedded sets. These fluvial sandstones and conglomerates are composed of intermediate-composition volcanic materials of the same composition as in surrounding debris-flow deposits.

Figure 17. Photograph of clay- to sand-sized volcaniclastic rocks filling a depression on the surface of upper Dog Springs debris-flow deposits. Unconformable contact between deposits indicated with dashed line. Exposure at end of canyon running directly south of old Baca Homestead.

#71

performed during the present study indicate that isolated ponding of water is the most likely origin of the deposits.

Two main types of sedimentary sequences compose the mudstone facies. One type consists of thinly laminated to very thin-bedded claystones, siltstones and mudstones occurring in thick, monotonous, vertical sequences. Laminations are generally well preserved and in an undisturbed state. Some bedding-plane surfaces show disruptions of the mud-sized material with trail-like casts of infilled coarser-grained sediments. Such turbation may represent the feeding trails of crawling organisms. Very little vertical disruption of horizontal bedding or lamination is present at outcrop scale. In thin section, some thinly laminated beds show vertical burrow-like disruptions consisting of fine-grained sand-filled casts. No fossils have been found in any of the exposures examined.

The second type of deposit consists of fine- to very coarse-grained normally graded beds, 30 cm to 1 m in thickness, overlain by thinly laminated to laminated, or thinly bedded mudstones and siltstones. This association occurs as vertical cyclic sequences measuring approximately 40 cm to 1.2 m in thickness (fig.18). Occasional thin-bedded, low-angle, medium-scale, cross-stratified sets are present in a sequence.

Figure 18. Photograph of cyclic sequence of volcaniclastic strata in the mudstone facies of the upper Dog Springs map unit. Each sequence consists of a normally-graded sandstone overlain by thinly laminated to laminated, or thinly bedded mudstones and siltstones. Hammer rests on graded bed found at the base of one sequence.

Graded beds may represent stream or slump generated, sediment-flows deposited into a small, quiet, standing body of water. Overlying laminated and thin-bedded mudstones and siltstones, present in each sequence, probably are the result of settling of suspended sediments associated with the sediment gravity flows.

The ponding of fine-grained material was probably caused by the disruption of a drainage network which was beginning to form during upper Dog Springs deposition. Discrete but discontinuous fluvial-sediment sequences found within upper Dog Springs debris-flow deposits may represent channelways disrupted by debris flows. The hummocky topography associated with the sites of debris-flow deposition (Macdonald, 1972, p. 180) was probably a major factor in the development of ponds. Streams may have emptied or were diverted into isolated low-lying areas in a hilly topography, or overflowed their channels into surrounding depressions.

Petrographically, rocks comprising the mudstone facies contain recognizable volcanic lithic fragments in the coarser-grained deposits. Within the silt- to fine-sand population, angular to subrounded grains of plagioclase, hornblende, biotite and opaque oxides are recognizable. Some laminae consist of concentrated horizons of opaque oxide grains. Microscopic constituents consist of clay

minerals and a dissemination of hematitic or limonitic staining. This imparts the reddish-brown oxidized color of these deposits.

Exotic blocks

Nonvolcanic material, ranging in size from sand to blocks of material hundreds of meters in diameter and tens of meters thick, are randomly distributed within debris-flow deposits of the upper and middle Dog Springs. Volcanic material consisting of boulders and breccia blocks, similar in composition to clast-sized constituents, are present within some debris-flow deposits. Non-volcanic components consist primarily of gray micritic limestones of Late Paleozoic age, shale, siltsone, and sandstone of the Permian Abo Formation, and sporadic occurrences of amphibolite and granite.

The term exotic block, as used by Coffin (1981) for rocks of similar appearance found within his study area, is extended here. The term refers to rock masses occurring in a lithologic association foreign to that in which the mass was formed (Bates and Jackson, 1980). In this discussion the word "block" will only be used in reference to material larger than boulder size as defined by Wentworth (1922). Monolithologic andesitic to dacitic boulders and blocks are

present throughout the middle and upper Dog Springs section. Most often they are more resistant to weathering than enclosing debris-flow deposits, and are exposed as isolated remnants on hilltops or along the walls of steep-sided canyons. In some instances it is difficult to determine whether an exposure represents an intrusive breccia or an exotic block. Volcanic exotic blocks present in the study area share many of the same physical characteristics as autoclastic and alloclastic breccias described by Parsons (1969). These deposits probably represent portions of such rocks which have been rafted into the area by debris-flows. The volcanic exotic blocks are monolithologic breccias with relatively low matrix percentages (25-35 %). These breccia blocks are well indurated and generally more resistant to weathering than surrounding debris-flow deposits. Volcanic exotic blocks have been differentiated and mapped where exposures suggest that they are incorporated within debris flows. Similar volcanic exotic blocks are described to the west by Harrison (1980, p.25) and Coffin (1981, pp. 61-66).

Nonvolcanic foreign clasts and blocks occur in a variety of sizes, but seem to show a correlation between size and composition. Clasts of red shale, siltstone and sandstone are abundant in certain debris-flow deposits and range from pebble to boulder size. Occasional cobble-sized clasts of amphibolite or granite are present in some debris-flow deposits in the upper Dog Springs. Limestone

ranges in size from sand to large blocks. The largest block observed in the study area (S.W. corner sec. 12, T.1N., R.7W.) has an exposed maximum diameter of approximately 830 m and thickness of 133 m. The very large limestone blocks occur only within the middle Dog Springs.

Compositionally, limestone exotic blocks are micritic with some chert or sparry calcite replacement. Some horizons within the limestones are fossil rich, containing rugose corals, crinoid columnals and stems, and fenestrate bryozoans. The age and geologic formation(s) from which the limestone blocks were derived is not known for certain. Previous investigators in the surrounding area who have documented the presence of limestone exotic blocks have inferred both Pennsylvanian and Permian ages (Givens, 1957, Laroche, 1981; Lopez, 1975). The clasts of reddish mudstones, siltstones, and sandstones found in some debris-flow deposits closely resemble rocks composing the Permian Abo Formation. Lopez (1975) and Harrison (1980) observed similar clasts in their study areas and suggested that they were from the Abo.

Coffin noted that exotic blocks in his and Harrison's study area were concentrated within the upper 107 m of the Dog Springs Member. No such relation is present in this study area. The abundance and stratigraphic position of exotic material is laterally variable. When a concentration

of exotic blocks is present in any one area, it occurs at approximately the same stratigraphic horizon.

The direction from which these nonvolcanic clasts were derived and transported may be inferred as southerly. South of the study area, outside the Baca depositional basin, the Spears rests on the Abo and Paleozoic limestones. At Tres Montosas (Wilkinson, 1976) and in the Kelly mining district (Blakestad, 1978) the Spears contains clasts from the underlying Abo. Limestone exotic blocks are restricted to Dog Springs Member of the Spears Formation and equivalent units present in the northern and central Gallinas Mountains (Robinson, 1981; Coffin, 1981; Laroche, 1981; this report), and northern and central Datil Mountains (Harrison, 1980; Lopez and Bornhorst, 1979). No limestone exotic blocks are reported in the southern Gallinas Mountains or within Spears exposures to the east in the Bear Mountains. Whether limestone exotic blocks are present in the area immediately west of the Datil Mountains is uncertain, since the area has not been mapped in detail. Along the southwestern margin of the Plains of San Augustin, Stearns (1962) reports that Spears-equivalent rocks overlie the Yeso, Glorieta and San Andres formations and Triassic(?) sandstones. No nonvolcanic clasts or blocks are described as being present in the volcaniclastic rocks within Stearn's area. The areally restricted occurrence of the limestone exotic blocks suggests that they where carried into the

study area along a north- northeasterly corridor running approximately through the northeastern portion of the Plains of San Augustin.

Exotic blocks consisting of both volcanic and nonvolcanic material are not uncommon features in debris-flow deposits. Occurrences are reported in the Absaroka volcanic field (Hay, 1954, pp. 613-615; Hay, 1956, p. 1874) and the Tuscan Formation of northern California (Anderson, 1933, p.225).

Moving exotic blocks with diameters of hundreds of meters and thicknesses of tens of meters by debris flows is certainly possible. Laboratory and theoretical analyses indicate that poorly sorted debris flows possess large buoyant forces (Hampton, 1979; Fisher, 1971; Rodine and Johnson, 1976). Debris flows can be characterized as highly concentrated non-Newtonian dispersions with high apparent viscosity, high bulk density, and have yield strength (Fisher, 1971). The fluid phase of the flow (i.e. water and sand/silt/clay) prevents interlocking of clasts and reduces shear strength thus enabling movement. Large buoyant forces are the result of high density and a vertical pressure gradient of downward increasing pore-water pressure. A likely additional source of support is dispersive pressure generated as the result of grain interaction during flow (Hampton, 1979).

The most difficult problem to be resolved is how the large exotic limestone blocks were incorportated into the debris flows. The two largest limestone blocks found in the study area (sec. 12, T.1N., R.7W., and sec. 31, T.2N., R.7W.) show very little deformation. Variations in the attitude of bedding along the strike of the blocks seems to be the result of rotation along fractures. This rotation might have occurred when the blocks where being incorporated into the debris flows or later during slumping that occurred in the area. The fractures along which this rotation has taken place are often far apart. Individual beds may be traced in an undeformed state for tens of meters (fig.19). In one case where the base of one of the largest limestone blocks is well exposed, the lower 60 cm to 1 m of the limestone is composed of a mass of brecciated cobble- to silt-sized carbonate material. Below this breccia zone, a meter or more of dark brownish-red shale mixed with limestone breccia is exposed. This breccia has a slight foliation and is suggestive of a cataclastic zone. The limestone block shows no sign of brecciation above this basal zone.

Mechanisms for incorporating the limestone blocks into the debris flows must take into account the overall physical characteristics of the blocks. The larger blocks are tabular masses with width-to-thickness ratios in some cases approaching 6:1. Several mechanisms could be used to

Figure 19. Photograph of large tablular-shaped exotic limestone block present in the middle Dog Springs map unit. Note undeformed limestone bed in foreground. Perimeter of block is indicated by dashed line. South-facing exposure, SE 1/4, NW 1/4 sec. 31, R.7W., T.1N.

account for the presence of these large limestone exotic blocks within the debris-flow deposits. Harrison (1980) postulated that the blocks of nonvolcanic material could have been gently floated upward by a slowly upwelling, brecciating magma, in a series of large volcanic vents. Coffin (1981) suggested a low-angle detachment fault moving blocks of limestone into a position for incorporation into debris flows. Another possible explanation is that the limestone was originally present on a sloping surface, and detached as large landslide blocks into flows travelling at the base of the slope. Such a mechanism would explain the large, relatively undisturbed, tabular shape of the larger blocks and the brecciated base resulting from detachment and shearing accompanying movement. Once in the debris flow, the blocks would be gently rafted along (Enos, 1977; Johnson, 1970).

Deformational structures related to slumping

A variety of deformational structures are exhibited by strata comprising the Dog Springs Member. Inclination of bedding varies from near horizontal to vertical and the strike of bedding varies widely both east and west of north. Individual debris-flow deposits, and blocks consisting of sequences of flows, have been rotated, folded, and faulted.

Strata showing a high degree of deformation are often confined between less deformed or nondeformed beds. The spatial distribution of disturbed bedding is stratigraphically confined to the interval between the top of the Baca Formation and the base of the Chavez Canyon Member. The Baca and Chavez Canyon show no signs of the type of deformation displayed by strata comprising the Dog Springs Member. As noted earlier, the depositional contact between the lower Dog Springs and Baca is conformable. Folding and general contortion of beds sometimes occurs directly above the Baca contact, but is variable, and may not be present until further upsection. In the northeastern portion of the map area, where relatively thin lower Dog Springs overlies the Baca Formation (sec. 12, R.7W., T.1N.), bedding is highly contorted. In this area, the lower Dog Springs-Baca contact occurs along a surface of detachment. A several-meter-thick zone consisting of highly contorted lower Dog Springs lithologies overlies undistrubed Baca strata. In the northwest corner of the study area, where exposures of the lower Dog Springs-Baca contact are present, no deformation occurs at the contact. Further upsection in the lower Dog Springs, a well-exposed surface of detachment is present. Gently dipping beds in the upper plate thrust over and fold underlying beds. Exposures of the middle Dog Springs in contact with the Baca are marked by a zone of detachment and highly contorted bedding. The

upper Dog Springs also contains rotated and contorted beds, but in general, does not show the degree of deformation which is present in the lower and middle portions. Strike directions of bedding in the upper Dog Springs are as variable as underlying deposits but the dips of beds are not as great.

The degree and location of deformation is variable both laterally and vertically within the Dog Springs Member, but, in general, is associtated with three portions of the section. These portions are: 1) along a detachment surface that sometimes occurs at the Baca-Dog Springs contact; 2) along a detachment surface that always occurs at the lower Dog Springs-middle Dog Springs contact; and 3) varying intervals throughout the middle and upper Dog Springs. The salient characteristics of the bedding within the Dog Springs Member can be listed as follows: 1) deformation is restricted to strata comprising the Dog Springs Member; 2) bedding attitudes are chaotic and bear no relationship to the tectonic strike of underlying or overlying units; 3) deformation is nonuniform, with highly deformed sequences of beds present between less deformed or nondeformed strata; 4) soft-sediment deformation structures such as clastic dikes and stringers are abundant; and 5) folded and thrusted beds indicate a compressional stress regime.

Such features are strikingly similar to deformation described as resulting from slumping. The process of slumping involves the penecontemporaneous deformation of sediments by gravity-induced sliding. Elastic, plastic and incipient viscous movement may be involved (Rupke, 1976). Slumped sediments partially retain their original sedimentary structures and their structural style is essentially the result of deformation rather than deposition (Woodcock, 1976).

Terrane that has undergone sedimentary slumping is indicated by the presence of a number of features. A summary of the characteristics associated with slumped masses has been compiled and modified by Rupke (1980, p. 376) and Helwig (1970, p. 176). Features that imply a slump origin include the presence of: 1) deformed beds occurring as a zone between undisturbed beds; 2) piled up, recumbent, or nappelike folds; 3) fold axes whose orientation shows no relation to the tectonic strike; 4) a wide range of deformational structures present within a single slump; 5) decollement surfaces and detached fold blobs; 6) chaotic structures not cut by open fractures or vein fillings; and 7) a "welded" contact above the zone of deformed beds, i.e., a depositional fit occurs between the irregularities of the deformed strata's upper surface and the base of the overlying bed. Miscellaneous indicators often associated with slumping are soft-sediment deformation

structures such as burrowed-folds, dewatering structures, and sand volcanoes (Woodcock, 1976)

Folded beds are most prominent along the detachment surface that occurs between the lower and middle Dog Springs map units. Approximately 0.5 km south of Cottonwood well (SW 1/4, sec. 33, R.7W., T.2N.) a spectacular exposure of folded lower Dog Springs strata is present. A sequence of tight folds with amplitudes of 50-60 m underlies a detachment surface with middle Dog Springs debris-flow deposits. A small-scale version of this relationship of folded grain-flow deposits separated by a detachment surface from overlying debris-flow deposits is present lower on the hill side (fig.20). Detached folds and roll-up structures (Potter and Pettijohn, 1977, fig. 6-8, p. 212) are also exposed along the Baca-middle Dog Springs contact in the northeast corner of the map area (fig.21). Additional indicators of soft-sediment deformation include the presence of clastic stringers or dikes which are present throughout the Dog Springs Member.

A variety of deformational styles are displayed by strata comprising the Dog Springs. Medium to thick plane-bedded sequences consisting of grain-flow deposits seem to be most susceptible to the development of folds and roll-up structures. Internally massive, very thick-bedded debris-flow deposits do not appear to be subject to fold

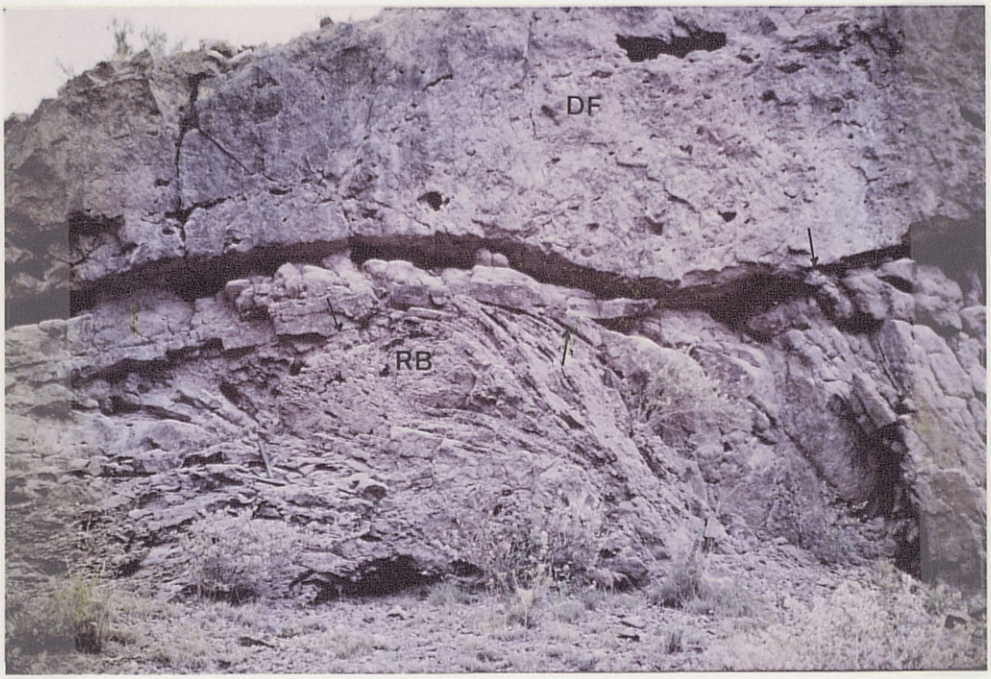

Figure 20. Photograph of folded beds in the lower Dog Springs map unit showing a detached upper contact. Rolled-up bedding (RB) is present near center of photo. Middle Dog Springs debris-flow deposit (DF) overlies folded grain-flow deposits. Location of detached surface between debris flow and grain-flow deposits indicated by arrows. West-facing exposure, SE 1/4, SE 1/4 sec. 32, R.7W., T.1N.

#87

Figure 21. Photograph of detached fold (DF) and roll-up structure (RS). West-facing exposure, NE 1/4, SW 1/4 sec. 7, R.6W., T.1N.

deformation, but rather have detached from their original depositional surface and are displaced as coherent blocks. Often these blocks have been rotated to steeply dipping positions. The size of the blocks which have been detached and rotated is quite impressive. Rotated sections tens to hundreds of meters thick, composed of multiple debris-flow deposits dipping very steeply, are present intermittently throughout the middle Dog Springs. Thrusting is indicated by the presence of slickenside surfaces at the base of some blocks. These blocks are positioned over other deposits with sharp angular discordance.

Interbedded slumped and undisturbed strata, as is present in the Dog Springs Member, has been noted by Jones (1936) in his study of slumping of submarine sediments. Such a condition is considered as an indication of intermittent emplacement of slump sheets in an area of continuous basin-facies sedimentation.

Slumping of sediments deposited on a slope occurs when the shear strengh of the sediments along a potential glide plane is exceeded by the shear stress acting downslope (Moore, 1961; Morgenstern, 1967). Shear strength is a highly variable quantity controlled by sedimentation rate, grain size, lithology, age, degree of consolidation and the pore water condition at the time of failure (Roberts, 1972). Rapid sedimentation, involving a large volume of volcanic

material transported by debris flows or mudflows, has been recorded in many volcanic regions within historic time (Macdonald, 1972). Similar depositional conditions probably existed during Dog Springs time. The absence of paleosols within the Dog Springs further supports a rapid emplacement of debris flows. Inundation by sediment gravity flows entraining significant amounts of water probably acted as an important factor in slump development. Loading induced by a rapid rate of deposition of water-saturated sediments may have resulted in the development of liquifaction of the sediments, which would initiate slumping. An additional factor which would contribute to a reduction in shear strength is sedimentation in a subaqueous environment. Deposited sediments would be unable to drain water and with loading would develop excess pore-pressure with resultant undrained slumping (Morgenstern, 1967).

The amount of material involved in slumping within the study area is very large. An estimated minimum volume of 41 km3 of slumped strata was present before erosion occurred. Slumping involving a large volume of material, particularly with large-scale features such as rotated blocks of debris-flow deposits and folded grain-flow beds with amplitudes of 50-60 m, have been attributed to seismic disturbances of great magnitude (Rupke, 1980, p. 375). It may be that earthquakes associated with volcanism occurred in the area while sedimentation was proceeding and acted as

an additional component in the triggering of slumping.

Exactly when the Baca lacustrine system no longer had an effect on Dog Springs deposition and deformation is difficult to determine. Subaqueous deposition did occur at least through lower Dog Springs time. Within the middle and upper Dog Springs no direct evidence of the presence of a lake has been observed. Without the occurrence of interbedded lacustrine sediments, it is not possible to demonstrate with any degree of certainty whether the debris flows present were deposited in a subaqueous or subaerial environment. Inundation by the debris flows comprising the middle Dog Springs probably resulted in infilling and displacement of water, leading to the final demise of the Baca lake system.

Particularly representative of disturbed beds found in the Dog Springs Member are deformed sediments found along the margins of flysch basins (Woodcock, 1976; Roberts, 1972; Helwig, 1970; Rupke, 1976) and on the fronts of fan-deltas which have developed in Cenozoic lakes (Theakstone, 1976; Stone, 1974; Postma, 1984).

The presence of features such as detached fold blobs, overriding or thrusted beds, and the extensive detachment surface occurring between the lower and middle Dog Springs map units, is characteristic of the distal portion or toe area (fig.22) of slump sheets (Lewis, 1971; Helwig, 1970;

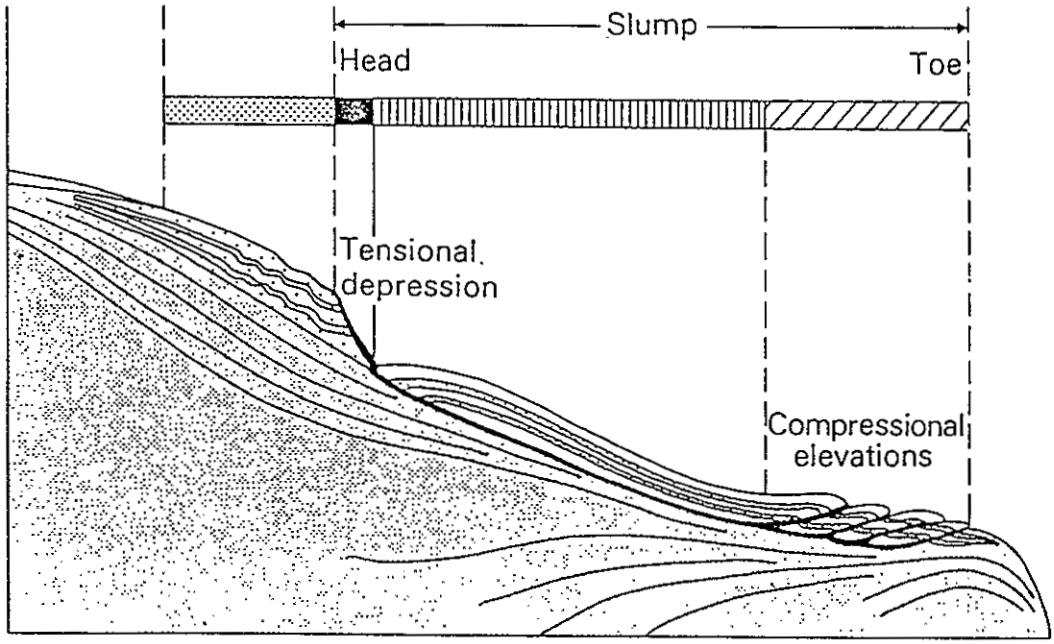

Figure 22. Diagramatic cross-section of a slump on a gentle slope. Unstippled beds have slumped. Diagonal cross-hatching overlies a zone of compressional folding and thrusting at toe of slump. Vertical hatching overlies a zone of undeformed or slightly deformed beds in the middle of the slump. Solid black overlies an exposed glide plane in a zone of tension at the head of the slump. Large stipples overlies disturbed beds associated with movement of the main slump (After Lewis, 1971).

Lajoie, 1972). The occurrence of these features within the Dog Springs Member suggests that the area lies within the distal portion of large slump deposits. The distance that the slumps have traveled is difficult to determine because slumped masses may travel many miles (Rupke, 1980). A deposit attributed to slumping in the Polish Carpathians has been traced 30 km in the direction of movement (Dzulyski and others, 1959, p. 1113).

Deformation of the Dog Springs Member and equivalent lower Spears sediments in the surrounding area is associated with sedimentary sequences consisting of debris-flow deposits, grain-flow deposits, and minor amounts of volcaniclastic conglomerates and sandstones. Occurrence of these deposits is restricted to the northern and central portions of the Gallinas and Datil Mountains (fig.23). This deformation is associated with Spears sediments deposited in the lacustrine and meanderbelt depositional systems of the Baca Formation (Compare fig.23 to fig.2).

Paleoslope indicators

Orientations of fold axes and bedding planes within slumped deposits have been used by many investigators as a means of determining the direction of the paleoslope (Stone, 1976). Caution must be taken in the interpretation of data

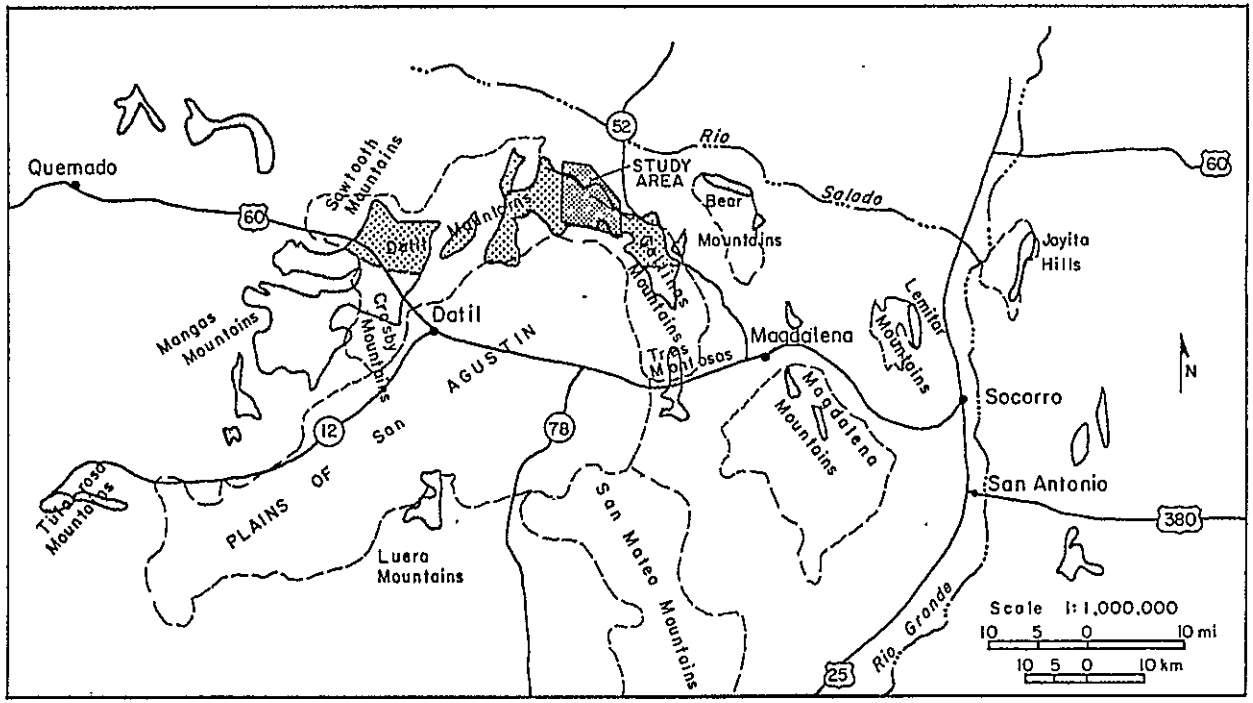

Figure 23. Approximate location of Spear's rocks in the study area and surrounding region that have a lower portion (Dog Springs Member and equivalent units) that contains disturbed bedding. Spear's deposits that have a lower portion consisting of debris-flow breccias, grain-flow deposits, exotic blocks, and lesser volcaniclastic conglomerates and sandstones, all of which have disturbed bedding, indicated by dark stippled pattern. Lower Spears deposits consisting predominantly of volcaniclastic comglomerates and sandstones with lesser debris-flow deposits indicated by light stippled pattern. Sources: Allen (1979), Blakestad (1978), Brown (1972), S. M. Cather (1984, oral commun.), Chamberlin (1974), R. M. Chamberlin (1984, oral commun.), Coffin (1981), Guilinger (1982), Harrison (1980), Laroche (1981), Lopez and Bornhorst (1979), G. R. Osburn (1984, oral commun.), Robinson (1981), Spradlin (1972), Stearns (1962), Wilkinson (1976).

because of the variability of orientation of slump structures at various positions in a slumped mass (Lajoie, 1972).

Several authors have plotted the strike of the axes of folds (Rupke, 1976; Helwig, 1970) and bedding (Jones, 1939) in slumped deposits. This data is commonly plotted on rose diagrams and interpreted based on the belief that as the mass slides down a slope it tends to acquire folds and corrugations approximately at right angles to the down-slope movement (Jones, 1939). Lajoie (1971) has shown by analogy with a deposit of slumped snow, that the strike of bedding and fold axes varies from near perpendicular to slope direction at the base of the slump, to orientations paralleling slope in its upper region (fig.24).

Also affecting the orientation and character of the slumped mass is the behavior of the beds comprising the slump under downslope movement. Most studies where paleoslope directions have been determined involved well-bedded, folded flysch deposits. In these deposits, strata had a tendency to fold, therefore the axes of folds were used in orientation plots. Strata composing the Dog Springs Member consist predominantly of debris-flow deposits and lesser grain-flow and minor fluvial deposits. Folded beds are present in the lower Dog Springs but only a few are exposed. The majority of beds comprising the Dog Springs

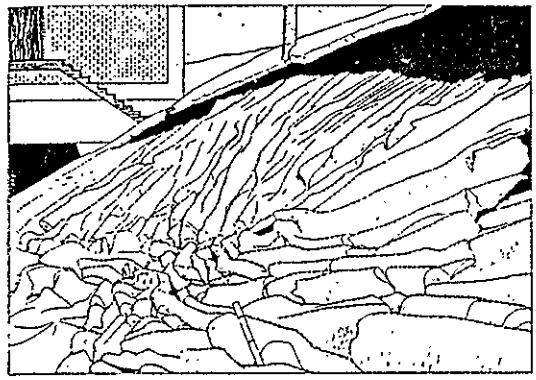

A

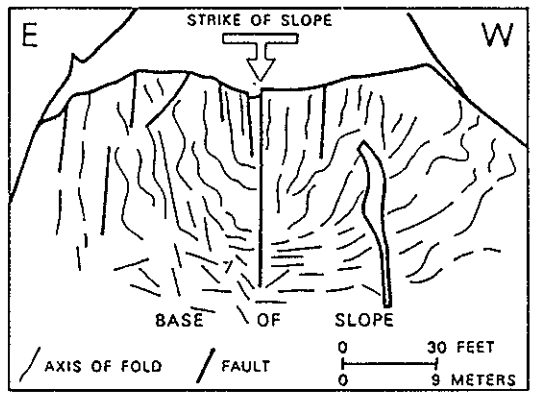

B

Figure 24. View of snow slump showing variations in the orientation of folded beds and faults within different areas of the slump sheet. A) oblique view of slump. Scale in foreground is 45 cm long. B) Map view of slump fold-axes orientations (From Lajoie, 1971).

Member have been disturbed by a non-plastic type of deformation. Blocks consisting of a stack of debris-flow deposits have detached from their depositional surfaces, moved as a coherent mass, and rotated to a new orientation during downslope movement. The movement of slump sheets composed of blocks of material has resulted in the chaotic appearance seen in the bedding of the middle and upper Dog Springs map units. Therefore, in this study, bedding plane surfaces, and not fold axes, were measured and used as a possible slump-direction indicator.

The direction perpendicular to the strike of disturbed beds has been plotted on a rose diagram in an attempt to discern both direction of slumping and paleoslope. Separate rose diagrams have been constructed for the lower, middle and upper Dog Springs, and for limestone blocks found in the middle Dog Springs (fig.25). The diagrams were constructed using only the northern half of the rose circle. Since the main body of the Mogollon-Datil volcanic field lies to the south of the study area, and there are no known volcanic rocks or source areas of equivalent age present to the north, the volcanic material present in the study area must have traveled from some direction in the southern hemisphere of the rose circle.

Figure 25. Rose diagrams illustrating the orientation of bedding within the Dog Springs Member. Diagrams constructed by plotting the perpendiculars to bedding strike directions within the northern hemisphere of a rose circle. Arrows indicate the position of the perpendicular to the average tectonic strike in the study area (approximately N.15°E.). Bedding orientations for the lower Dog Springs, A); middle Dog Springs, B); upper Dog Springs, C); and exotic blocks present in middle Dog Springs, D). Class sizes encompass 10 degree intervals on the rose circle. Vector mean expressed as azimuth reading. Vector strength should be considered between 0.5 and 1.0; 0.5 = random distribution. Paleocurrent plot program written by Sue Daut (1978, Iowa Geological Survey), adapted by Kenneth Lemley (1984, New Mexico Institute of Mining and Technology).

LOWER DOG SPRINGS

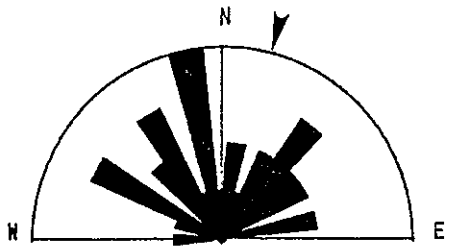

A) 30 measurememts
Vector mean = 17.3
Vector strength = 0.67
Resultant = 21.16
Radius = 4 measurements

MIDDLE DOG SPRINGS

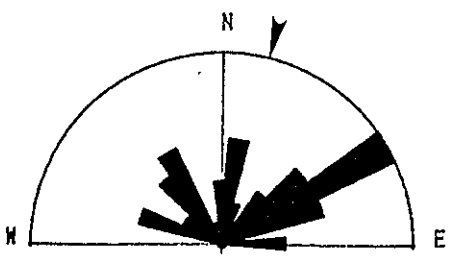

B) 56 measurements
Vector mean = 0.3
Vector strength = 0.71
Resultant = 37.33
Radius = 9 measurements

UPPER DOG SPRINGS

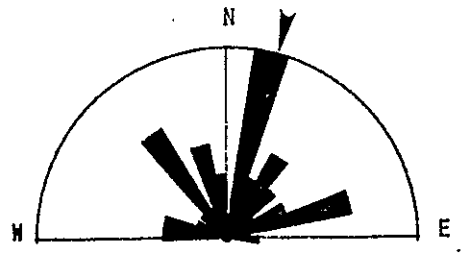

C) 39 measurements
Vector mean = 6.8
Vector strength = 0.69
Resultant = 26.95
Radius = 8 measurememts

EXOTIC LIMESTONE BLOCKS

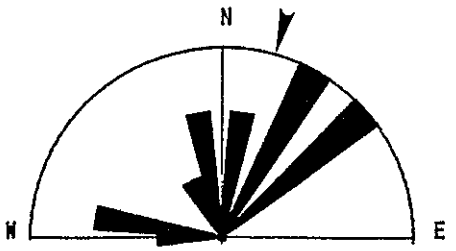

D) 15 measurements
Vector mean = 359.6
Vector strength = 0.71
Resulant = 10.69
Radius = 3 measurements

Plotted measurements show that the strike of bedding has a wide range of orientations. The difference in the mean vector directions for the 4 categories plotted is 17.7 degrees, between azimuths 359.6 and 17.3 . The largest directional size class for the middle and upper Dog Springs, and for the limestone exotic blocks of the middle Dog Springs all lie within the northeast quadrant of the rose diagram.

The rose diagrams show that the orientation of the slumped beds is variable. This variance is to be expected within a large area that has undergone slumping. Deformational structures, such as thrusted and folded beds, and an extensive detachment surface occurring between the lower and middle Dog Springs, suggest that the area occurs near the toe of slump sheets. Therefore, in conjunction with Lajoies (1972) observed orientation of bedding at the base of a slumped mass, there should be some predominant set of bedding orientations whose strike is perpendicular to the slope. A common preferred orientation among the largest directional size classes in three of the four cases tested is significant. It infers that the direction of slumping was controlled by a north to northeast-oriented paleoslope.

Diagenesis

Secondary mineralization is present within nearly all deposits comprising the Dog Springs Member. Secondary minerals include calcite, phyllosilicates, hematite, chlorite, quartz, heulandite, and celadonite.

Calcite occurs as a replacement mineral and void-filling cement. It is found within rock fragments and in the matrix of debris-flow and grain-flow deposits. It commonly replaces groundmass constituents of clasts, forming irregularly-shaped, raggedy-edged patches of microcrystalline to very fine-grained crystals. Occasionally it replaces plagioclase phenocrysts. It is also present as a void-filling cement consisting of an interlocking mosaic of sparry crystals. Calcite is by far the most abundant secondary mineral present in Dog Springs deposits.

Phyllosilicates are mostly associated with the matrix portion of the rocks. Minor amounts of sericitic alteration occur along fractures in some plagioclase phenocrysts or as a replacement of plagioclase microlites in the groundmass of lithic fragments. Petrographic examination of the matrix indicates the presence of sericite, illite (?) and smectite clays (?). These minerals occur as intergrowths or replacements of finely pulverized matrix constituents.

Chlorite occurs as a void-filling and replacement mineral. Void-filling chlorite is present as fibrous to thin platey crystals arranged perpendicular to the margins of microvesicles in some clasts (fig.26). It is also present as a replacement product, most often as aligned crystals within hornblende or biotite. The chlorite varies from colorless to pale green in plane polarized light.

Heulandite, a mineral in the zeolite group, is most prominent as a pore-filling cement in coarse-grained volcaniclastic sandstones of the lower Dog Springs. Colorless, euhedral, tabular crystals of heulandite are best developed where a large void space was originally present in the rock (fig.27).

Secondary silica is sporadically present throughout Dog Springs deposits. It generally occurs filling voids, either as a mosaic of anhedral crystals or as fibrous chalcedony. It is also present in clasts as blotchy accumulations of fine- to medium-grained crystals grading into cryptocrystalline groundmass. This crystal form is associated with porphyritic dacitic clasts found within middle Dog Springs deposits. Such silica may be of a deuteric origin.

Hematite occurs as an alteration product associated with the breakdown of magnetite and ferromagnesian minerals. It is also present as alteration halos around oxyhornblende

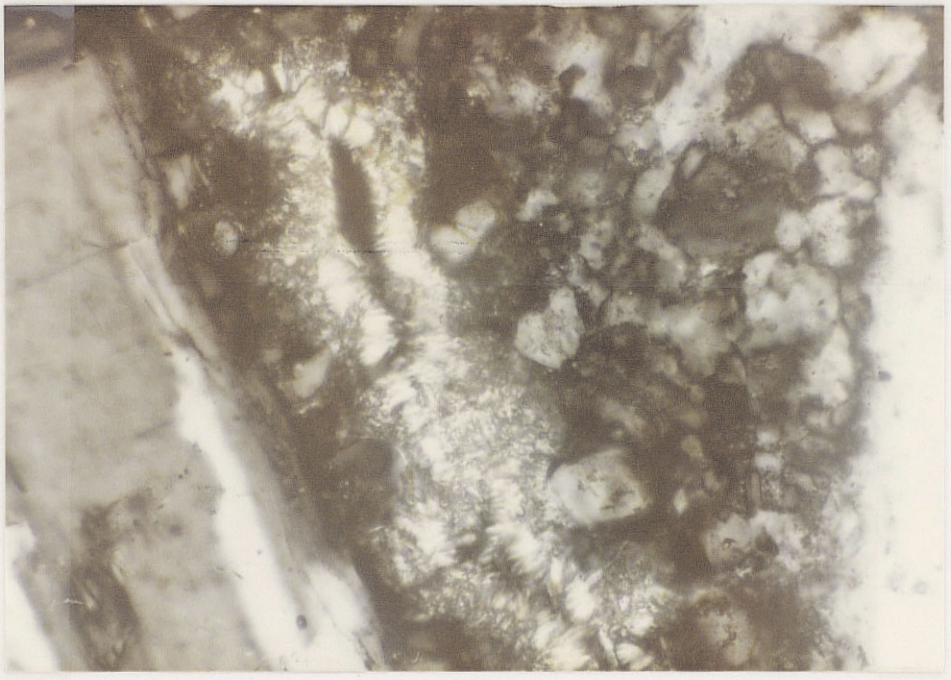

Figure 26. Photomicrograph of pore-filling chlorite in microvesicle of a volcanic clast from the upper Dog Springs map unit. Note the platey to fibrous chlorite is perpendicular to vesicle wall. Photo taken in cross-polarized light. Field of view between points A and B = 0.325 mm.

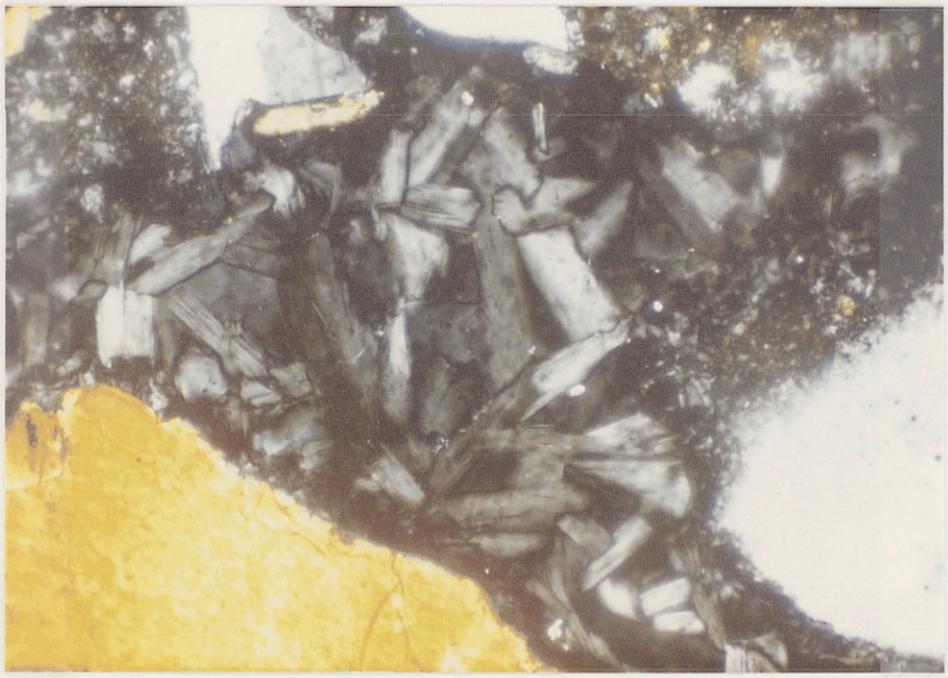

A B

Figure 27. Photomicrograph of tablular crystals of heulandite filling large pore space in volcanic lithic graywacke present in the lower Dog Springs map unit. Photo taken in cross-polarized light. Field of view between points A and B = 0.65 mm.

#104

and magnetite crystals. It is commonly found within the matrix of debris-flow breccias where finely pulverized and disseminated iron-bearing minerals have altered to hematite, imparting a murky deep-red to reddish-brown staining to the rock.

Celadonite, a variety of the mineral glauconite, is found as a vesicle-filling mineral in upper Dog Springs andesitic clasts. It occurs as pleochroic, yellow-green to lemon-yellow radially fibrous to vermicular crystals (fig.28). Granular anhedral crystals of epidote are present, but are very scarce. The epidote observed was associated with debris-flow deposits having a high degree of chloritization.

The secondary minerals present within the Dog Springs Member were probably precipitated during early burial diagenesis. Surdam and Boles (1979) report that carbonate, phyllosilicate, and zeolite cements precipitate during hydration reactions that occur in the early stages of diagenesis of volcaniclastic sediments.

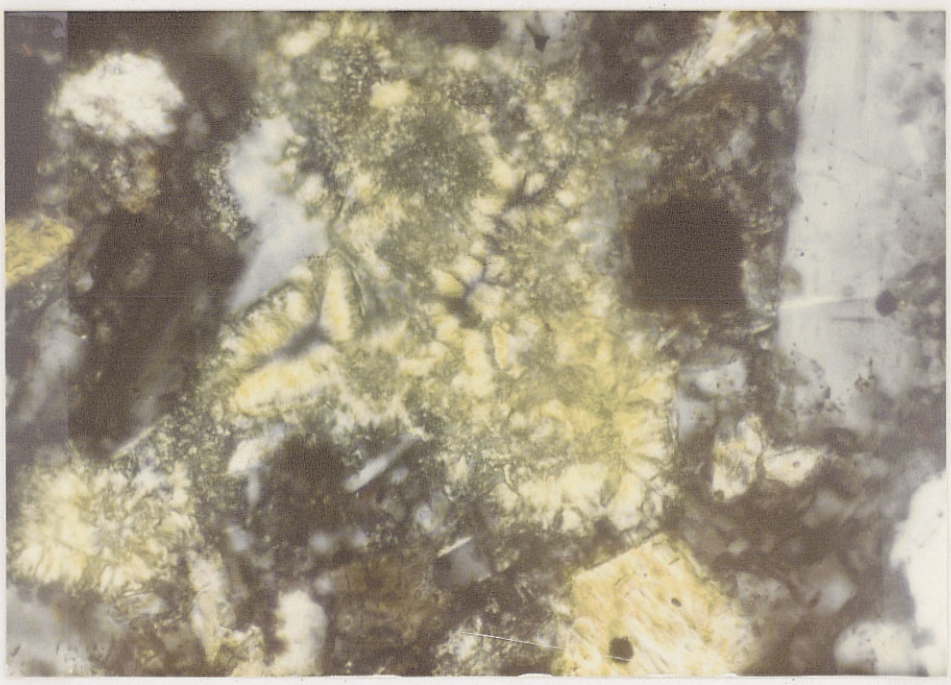

A B

Figure 28. Photomicrograph of vesicle-filling celadonite in andesite clast present in the upper Dog Springs map unit. Photo taken in cross-polarized light. Field of view between points A and B = 0.325 mm.

Chavez Canyon Member

The Chavez Canyon Member of the Spears Formation consists of a sequence of light brown to gray, volcaniclastic pebble to cobble conglomerates, sandstones, and minor debris-flow deposits. This unit lies within the stratigraphic interval above the Dog Springs Member and below the Rock House Canyon Tuff. The type section of the unit is located approximately 3.7 km west of the study area along Chavez Canyon (S1/2 sec. 27, T.2N., R.8W., unsurveyed, Dog Springs 7 1/2-min quadrangle). Within the area investigated, the Chavez Canyon Member conformably underlies the Rock House Canyon Tuff and rests with angular unconformity upon the Dog Springs Member. This unconformable relationship has been noted as far west as the Chinchbug Well area (N.E. 1/4 sec. 9, T.1N., R.9W.) by Harrison (1980). To the east, within the Bear Mountains, braided-stream deposits similar to, but finer grained than, those composing the Chavez Canyon are present (Massingill, 1979; Brown, 1972). These deposits are not stratigraphically restrained by rocks equivalent to the Dog Springs Member below, or Rock House Canyon Tuff above. To the southwest, in the Datil area, along White House Canyon, Bornhorst (1976) reports a 60 m section composed of feldspathic sandstone with minor interbedded pebble conglomerate comformably overlying mudflow breccia deposits.

These volcaniclastic rocks underlie the Datil Well Tuff. South-southeast of the study area, in the southern Gallinas Mountains (Chamberlin, 1974) and Tres Montosas area (Wilkinson, 1976), rocks with characteristics similar to those of the Chavez Canyon Member occur underlying the Tuff of Nipple Mountain (Rock House Canyon Tuff). An underlying unit equivalent to the Dog Springs Member is apparently not present in these areas, although exposures of the lower Spears are very limited.

The Chavez Canyon Member varies laterally in thickness. Cross-sectional measurements indicate a west to east thickness change from approximately 60 m near the southwest corner of the study area to 249 m in the southeast. An anomalously thin, poorly exposed, 24-m-thick section of the unit occurs within the upper portion of the hill 300 m northwest of Long West Windmill. Construction of an east-trending long section, based on a composite of north- to north-northeast-trending cross-sections, illustrates thickness changes in the unit (fig.29). The consistency in thickness along strike of the overlying Rock House Canyon Tuff, indicates that the tuff was deposited on a relatively planar surface. Therefore, the base of this ash-flow tuff was used as a datum in the construction of the long section. The geometry of the Chavez Canyon is that of a laterally thinning-and-thickening deposit, most probably resulting from the infilling of broad areas of low relief present on

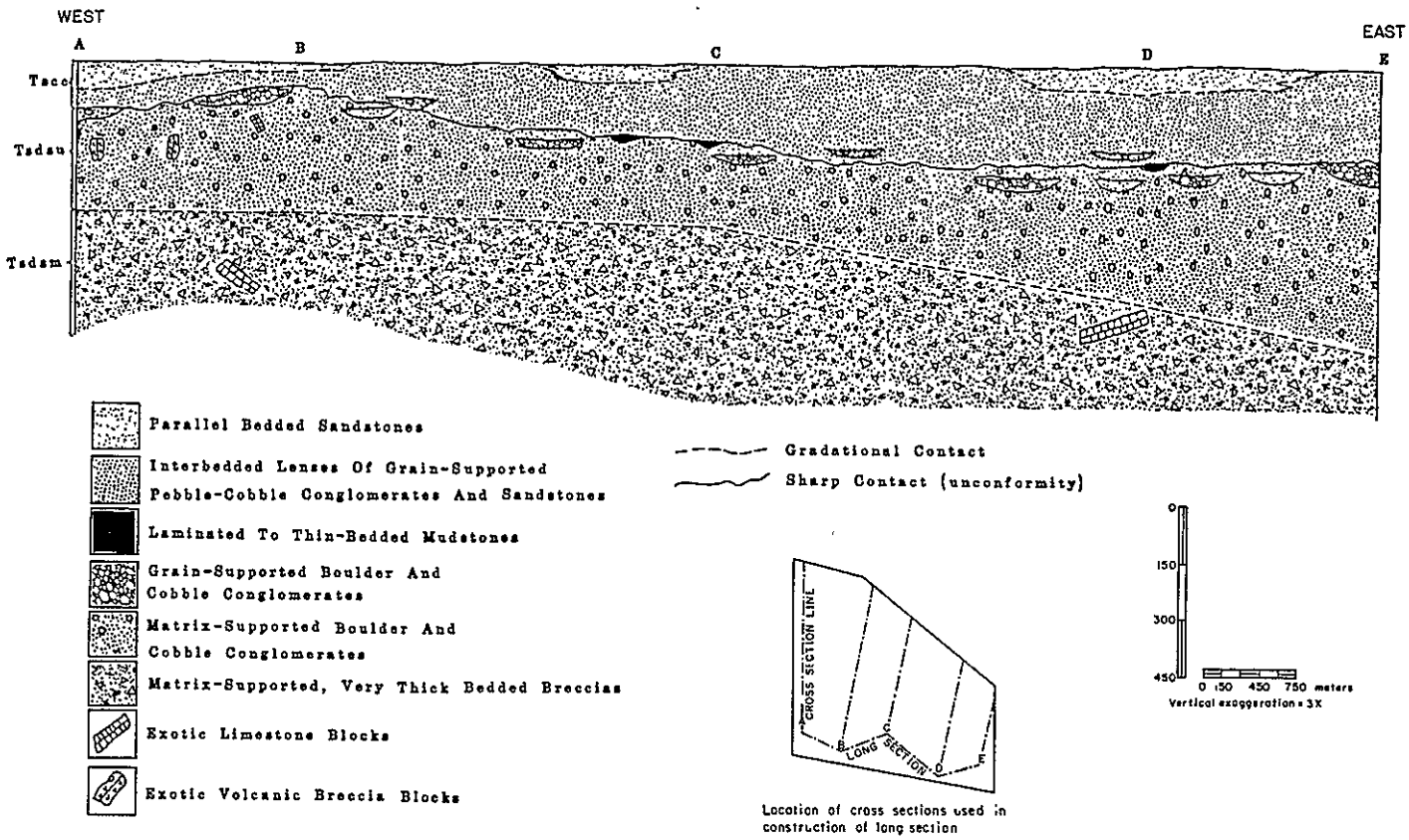

Figure 29. Long Section illustrating thickness and lithologic variations in the Chavez Canyon Member (Tscc) and middle (Tsdsm) and upper (Tsdsu) Dog Springs map units.

the upper surface of the Dog Springs Member.

Exposures of the Chavez Canyon Member in the study area are scattered. Generally the unit underlies extensive talus, colluvium and landslide deposits from superjacent ash-flow tuff deposits. The best exposures of the unit occur where steep erosional hillside scarps are present. The lower part of the Chavez Canyon, where exposed, consists of interbedded lenses of volcanic conglomerates, sandstones and occasional debris-flow deposits. One of the best outcrops of a complete section of the Chavez Canyon Member occurs at the end of the canyon running directly south of the old Baca Homestead. Plane-bedded, medium-grained, moderate- to well-sorted, volcaniclastic sandstones containing occasional lens-shaped volcanic conglomerates, occupy the lowest 15 m of the section. Above this is approximately 185 m of interbedded, lens-shaped, clast- and matrix-supported, pebble to cobble conglomerates and sandstones. Sandstones have planar bedding or low-angle cross-stratification. Sandstone beds generally pinch out in 12 to 15 m laterally. They are subordinate to conglomeratic deposits and comprise approximately 20-30 percent of the section. Conglomeratic beds are lens-shaped with large length-to-thickness ratios. Some conglomeratic lenses measure 75 m across, with a thickness of only 9 to 12 m. Lower surfaces of these conglomerates are planar to broadly concave upward, indicating that very little scouring

occurred prior to deposition. This thick sequence of interbedded conglomerates and sandstones make up the main body of the Chavez Canyon Member (fig.30). Twenty-five pebble and cobble imbrication directions were measured at several points along this portion of the section and indicate a north to northeast paleoflow direction.

Clast sizes in conglomeratic beds range from pebbles to boulders on the Wentworth scale. Clasts consist predominantly of dark, subrounded to rounded, porphyritic to microporphyritic, andesitic to dacitic rocks similar to those present in the upper portion of the upper Dog Springs Member. Also present are lighter colored porphyritic hornblende and biotite bearing dacitic clasts characteristic of middle Dog Springs deposits. These clasts are white to light blue to green in color and occur in an intensely weathered, very friable condition. Several other clast types are sporadically present. Subordinate clast types include: pebble- to cobble-sized clasts of a flow banded dark-gray-and-black vitrophyre, granite, and brownish-red highly vesicular rocks.

The upper part of the Chavez Canyon is laterally variable in lithology. It consists of a sequences of plane-bedded volcaniclastic sandstones or interbedded sandstones and conglomerates, similar to underlying lithologies. Sequences composed predominantly of sandstones

Figure 30. Photograph of interbedded volcaniclastic pebble-cobble conglomerates and sandstones comprising the main body of the Chavez Canyon Member. Sandstone beds are less resistant to weathering and are inset into the bluff. Hammer for scale at lower right center of photo. South-facing exposure approximately 1.2 km west of Long West Windmill.

consist of light-gray, thin- to very thin-bedded planar strata, occasionally separated by laminated mudstones and siltstones. Sparse scour surfaces with 15-20 cm of relief are filled by low angle cross-stratified beds.

Sandstones present in the Chavez Canyon Member generally consist of medium- to very coarse-grained, angular to subangular grains of feldspar, hornblende, biotite, pyroxene, volcanic lithic fragments and minor amounts of sanidine and quartz. Lithic fragments are mainly composed of clinopyroxene and hornblende bearing andesitic to dacitic rocks with similar petrographic characteristics as noted in the upper Dog Springs Member. In the upper portion of the Chavez Canyon Member, clasts containing ferromagnesian phenocrysts of pyroxene and olivine replaced by iddingsite are present. Petrographically, these sandstones can be classified as lithic arkoses and feldspathic litharenites (Folk, 1974, p.129). Calcite acts as the main cementing agent in the rocks with lesser hematite, phyllosilicate, silica and zeolite cements. In general, the rocks that compose the Chavez Canyon Member contain less matrix and more pore space than those of the Dog Springs Member. Some sandstones present within the Chavez Canyon Member have porositys of 10-15 percent.

Depositional model

Pebble and cobble imbrications indicate a north to northeast flow-direction during deposition of the Chavez Canyon Member. A cross-sectional profile, nearly perpendicular to this flow direction, (fig.29) shows that the Chavez Canyon was deposited on a surface with considerable relief. A sharp angular unconformity and contrast in sedimentologic character exists between deposits of the Dog Springs and Chavez Canyon Members. The contact between these two units represents a discrete change in depositional processes from debris-flow deposition characterizing the Dog Springs Member to fluvial sedimentation during Chavez Canyon time. A short-lived, volumetrically small component of debris-flows were deposited during the initial phase of Chavez Canyon sedimentation.

Lateral thinning and thickening of Chavez Canyon deposits indicates that initial sedimentation occurred in low-lying areas on the upper Dog Springs surface. When infilling of depressions was completed a laterally contiguous surface of deposition developed. The interbedded lens-shaped conglomerates and sandstones composing the main body of the Chavez Canyon Member are similar in sedimentologic character to mid-fan deposits of the Van Horn

Sandstone in Texas (fig.31A). Mid-fan deposits of modern braided outwash fans in glacial areas (fig.31B) also show similarities with respect to bedforms and grain size as deposits preserved in the Chavez Canyon Member. Initial Chavez Canyon deposition was probably largely controlled by Dog Springs topography. Braided streams followed and eventually filled low-lying areas. With time, a laterally contiguous surface of deposition evolved. At this point, an expansive plain of braided streams or coalescing braided alluvial fans dominated the system.

Basaltic andesite flow

Within the southwest corner of the map area, on hilltop 8152, south of the Long West Windmill, a remnant of a basaltic-andesite flow(s) is present. This flow lies above the Chavez Canyon Member and below the Rock House Canyon Tuff. A north- to north-northwest-trending, high-angle normal fault, displaces the flow. A portion of the flow caps the hilltop on the western, up-thrown side of the fault, with the basal 1.5 to 3 m of the Rock House Canyon Tuff lying above the flow on the eastern down-thrown side of the fault. The flow(s) is approximately 12 m in thickness. No other outcrops of this unit were noted during mapping, either because the flow is not present or because talus and landslide deposits are covering it.

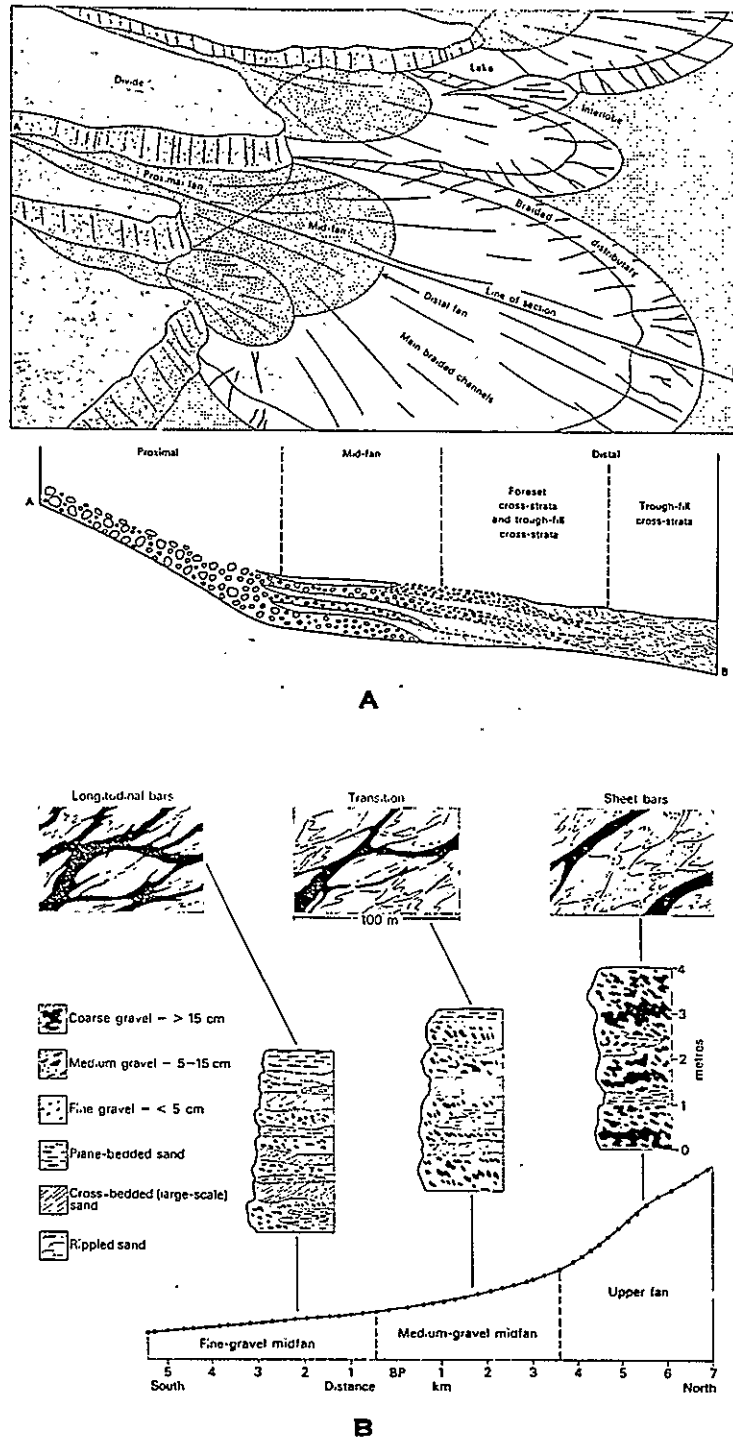

Figure 31. Longitudinal profiles of alluvial fan deposits. A) Distribution of facies and environments in humid alluvial fan deposits of the Van Horn Sandstone, Texas (After McGowen and Groat, 1971). B) Changes in bar type, slope and structure along a braided outwash fan (After Boothroyd, 1972).

In hand sample, a fresh surface of the rock is medium gray (N 5) to medium bluish-gray (5 B 5/1), weathering to a pale yellowish-brown (10 YR 6/2). Chalky to clear, euhedral to anhedral plagioclase phenocrysts stand out on weathered surfaces. Some of these phenocrysts have long dimensions of up to 6 mm. Iron oxide replaced olivine occurs as orange-brown specks, contrasting against the drab gray color of the groundmass. Occasionally calcite amygdules are present.

Petrographically, the rock has a porphyritic to seriate texture. The groundmass is nearly holocrystalline, containing only a trace to 1 percent glass. Plagioclase microlites present are disposed in a subparallel manner. Groundmass constitutes consist of in decreasing order of abundance, plagioclase, opaque oxides, clinopyroxene and orthopyroxene.

Plagioclase, clinopyroxene, olivine, and opaque oxides occur as phenocrysts. Plagioclase phenocrysts compose about 10-15 percent of the rock. They are characterized by a sieve texture and often have irregularly shaped, resorbed crystal margins (fig.32). Inclusions of opaque oxides and clinopyroxene are present in some grains. Plagioclase phenocrysts occur both as single crystals and glomeroporphyritic accumulations. Crystals are commonly zoned in combination with carlsbad and albite twinning.

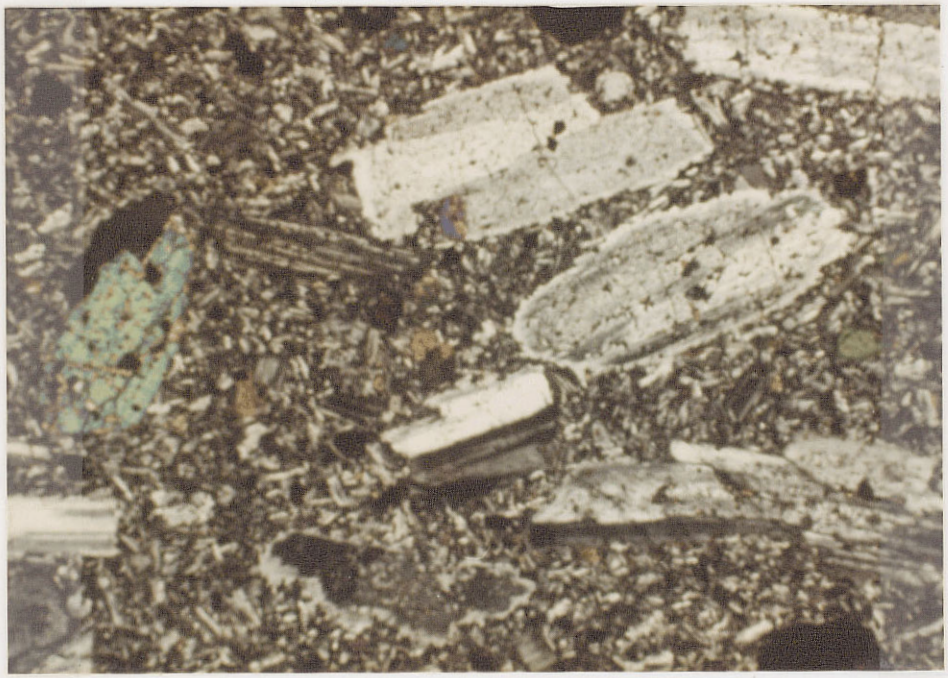

A B

Figure 32. Photomicrograph of basaltic andesite from flow which locally overlies the Chavez Canyon Member. Note sieve texture and resorbed crystal margins on plagioclase phenocrysts. Photo taken in cross-polarized light. Field of view between points A and B = 6.5 mm.

Plagioclase has an Anorthite content of 52 (maximum value from 5 grains, Michel-Levy method). Clinopyroxene phenocrysts compose approximately 6 percent of the rock. Crystals range from 3 mm in longest dimension to groundmass-sized constituents. Approximately 2 percent of the rock is composed of subhedral to anhedral opaque oxide phenocrysts. Opaque oxides increase in amount to 4-5 percent within the groundmass. Relict olivine occurs as phenocrysts composing about 2-3 percent of the rock by volume. The olivine has been replaced by iddingsite/hematite and commonly has an opaque outer rim with a core which is reddish-brown to golden-brown in color.

This flow represents the most northern known occurrence in the Gallinas Mountains of similar flows that occur at approximately the same stratigrahic level. To the south, Laroche (1981), Chamberlin (1974) and Wilkinson (1976) describe a "turkey-track" andesite lying below the Tuff of Nipple Mountain (Rock House Canyon Tuff). Chamberlin also found andesitic flows interbedded within the overlying ash flow tuff. To the east, in the southern Bear Mountains, Brown (1972) used a blue-gray amygdaloidal turkey track andesite flow below the Tuff of Nipple Mountain as the base of the upper member of the Spears. To the southwest, in the Datil area (Lopez, 1975; Bornhorst, 1976) a porphyritic andesitic flow underlies the Datil Well Tuff and overlies a feldspathic sandstone member of probable equivalence to part

of the Chavez Canyon Member.

Rock House Canyon Tuff

The Rock House Canyon Tuff is a poorly to moderately welded, crystal-poor, moderately pumiceous, rhyolite ash-flow tuff. The unit lies within the stratigraphic interval above the Chavez Canyon Member of the Spears Formation and below the Rincon Windmill Member. The type section of the Rock House Canyon Tuff is located approximately 1 km from the southwest edge of the study area, at the junction of Rock House Canyon and Long Canyon (SW 1/4 sec. 13, T.1N., R.8W., unsurveyed Dog Springs 7 1/2 min quadrangle). This unit is regionally extensive and is correlative to the west and southwest with the tuff of Rock House Canyon (Coffin, 1981) and the tuff of Main Canyon (Lopez, 1975; Bornhorst, 1976; Harrison, 1980), and to the east and southeast with the tuff of Nipple Mountain (Brown, 1972; Chamberlin, 1974; Wilkinson, 1976; Laroche, 1981). Because of its lateral persistence and excellence as a marker bed, earlier investigators in the region used the Rock House Canyon Tuff (tuff of Nipple Mountain) to divide the Spears into upper and lower members.

No age date is available at this time on the unit. Based on known outcrop and thickness patterns Harrison (1980) proposed a possible source area for the unit beneath the eastern Plains of San Agustin or further south.

Within the southwest portion of the study area the Rock House Canyon Tuff is exposed as highly jointed cliff faces and extensive dip-slope surfaces. Exposures within the southeast portion of the map area are largely obscured by talus and landslide deposits. The unit has a relatively consistent thickness, varying from approximately 60-72 m.

Within the study area the Rock House Canyon Tuff is a multiple-flow, simple cooling unit. The lower 9-12 m of the tuff weathers to a flaggy grus. A fresh surface of this basal portion is light brownish-gray (5 YR 6/1), weathering to pinkish gray (5 YR 8/1). The main body of the unit weathers in a blocky to massive manner. A fresh surface on the rock is very light gray (N8), weathering to light brown (5 YR 6/4).

The basal flaggy-weathering part of the unit is poorly welded but well indurated. In thin-section, it is composed of approximately 2-3 percent phenocrysts of sanidine, plagioclase and biotite. Sanidine is most abundant, comprising about 1-2 percent of the rock. It occurs as 0.2-1.5 mm, subhedral to anhedral crystals which often have embayed margins. Carlsbad twinning is common. Plagioclase

is present in trace amounts to approximately 1 percent of the rock. It often has corroded or deeply embayed crystal margins. Both single crystals and glomeroporphyritic accumulations occur. Combined albite and carlsbad twinning is common. Trace amounts of biotite are present. These crystals commonly have subhedral crystal outlines. Subrounded to angular volcanic lithic fragments with seriate to microporphyritic textures occur in trace amounts. Lithic fragments are predominantly composed of plagioclase with lesser biotite and magnetite. Pumice, glass bubbles and shards are well preserved, showing little compaction in this lower portion. Spheriolite and axiolite development is common.

The basal well-indurated portion of the Rock House Canyon Tuff grades upward to a poorly to moderately welded upper section. This upper section composes approximately 85 percent of the unit. Crystal and lithic content remain approximately the same as in the basal portion. The amount and size of pumice increases slightly upsection, with uncompressed pumice, 2-3 cm in size, present at the top of the unit. Primary pumice structure is preserved in some instances, whereas, spheriolite development has destroyed it in others. Groundmass constituents range from partly devitrified, with glass shards displaying axiolitic textures, to pervasively devitrified with the development of a granular texture.

Rincon Windmill Member

Within the study area, the Rincon Windmill Member of the Spears Formation consists of light brownish-gray to moderate reddish-orange volcaniclastic sandstones and conglomerates. This unit is present as noncontinuous exposures ranging in thickness from a maximum of approximately 37 m to a minimum of 12 m. Rocks composing the unit are poorly to moderately indurated, generally forming talus covered slopes. Landslide, talus and colluvium from overlying ash-flow tuffs generally cover exposures at this stratigraphic level.

The type section of the Rincon Windmill Member is located approximately 8 km west of the southwest corner of the study area, 2 km north-northwest of Rincon windmill (NW 1/4, NW 1/4, sec. 18, T.1N., R.8W., unsurveyed Dog Springs 7 1/2 min quadrangle). At the type section, the Rincon Windmill can be divided into two separate units by the interlayered Blue Canyon Tuff. The interval below the Blue Canyon Tuff consists of volcaniclastic sandstones and pebble to cobble conglomeratic beds. The interval above the Blue Canyon is predominantly composed of fluvial volcaniclastic sandstones, overlain by 10.5 m of eolian sandstones. Mapping by Harrison (1980) and Coffin (1981) showed the interlayered Blue Canyon Tuff to be discontinuous, and

combined the upper and lower portions of the Rincon Windmill into a single unit. The Blue Canyon Tuff is also discontinuously present is this study area. When present, it overlies exposures of the Rincon Windmill. A thin, laterally discontinuous sequence of volcaniclastic sandstones overlies the Blue Canyon Tuff within the southwestern part of the map area, but is not at a mappable scale.

The Rincon Windmill Member is stratigraphically correlative to Tdh2 of Givens (1957), the middle sedimentary unit of Lopez (1975), the second volcanic sedimentary unit of Bornhorst (1976), the middle sedimentary unit of Harrison (1980), and the middle volcaniclastic rocks of Coffin (1981). The sequence of eolian and fluvial sandstones which comprise the upper part of the Rincon Windmill above the Blue Canyon Tuff, as described by Bornhorst, Harrison and Coffin, is not present in the study area. The Rincon Windmill Member shows a rapid decrease in thickness from the Datil Mountains-northwest Gallinas Mountains area, into the northeast Gallinas Mountains. Lopez (1975), Harrison (1980) and Coffin (1981) report a maximum thickness for the Rincon Windmill of 130-150 m. A maximum exposed thickness of 37 m is present in this study area.

Within the map area, the Rincon Windmill conformably overlies the Rock House Canyon Tuff. It underlies the Blue Canyon Tuff conformably and Hells Mesa Tuff disconformably. The unit consists of a sequence of interbedded volcaniclastic sandstones and pebble to cobble conglomerates. Occasional boulder-sized material is present within channel-lag deposits. Bedforms vary from thin to thick planar-beds, to medium-scale low angle cross-stratified beds. Volcaniclastic sandstones are poorly sorted, containing subangular to subrounded grains and lithic fragments. Lithic fragments consist of aphanitic and porphyritic intermediate to basaltic rocks. Occasional ash-flow tuff clasts are also present. Grains consist of hornblende, clinopyroxene, plagioclase, and biotite.

This unit shows a change in color as traced laterally through the area. In the southwest portion of the study area it is light brownish gray (5 YR 6/1), changing to a moderate reddish orange (10 R 6/6) in the southeast. This color change is associated with an increase in limonite which acts as a stain, and as a cementing agent for the sediments present in the southeast (fig.33). Other cementing agents include calcite, silica, and phyllosilicates.

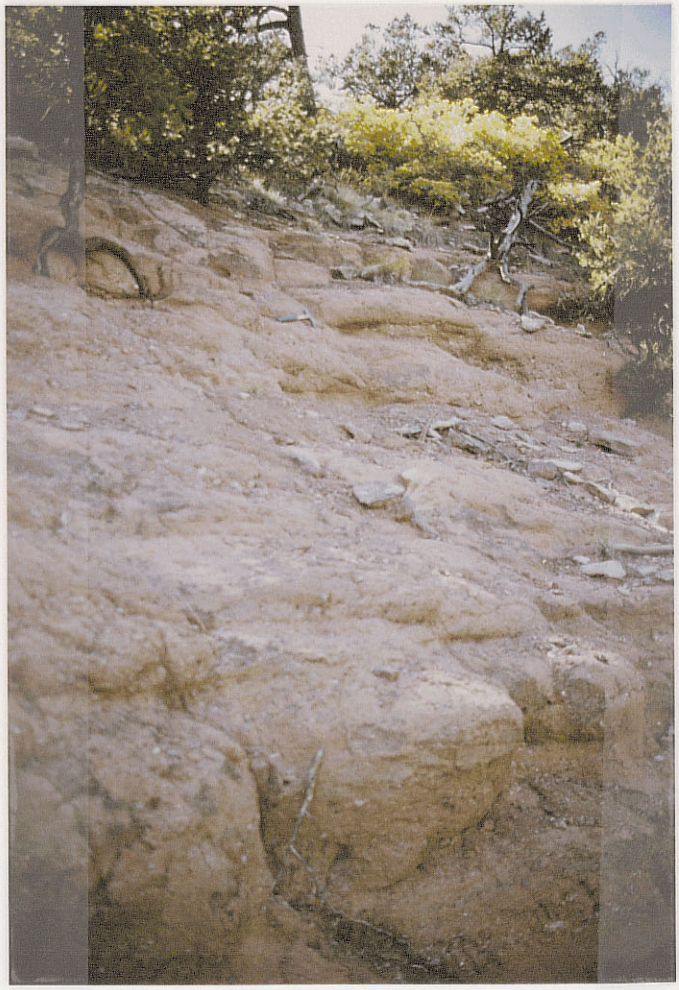

Figure 33. Photograph of limonite-stained sandstone and conglomerate beds of the Rincon Windmill Member. North-facing exposure on Indian Mesa, approximately 2 km south-southwest of North Basin Well.

#126

It is interpreted that this sequence of interbedded volcaniclastic sandstones and conglomerates represents a continuum of mid-fan or braided plain alluvial sedimentation which began during deposition of the Chavez Canyon Member. Sedimentation was interrupted in the area during emplacement of the Rock House Canyon Tuff.

Blue Canyon Tuff

The Blue Canyon Tuff is a poorly to moderately welded, crystal-rich, biotite-rich, quartz-poor, quartz-latite tuff. This unit is the uppermost ash-flow tuff present in the study area that is part of the Datil Group. Three radiometric dates are available on the unit from samples collected in the Datil area. Dating by the K-Ar method on biotite yielded ages of 33.3 $\pm$ 1.2 my and 29.7 $\pm$ 2.2 m.y.B.P (Osburn and Chapin, 1983); fission track dating of zircon yielded an age of 32.2 $\pm$ 1.7 m.y.B.P. (Bornhorst and others, 1982). The type section of the Blue Canyon Tuff is located approximately 20 km west-southwest of the southern corner of the map area and 11 km north of Datil, near the junction of Blue Canyon and Main Canyon (NE 1/4, SE 1/4, sec. 1, T.1S., R.10W., Cal Ship Mesa 7 1/2 min quadrangle).

The Blue Canyon Tuff is correlative to the lower part of unit Tdh3 of the Hells Mesa member (Givens, 1957), the quartz-latite tuff of Blue Canyon (Bornhorst, 1979; Lopez and Bornhorst, 1976), the tuff of Blue Canyon (Lopez, 1975; Harrison, 1980; Coffin, 1981), and map unit Tst2 of the Spears formation (Mayerson, 1979). A maximum thickness of 50 m is reported for the unit in the southwest Crosby Mountains (Bornhorst, 1976). Within the study area it is present as 0 to 12-m-thick exposures. Mayerson (1979) reports a thickness of 4.6 m or less, for isolated remnants of the unit present just east of the study area in the Corkscrew Canyon-Adobe Spring area.

Within the area mapped for this study, the Blue Canyon Tuff is poorly exposed. Outcrops of the unit consist of a slightly more resistant, minor ledge above conglomeratic to sandy beds of the Rincon Windmill Member and below the Hells Mesa Tuff. A fresh surface of the Blue Canyon Tuff is pinkish gray (5 YR 8/1) to very light gray (N 8), weathering to a moderate yellowish-brown (10 YR 6/2). Crystal content in the unit ranges from approximately 13-17 percent, consisting of 5-6 percent plagioclase, 3-4 percent biotite, 3-4 percent sanidine, 1-2 percent hornblende, and a trace to 1 percent opaque oxides. Lithic fragments and pumice are conspicuous components. Orange to reddish-brown, subrounded to rounded, volcanic lithic fragments, 0.5-4 mm in size, compose approximately 1-2 percent of the rock.

Approximately 4-5 percent of the rock is composed of slightly compressed to round pumice.

In thin-section, plagioclase occurs as subhedral to anhedral crystals, 0.5-2 mm in size. Albite and carlsbad twinning are most common; zoned crystals are less abundant. A plagioclase compostion of An 36 was obtained from 10 grains from two thin-sections (Michel-Levy method). Pleochroic greenish-yellow to deep brown-red biotite is present, generally as euhedral crystals 0.5-2 mm in size. Euhedral to subhedral, 0.5-1 mm hornblende has pleochroic yellow-orange to orangish-red colors. Sanidine occurs as subhedral to anhedral crystals, 0.5-1 mm in size.

Hells Mesa Tuff

The Hells Mesa Tuff is a moderately to densely welded, crystal-rich, moderately quartz-rich, quartz-latite to rhyolite ash-flow tuff. This unit is regionally extensive within the northeastern Mogollon-Datil volcanic field except within the southern Chupadera Mountains and northern Jornado del Muerto (Osburn and Chapin, 1983). Tonking (1957) originally defined the Hells Mesa Member of the Datil Formation for exposures of vitric rhyolite tuffs that occur below the La Jara Peak Member in the eastern and northern Bear Mountains. Chapin (1971) raised the Hells Mesa Tuff to

formational status. The Hells Mesa Tuff has more recently been defined as the crystal-rich, quartz-rich, lower portion of Tonking's (1957) original Hells Mesa Member (Chapin and others, 1978; Osburn and Chapin, 1983) and is correlative to: map unit Tdh4 and the lower portion of Tdh5 of the Hells Mesa Member (Givens, 1957); the tuff of Goat Springs (Brown, 1972); the tuff of Ary Ranch, and tuff of Rock Tank (Lopez and Bornhorst, 1979).

The type section of the Hells Mesa is located in the northeastern Bear Mountains approximately 0.4 km southwest of Bluff Springs (center of side common to sec. 36, T.2N., R.5W. and sec. 31, T.2N., R.4W., Mesa Cencerro 7 1/2 min quadrangle). seventeen radiometric dates derived by K-Ar, fission track and 40Ar/39Ar methods are presently available for the Hells Mesa Tuff. The 40Ar/39Ar dates are the most accurate and indicate an age of about 32.2 m.y.B.P. (Laura Kedzie, 1984, oral commun.) The source for the unit has been established as the Socorro cauldron (Eggleston, 1982; Osburn and Chapin, 1983).

Within the study area, the Hells Mesa Tuff is disconformable with the underlying Blue Canyon Tuff or Rincon Windmill Member of the Spears, and the overlying La Jencia Tuff. The unit characteristically weathers in a flaggy to slabby manner along foliated surfaces (fig.34). Vertical jointing contributes to the formation of boulder

Figure 34. Photograph of typical weathering character of the Hells Mesa Tuff. Note weathering of slabby to flaggy blocks which form extensive talus deposits. North-facing exposure present at the top of Indian Mesa.

size blocks which often form extensive talus and landslide deposits. The Hells Mesa Tuff forms the main cap rock at the top of the extensive erosional escarpment present in the southeastern portion of the map area. Weathered exposures of the unit form gentle dip slopes or rounded hills when capped by the overlying La Jencia Tuff.

The Hells Mesa Tuff changes in thickness from a maximum of approximately 153 m in the south-central and southeast portion of the map area to 12 m in the southwest. The subjacent Rock House Canyon Tuff or Rincon Windmill Member display no major changes in thickness or discontinuity in lateral extent. The reduction in thickness of the Hells Mesa Tuff in the southwest portion of the map area is believed to have been caused by post-emplacement erosion. Documentation of a 3-m.y. hiatus between eruption of the Hells Mesa Tuff and the overlying La Jencia Tuff (Laura Kedzie, 1984, oral commun.) and observations of post-Hells Mesa--pre-La Jencia Tuff erosional channels (Wilkinson, 1976; Mayerson, 1979; Coffin, 1981) indicate a regional unconformity at this stratigraphic level. The presence of the overlying La Jencia Tuff above both thin and thick exposures of the Hells Mesa Tuff indicates that the thickness change is not the product of more recent erosion.

In hand sample, the main body of the Hells Mesa Tuff is pale red (5 R 6/2) in color, with grayish-red (5 R 4/2) compressed and foliated pumice. Phenocrysts comprise approximately 40-45 percent of the rock. Plagioclase and sanidine are most abundant, with lesser biotite, hornblende, quartz and opaque oxides. Copper-colored biotite and clear to smoky quartz are conspicuous components of the rock.

Quartz increases in abundance upsection. Exposures of the basal 9-12 m contain 0 to trace amounts of quartz, increasing to 3-4 percent for the main portion of the unit and 8-10 percent for the uppermost 12-15 m. This upper, relatively quartz rich, 12-15 m of the Hells Mesa Tuff is only preserved where it underlies the La Jencia Tuff in the south-central to southeast portion of the study area. The increase in quartz noted for the top of the unit is accompanied by a change from pale-red slabby weathering rocks, to very light-gray (N 8) to pinkish-gray (5 YR 8/1) massive to blocky weathering exposures. This uppermost portion is poorly to moderately welded with slightly compressed white to very light-gray pumice, as large as 2-3 cm in maximum diameter. Drusy vapor-phase minerals are often present in open spaces.

In thin section, plagioclase and sanidine occur in near equal amounts, each comprising approximately 15-17 percent of the rock. Plagioclase commonly occurs as euhedral to

subhedral laths, 0.5-2.5 mm in size. Most crystals have combined albite and carlsbad twinning; zoned crystals are less abundant. The compostion of plagioclase is approximately An 28 (from 13 grains in 3 thin-sections; Michel-Levy method). Sanidine is present as 0.1-2 mm subhedral to anhedral crystals. It occurs both as untwinned and carlsbad twinned crystals, many of which are fractured or have deeply embayed margins.

Biotite, hornblende, quartz, and opaque oxides comprise the remainder of the phenocryst population. About 2-5 percent, strongly pleochroic, yellow-red-brown to dark orange-red biotite is present in the rock. Crystals are euhedral to subhedral, with some having broken ragged margins. Some biotite is almost totally replaced by opaque oxides. Hornblende is present from trace amounts to about 2 percent of the rock. Euhedral to subhedral, 0.5-1.5 mm hornblende crystals have a lime-green to yellow-brown pleochroism. Quartz often has an idiomorphic hexagonal shape, with rounded corners and straight or embayed crystal margins. Opaque oxides comprise 1-3 percent of the rock, occurring in a wide range of sizes, but generally not exceeding 1.5 mm in maximum diameter.

The original glassy components present in the groundmass of the Hells Mesa tuff are moderately to densely welded. Pumice fragments vary in shape from slightly

compressed to length-to-width ratios as much as 6/1. Well-developed axiolitic and spheriolitic devitrification minerals normally completley fill former pumice. Crystals present in relict pumice are extremely deformed. Biotite grains are often bent or broken, with plagioclase and sanidine occurring in a shattered state. Glass shards present in the groundmass are compressed and distorted and completely devitrified. Some rap around crystals, resulting in a pseudoflow texture. A fine dissemination of reddish-brown interstitial opaque oxides in the groundmass imparts a reddish color to the rock.

La Jencia Tuff

The La Jencia Tuff consists of poorly to moderately welded, crystal-poor, quartz-poor, one feldspar rocks which form a multiple-flow, compound-cooling unit. The La Jencia Tuff is the new name proposed by Osburn and Chapin (1983) for what has been referred to previously as the lower member of the A-L Peak Tuff. The unit is present throughout the northeastern Mogollon-Datil volcanic field. The type locality for the La Jencia Tuff is located along the west side of the La Jencia Basin in the southern Bear Mountains, approximately 26 km southeast of the study area (NW 1/4 sec. 22, T.1S., R.4W., Magdalena NW 7 1/2 min quadrangle). The type section of the La Jencia Tuff is the lower cooling unit

of Brown's (1972) tuff of Bear Springs. The lower tuff of Bear Springs was miscorrelated by Deal (1973), Chapin and Deal (1976) and Deal and Rhodes (1976) to a 600 to 700-m-thick sequence of tuffs exposed on A-L Peak in the northern San Mateo Mountains. This resulted in the introduction of the stratigraphic term A-L Peak Tuff and its use by subsequent workers in the region who used Brown's (1972) lower tuff of Bear Springs for correlation purposes. Therefore, to avoid further confusion, it has been proposed by Osburn and Chapin (1983) that the term A-L Peak Tuff be abandoned, and Brown's lower tuff of Bear Springs be renamed the La Jencia Tuff.

The La Jencia Tuff is equivalent to the middle portion of Tonking's (1957) Hells Mesa member, Tdh5 and most of Tdh7 as mapped by Givens (1957) within the study area, Chamberlin's (1974) lower cooling unit of the A-L Peak Formation, Lopez's (1975) and Bornhorst's (1976) A-L Peak Rhyolite Tuff, Wilkinson's (1976) A-L Peak Tuff, Coffin's (1981) and Laroche's (1981) lower cooling unit of the A-L Peak Tuff, and Harrison's (1980) lower member of the A-L Peak Formation. The unit was erupted from the contemporaneous Sawmill Canyon and Magdalena cauldrons (Chapin and others, 1978; Petty, 1979; Bowring, 1980; Osburn and Chapin, 1983). The age of the La Jencia Tuff was formerly estimated to be about 31 m.y., based on a 30.9 $\pm$ 1.5 m.y. K-Ar whole rock date on the basaltic andesite of

Deep Well (Twin Peaks) that overlies the unit (Osburn and Chapin, 1983). However, recent 40Ar/39Ar dating by Laura Kedzie (1984, oral commun.) indicates an age of approximately 29 m.y.B.P. for the La Jencia Tuff. Two K-Ar biotite dates of 29.7 $\pm$ 1.1 m.y. and 30.2 $\pm$ 1.1 m.y. from associated tuffs present within the cauldron-fill of the Sawmill Canyon cauldron (Osburn and Chapin, 1983) are in reasonably good agreement with the 40Ar/39Ar dates.

Within the study area the La Jencia Tuff is present as remnants on isolated hilltops. The unit weathers to slabby to blocky talus covering rounded hills. It is disconformable with the underlying Hells Mesa Tuff and overlying Vicks Peak Tuff. The unit is approximately 40-43 m thick along the south-central margin of the map area where it is capped by the Vicks Peak Tuff. It thins or has been removed by erosion to the east and west. The contact of the unit with the overlying Vicks Peak Tuff was mapped at the occurrence of a red-to-brown vitrophyre present at the top of the La Jencia Tuff. This vitrophyre has also been noted by Harrison (1980) in outcrops of the unit to the west. Exposures of the La Jencia and Vicks Peak Tuffs to the west are separated by basaltic-andesite flows of Deep Well (formerly basaltic andesite of Twin Peaks; see Osburn and Chapin, 1983), or a discontinuous sequence of volcaniclastic rocks (Coffin, 1981). Mafic flows are present separating these two units to the south and east of the study area.

These flows, referred to as the La Jara Peak Basaltic Andesite, have been noted by Chamberlin (1974), Wilkinson (1976) and Laroche (1981) to the south, and by Brown (1972) and Mayerson (1979) to the east.

Where a complete section of the La Jencia Tuff is present in the area mapped for this study, the unit contains an upper vitrophyre and a lower vitrophryic to densely welded zone. The lower vitrophyric to densely welded zone is discontinuous and is not present in the southwest corner of the map area. An unwelded to poorly welded zone approximately 3-9 m thick is present everywhere and forms a blocky weathering ledge at the base of the unit. This lower portion varies in color from light brownish gray (5 YR 6/1) to pale red (5 R 6/2), weathering to light brown (5 YR 6/4). Uncompressed to slightly compacted pumice as large as 2 cm in diameter are present within this zone. In thin section, glass shards are slightly compacted and partly lineated. Shards are devitrified to axiolites with relict features such as bubble walls outlined by a reddish iron-oxide staining. Most pumice fragments are cavernous with a thin rind of granular to axiolitic devitrification products around their margins.

A grayish-red (10 R 4/2) vitrophyric to densely welded zone, approximately 0.6-3 m in thickness, discontinuously occurs above the partially welded base. Within this zone

pumice and shards are compressed and form a eutaxitic foliation.

Above the basal poorly welded zone, or the densely welded zone when present, is a zone of partial to moderate welding. This 24 to 31-m-thick section increases in vapor-phase crystallization upward. The zone is characterized by light brownish-gray (5 YR 6/1) to medium light-gray (N6) fresh exposures which weather to pale-brown (5 YR 5/2), slabby-to-flaggy rubble. Rocks comprising this zone are well indurated. An increase in pumice size and vapor-phase crystallization within pumice occurs upward. Eutaxitic textures are well developed in the upper portion of this zone. Petrographically, glass shard structure is nearly completely destroyed and replaced by a fine granular texture in the upper portion of this vapor-phase zone. Pumice fgragments are slightly to well compressed. They often have an axiolitic margin 0.05 mm in width, and an increasingly coarser-grained central portion consisting of a mosaic of vapor-phase quartz and potassium feldspar.

Where preserved by the overlying Vicks Peak Tuff, a poorly-welded, poorly-indurated zone 1.5-3 m in thickness is present. Pumice fragments are mainly uncompressed and cavernous, often with a thin rim of vapor-phase minerals. Above this poorly welded zone is a 1-1.5 m thick, dark reddish-brown (10 R 3/4) to grayish-red (5 R 4/2)

vitrophyre. Pumice fragments present in this upper vitrophyre are microvesicular, glassy, and light gray (N7) to light brown (5 YR 5/6) in color. The upper poorly welded zone and upper vitrophyre represent a reversal in welding and emplacement of an upper flow, of which the basal portion is all that remains.

Phenocryst composition is relatively consistent through the zonal variations noted in the La Jencia Tuff. Sanidine (actually anorthoclase; J. I. Lindley, 1984, oral commun.) is predominant, comprising approximately 2-6 percent of the rock. Hornblende, plagioclase, clinopyroxene and biotite each occur in amounts less than 1 percent. Opaque oxides are generally scarce, but are present in amounts up to 2 percent within the groundmass of the basal unwelded zone. Intermediate to basaltic lithic fragments are present from trace amounts to about 2 percent of the rock.

Euhedral to subhedral anorthoclase phenocrysts average 1 mm in size and commonly have straight crystal edges and rounded corners. Single untwinned anorthoclase is most common, with a lesser proportion of crystals with carlsbad twinning. In hand sample, anorthoclase often has a distinctive iridesence.

Subrounded to rounded volcanic lithic fragments average 1-1.2 mm in size. They are mainly composed of hornblende, clinopyroxene and plagioclase phenocrysts set in a groundmass of iron-oxide stained glass and plagioclase microlites. Volcanic lithic fragments containing relict olivine replaced by iddingsite are occasionally present.

Vicks Peak Tuff

The Vicks Peak Tuff consists of poorly to moderately welded, crystal-poor, quartz-poor, one-feldspar rocks which form a multiple-flow, simple cooling unit. The Vicks Peak Tuff was originally referred to by Farkas (1969) as the Vicks Peak Rhyolite for exposures on Vicks Peak at the south end of the San Mateo Mountains. It was later redefined by Deal and Rhodes (1976). Osburn and Chapin (1983) have proposed a principal reference section for the Vicks Peak Tuff in the southern Bear Mountains (S 1/2 sec. 22, T.1S., R.4W., Magdalena NW 7 1/2 min quadrangle) because of poor constraints on the unit in the area where it was originally defined. This new reference section is the upper cooling unit of Brown's (1972) tuff of Bear Springs.

The Vicks Peak Tuff is present throughout the region and is correlative to: the uppermost part of Tdh7 as mapped by Givens (1957) within the study area; Tdrp2 within the

southeastern corner of the area mapped by Stearns (1962) as correlated by Fodor (1976), the tuff of Wahoo Canyon (Lopez, 1975; Bornhorst, 1976; and Fodor, 1976); the pinnacles member of the A-L Peak Tuff (Mayerson, 1979; Harrison, 1980; and Laroche, 1981); the middle cooling unit of the A-L Peak Tuff (Chamberlin, 1974); and the upper cooling unit of the A-L Peak Tuff (Coffin, 1981).

The source of the Vicks Peak Tuff is considered to be the Nogal Canyon cauldron, located in the southeastern San Mateo Mountains (Deal and Rhodes, 1976; Osburn and Chapin, 1983). A fission track date of 31.3 $\pm$ 2.6 m.y.B.P. on zircon (Bornhorst and others, 1982) was the only radiometric date on the Vicks Peak Tuff prior to the recent 40Ar/39Ar dating by Laura Kedzie. The 40Ar/39Ar dating indicates an age of approximately 29 m.y.B.P. for the Vicks Peak Tuff, essentially indistinguishable from the age of the La Jencia Tuff (Laura Kedzie, 1984, oral commun.).

Two isolated hilltop remnants of the Vicks Peak Tuff are present resting disconformably on the La Jencia Tuff within the study area. These outcrops are located along the central portion of the southern border of the area mapped. The maximum exposed thickness of the unit is approximately 27 m. This maximum thickness is the result of infilling by the Vicks Peak within a small trough-like depression carved on the La Jencia Tuff. Outcrops of the Vicks Peak Tuff

weather to slabby rubble-covered rounded hilltops. In its lower portion, the Vicks Peak is a light brownish-gray (5 YR 6/1) color on a fresh surface, weathering to grayish-orange pink (5 YR 7/2). The upper part of the unit is light gray (N7), weathering to light olive-gray (5 Y 6/1).

The basal 1.2 m of the Vicks Peak Tuff is unwelded, poorly indurated, and contains a concentration of spherical pumice. Above this is a zone containing porcelainous-looking, generally massive, well-indurated rocks. Pumice fragments are moderately compressed and relatively large. Oblong-shaped pumice with maximum diameters of 6-7 cm are occasionally present. Complete filling of pumice by round spheriolites is common. This zone grades upward to an interval characterized by lesser induration, with pumice and void space generally filled by drusy- to grainy-textured vapor-phase minerals. In thin section, glass shards comprising the groundmass are totally altered to a granular texture, which contains disseminated fine-grained opaque minerals. Pumice fragments have a 0.1 mm thick rind of axiolite crystals. Relict pumice sites often coarsen inward with a mosaic of very fine- to coarse-grained, anhedral vapor-phase potassium feldspar and lesser quartz. Occasionally pumice in this upper zone has not been affected by vapor phase crystalization. These dark black pumice fragments have wispy flame-like outlines and internally retain frothy pumice structure. Most pumice

fragments in this zone are moderately compressed.

Total crystal content in the Vicks Peak ranges from approximately 3-6 percent. Anorthoclase is predominant, comprising 3-5 percent of the rock. In hand sample, anorthoclase has a distinctive tabular shape and often shows a chatoyant blue color. Anorthoclase phenocrysts range from 0.3-3 mm in diameter and average 0.7 mm. Petrographically, anorthoclase occurs as euhedral to subhedral crystals, occasionally with carlsbad twinning and embayed crystal margins. Biotite, hornblende, and andesitic to basaltic lithic fragments each comprise less than 1 percent of the rocks volume. Approximately 10-15 percent of the rock is composed of pumice, which imparts a eutaxitic foliation.

Intrusives and flows

Mafic dike(s)

Several short segments of a mafic dike, or dikes, are exposed in the northeast portion of the map area. The exposures occur near the mountain front-piedmont slope transition. The dike(s) seems to be controlled by a steeply dipping, N45^{o}W, 3.2-km-long fracture cutting the Baca Formation. The Baca is the youngest unit intruded by the dike. The dike's trend parallels the well developed N45

W-trending swarm of fractures and faults that transect the western portion of the map area. Age of the dike is unknown, but it was probably intruded during Neogene extension in the region. Dikes of similar northwest orientation in the Pie Town area have been dated at approximately 28 m.y.B.P. (Lauglin and others, 1983). Massingill (1979) reported ages of 24.3 $\pm$ 0.8 and 24.8 $\pm$ 0.6 m.y.B.P. for north-trending dikes with similar characteristics in the Riley-Puertecito area.

The mafic dike present in the study area maintains a width along strike of 1.8-2.4 m. Its trend is linear, splaying off only slightly in places. It differs somewhat in its weathering character depending on the nature of the intruded country rock. Where the dike has intruded Baca mudstones it stands as a slightly elevated ridge with little alteration effects in the surrounding country rock. Where it has intruded Baca sandstones, it occupies a saddle between resistant ridges of silicified and calcified, bleached yellow sandstone. This altered zone extends outward 1.2-1.5 m from the dike's margin. The dike is pervasively altered and deeply weathered to a grus which is greenish black (5 G 6/2) to greenish gray (5 GY 6/4) on fresh surfaces, weathering to grayish olive green (5 GY 3/2) with dusky-yellow (5 Y 6/4) blotches of limonitic staining. In hand sample, the rock contains phenocrysts of plagioclase, biotite, and ferromagnesian minerals, set in an

aphanitic groundmass. Plagioclase phenocrysts are kaolinized and chalky white in color. Ferromagnesian minerals and groundmass constituents are generally chloritized. The crumbling nature of the rock precluded petrographic analysis.

Basaltic flows and related dike rocks

A small remnant of a basaltic lava flow(s) is present on a hilltop in the north-central portion of the map area, approximately 1.6 km west-northwest of the old Baca Homestead (SE 1/4 sec. 28, R.7W., T.2N.). It overlies with angular unconformity chaotically bedded debris-flow deposits of the middle Dog Springs map unit. The flow(s) is approximately 12.2 m in thickness. Its lower contact is generally obscured by the blocky talus it produces. The main body of the flow is a dense microvesicular mass, with the top of the flow being somewhat scoriaceous in places. North-northeast- to northwest-trending basaltic dikes are present within 305 m of the flow. The most northern of the basaltic dikes falls on a line projected along the trend of the mafic dike(s) that intrudes the area. The northwest trend of this basaltic dike is most likely related to the same fracture set that controls the orientation of the mafic dike(s) in the area. A N20°E basaltic dike lies approximately 46 m southeast of the northwest-trending dike.

This dike's north-northeast trend contrasts with the general structural grain of the area.

The flow and nearby dikes are considered to be associated because of the similarity in color, mineralogy, texture and degree of weathering. Both are very fresh, much less altered than other lava flows or intrusives in the study area. Approximately 4.8 km north, on Table Mountain, an extensive bench composed of a sequence of similar looking flows caps the Crevasse Canyon Formation. It is interpreted that these two locations contain the same flow. Callender and others (1983) indicate an age of 3.1 m.y.B.P. for related basaltic flows present north of the Rio Salado.

In hand sample, the flow rock is dark gray (N3) on a fresh surface, weathering to a light gray (N 7) or a limonite-stained moderate yellowish brown (10 YR 5/4). Microphenocrysts of plagioclase and ferromagnesian minerals are set in an aphanitic groundmass.

Petrographically, the rock has a microporphyritic to seriate, microvesicular texture. Plagioclase, clinopyroxene and olivine phenocrysts grade in size into a groundmass which also contains magnetite, orthopyroxene and glass. Phenocrysts are no larger than 2 mm in maximum diameter. Euhedral to subhedral plagioclase phenocrysts comprise about 15-20 percent of the rock. Plagioclase phenocrysts are arranged in a subparallel manner, while those within the

groundmass are randomly oriented. Pericline and albite twinning are common and are often found in combination with carlsbad-twinned and zoned crystals. Anorthite content of the plagioclase is approximately An54 (10 grains, Michel-Levy method). Euhedral to subhedral, commonly zoned, clinopyroxene phenocrysts comprise 5-6 percent of the rock by volume. Olivine phenocrysts comprise 4-5 percent of the rock. These crystals generally occur as subhedral to anhedral forms, but occasionally, euhedral, elongate, 6-sided olivine crystals are present. Olivine often has a mottled birefringence with patchy replacements of reddish-brown iddingsite. Reaction rims of clinopyroxene are present on some olivine crystals. Iron oxides are rare as phenocrysts, but are common within the groundmass. They comprise approximately 15-20 percent of the rock.

Surficial Deposits

Piedmont slope, highland gravel, and Long Canyon gravel deposits

Three distinct surficial deposits, and associated surfaces of erosion, have been differentiated and mapped within the study area. The oldest deposit is related to a late Tertiary erosional event, which is recorded by a veneer of material covering a high-level erosion surface. Two

younger Quaternary deposits have been differentiated based on their location, extent and thickness. One deposit consists of material derived from adjacent highland areas along the northeast front of the Gallinas Mountains and forms a portion of an extensive piedmont. The other deposit consists of a thin accumulation of gravels occurring on an erosion surface developed in the Long Canyon area.

The oldest of the deposits, referred to as Highland Gravels on the map, is found on a gently northwest-inclined, high-level erosion surface present along the west-central border of the map area, approximately 2.4-3.2 km west and northwest of Cottonwood Well. The erosional surface consists of a moderately undulating to gently inclined bench lying above the 7600 ft contour. This surface cuts deposits of the middle and upper Dog Springs, Chavez Canyon Member, and Rock House Canyon Tuff. A thin mantle of unconsolidated to poorly lithified gravel, approximately 0-15 m in thickness, covers the surface. The deposit consists of pebbles to small boulders of Rock House Canyon Tuff, La Jencia Tuff, Hells Mesa Tuff and Dog Springs Member lithologies. Gravels associated with this high-level erosional surface north of the Thompson Canyon fault consist almost exclusively of ash-flow tuff clasts. This high-level erosion surface and associated gravel deposits are most likely Pliocene in age. Pliocene basaltic flows with interbedded gravels containing lithologies similar to the

highland gravels, lie on an equivalent erosion surface north of the Rio Salado (John Hawley, 1984, oral commmun.).

An extensive piedmont deposit is present along the northern portion of the map area. This deposit consists of a veneer of dissected alluvial fan and colluvial deposits covering a shallow bedrock pediment. Such a setting is characteristic of the upper piedmont slope as defined by Gile and others (1981). These piedmont deposits range in thickness from approximately 3 to 13.7 m and consist of sand- to small boulder-sized material derived principally from the Dog Springs Member. The extensive piedmont present in the northeastern Gallinas Mountains may be the result of a lowering in the base-level of the ancestrial Rio Salado.

In the southwest portion of the map area, a thin accumulation of gravels is present on a gently inclined erosional surface. These gravels are related to erosion occurring within Long Canyon. Material is actively being moved across a sloping surface of erosion from elevated areas into the main drainage axis of Long Canyon. A thin accumulation of 0-3 m of sand- to cobble-sized constituents covers bedrock in the area.

Talus, colluvium and landslide deposits

Talus, colluvium and landslide deposits form an extensive cover extending along the prominent erosional escarpment found in the northeastern Gallinas Mountains. Talus and colluvium mantle a large portion of the bedrock in the study area, but have been mapped predominantly in areas where they obscure geologic contacts. Landslide deposits, consisting mainly of blocky cobble to boulder-sized material and occasional slump blocks, occur extensively along the northeast-facing escarpment of the Gallinas Mountains. Many of the landslide deposits consist almost exclusively of material derived from a specific stratigraphic unit. In such cases the deposit has been mapped in reference to the unit from which it originated. Large hillside hummocks and table-like benches present along the escarpment are mainly the result of a resistant capping of landslide debris derived from ash-flow tuffs. This debris overlies less resistant volcaniclastic rocks of the Chavez Canyon Member.

Alluvium

Alluvial deposits have been mapped in areas of modern ephemeral stream deposition and in some cases include terrace deposits and older soil-stabilized alluvium. A

well-developed terrace deposit, consisting of approximately 3 m of silty to sandy material, is present within Long Canyon and exposed along near-vertical eroded banks of the present arroyo. This terrace represents materials that have escaped degradation during arroyo cutting which the area has been experiencing since the 1800's (Givens, 1957). The majority of alluvium mapped consists of unconsolidated to poorly lithified sand and gravel.

STRUCTURE

The area mapped for this study lies within a tectonic and physiographic transition between the Colorado Plateau to the north, Rio Grande rift to the east, and Mogollon-Datil volcanic field to the south. Strata within the area, aside from disturbed bedding within the Dog Springs Member, display a south-southwesterly dip, which ranges from approximately 5 to 10 degrees. This southward tilting of the strata represents a large monoclinal flexure along the southern margin of the Colorada Plateau. Easterly, north-northwesterly, and northwest-trending high-angle normal faults and fractures displace strata within the area.

Folds

A broad southeast-plunging syncline has been described to the west of the study area by Givens (1957), Harrison (1980) and Coffin (1981). The axis of the syncline trends southeasterly through the middle portion of area mapped by Harrison and disappears to the south beneath the North Lake Basin. The eastern limb of the syncline extends to the southwest corner of the area mapped during this study.

Initial development of the syncline has been inferred by Harrison (1980) as occurring shortly after the emplacement of the Hells Mesa Tuff (approximately 32 m.y. ago). A deeply dissected erosional surface developed on the Hells Mesa Tuff in the area of the southeast-plunging synclinal flexure (Harrison, 1980; Coffin, 1981; this report). Marked thinning of Hells Mesa Tuff occurs in the southwest corner of the map area, coincident with the furthest extent of the eastern limb of the syncline. Synclinal development seems to be have continued at least until time of deposition of the Vicks Peak Tuff (approximately 29 m.y. ago). To the west of the study area, southeast-trending paleovalleys cut post-Hells Mesa stratigraphic units and are filled by the Vicks Peak Tuff (Harrison, 1980; Coffin, 1981).

Faults

Three distinct fault-related structural elements occur within the study area. North-northwest- to northwest-trending high-angle normal faults are exposed within the southwest to south-central portion of the map area. Long, northwest-trending fractures are present within the western portion of the area mapped. An east-trending, steeply-inclined normal fault transects the northern portion of the area.

The east-trending major fault running through the northern portion of the study area represents the eastern extension of the Thompson Canyon fault, mapped by Harrison (1980) and Coffin (1981) to the west. This east-trending fault can be traced for approximately 20 km from the study area to the west. The trend of the fault is discordant to the predominant northwest-oriented structural grain of the area. An estimated 250 m of down-to-the-north displacement is present on the fault near its intersection with the western border of the map area (cross section B-B', plate 1). Displacement decreases towards the east. Other transverse faults have been reported in the surrounding area (Brown, 1972; Chamberlin, 1974; Lopez, 1975; Bornhorst, 1976; and Laroche, 1981). Coffin (1981) has inferred intermittent movement on the fault beginning during deposition of the Chavez Canyon Member. He sites evidence of growth-fault movement by the greater thickness of Chavez Canyon sediments on the north down-thrown side of the fault. More recent movement is indicated by the termination of gravel deposits along the fault (Harrison, 1980; Coffin, 1981, this report). Reverse drag has been reported on the Thompson Canyon fault to the west of the study area (Coffin, 1981). Reverse drag is not evident within this map area because of the masking effect of disturbed bedding within the Dog Springs Member through which the fault traverses. The Thompson Canyon fault has apparently also acted as the

headwall of a large slump consisting of debris-flow deposits that detached and moved in a north-northeasterly direction (see cross-sections B-B' and C-C', plate 1). Movement of the slump has removed approximately 160 m of lower Dog Springs deposits along its eastern margin. Thus, the Thompson Canyon fault may have originated as a down-to-the-basin growth fault during deposition of the Dog Springs Member. The reverse drag reported by Coffin (1981) suggests a listric geometry for the fault.

High-angle normal faults trending between N11°W and N45° W occur within the south-central portion of the map area. A 3.1-km-wide down-dropped block occupies the area between the eastern and western fault traces. Maximum displacement of this small graben ranges from approximately 104 m on the west, occurring between two step faults, to 195 m on the easternmost bounding fault. Faults having lesser displacements, with down-to-the-west and down-to-the-east movements occur within the graben block. The Vicks Peak Tuff is the youngest unit effected by this faulting. Small-displacement north to northwest-trending normal faults probably occur in the northern portion of the map area within the Dog Springs Member. The chaotic nature of the bedding and lack of sufficient marker horizons prohibited mapping of their trend or sense of displacement with any degree of certainty.

A well-defined set of N45°W fractures is concentrated within the western half of the map area. These fractures can be traced in some instances for several kilometers. They parallel the prominent northwest-trending erosional escarpment found in the northeast Gallinas Mountains. The sharply defined lineation of the escarpment in the area 1.8 km southwest of Cottonwood Well and near the Gallinas triangulation station (southeast portion of map), suggests that the fracture set may be acting as a control in the escarpment's development. The accumulation of landslide deposits in the southeast portion of the map area, along the northwest-trending escarpment, seems to be related to this fracture system. In the area of the Gallinas triangulation station large blocks of ash-flow tuff apparently have caved along these fractures, initiated by erosional undercutting of subjacent, less-resistant, volcaniclastic strata.

Uplift of the Colorado Plateau

The gradual distal thinning and accompanying facies changes one would expect with the northward aggradation of the Spear's volcaniclastic apron is abruptly terminated by erosion within the northern Gallinas Mountains. The north to northeast-oriented paleoslope controlling deposition of Spear's sediments has been replaced by a south-southwest tectonic dip. This dip reversal is related to the

development of a monoclinal flexure along the southern margin of the Colorado Plateau. Creation of the monocline is a result of uplift of the Colorado Plateau structural block. Initial uplift of the southeast portion of this structurally coherent entity is considered to have occurred during the early Miocene (Bruning and Chapin, 1974; Chapin and Seager, 1975). Development of a highland area north of the Gallinas Mountains is indicated by the southeast paleoflow direction of volcaniclastic fanglomerates deposited in the northwest portion of the Miocene Popotosa basin (see Chapin and Seager, 1975, Fig.5). As the Colorado Plateau rose, the northernmost portion of the Spear's volcaniclastic apron, and overlying deposits, were stripped and redeposited to the south into the broadly-downwarping Popotosa basin and perhaps into the San Agustin Basin.

CONCLUSIONS

The stratigraphic and structural relationships apparent within the study area suggest the following geologic history for the northeastern Gallinas Mountains. During the latest Eocene to earliest Oligocene (about 39 m.y.B.P.) a northerly aggrading volcaniclastic apron began to develop around the northeast margin of the Mogollon-Datil volcanic pile. The sedimentary characteristics of the basal portion of the Dog Springs Member indicate that initial volcaniclastic sedimentation in the area occurred as subaqueous grain flows into the lacustrine portion of the Baca basin. This was followed by a rapid influx of debris flows which led to the demise of the Baca lacustrine system. Large exotic blocks and/or clasts of Paleozoic limestone, Permian Abo Formation and volcanic breccia were rafted into the area by debris flows. Chemical analysis of volcanic clasts from debris-flow deposits indicate that initial volcanism in the area was dominated by extrusion of high-potassium dacites and andesites.

Intermittent slumping and resulting soft-sediment deformation of deposits accompanied continuous basin sedimentation. Slumping occurred on a large scale as indicated by the presence of extensive detachment surfaces, folds with amplitudes of 50-60 m, and cutting out by slump

faulting of thick sections of the lower portion of the Dog Springs Member.

Debris-flow-dominated deposition characterizing the Dog Springs Member abruptly changed to fluvial-dominated processes during deposition of the Chavez Canyon Member. Infilling of low-lying areas on the surface of the Dog Springs Member by braided streams eventually led to the construction of an extensive contiguous surface of alluvial sedimentation.

Emplacement of the Rock House Canyon Tuff briefly interrupted deposition of volcaniclastic sediments in the area. It also signaled the beginnings of cauldron development which would eventually lead to the cessation of Spear's sedimentation. The thin accumulation of sedimentary deposits comprising the Rincon Windmill Member records the end of construction of the large volcaniclastic apron of the Spears Formation.

Increasing cauldron development and the blanketing of the region by ash-flow sheets (Hells Mesa, La Jencia, and Vicks Peak Tuffs) resulted in the closing off of source areas for the Spears. Following emplacement of the Hells Mesa Tuff (about 32 m.y.B.P.), a 3-m.y. hiatus occurred prior to deposition of the La Jencia Tuff. An extensive surface of erosion, having considerable relief within the study area, developed within the region. Erosional thinning

of the Hells Mesa Tuff in the southwest corner of the study area occurred as a broad, southeast-plunging syncline developed to the west. About 29 m.y.B.P. the La Jencia and Vicks Peak Tuffs were deposited nearly concurrently

Uplift of the Colorado Plateau in the early Miocene resulted in a reversal from a north to northeast paleoslope to a south-southwest tectonic dip in the area. The most northerly deposited portion of the Spear's volcaniclastic apron, and overlying volcanic rocks, were stripped and redeposited to the south as the Plateau rose.

High-angle normal faults and fractures have developed in the area during the last 30 m.y., concurrent with extension along the Rio Grande rift. These zones of weakness have acted as pathways for the intrusion of late Oligocene and Pliocene dikes.

A high-level erosion surface and accompanying thin gravel deposits records late Tertiary degradation of the area. An extensive piedmont began to develope along the northeast front of the Gallinas Mountains during the Quaternary.

REFERENCES

Allen, P., 1979, Geology of the west flank of the Magdalena Mountains, south of the Kelly district, Socorro County, New Mexico: M.S. thesis, New Mexico Institute of Mining and Technology, 153 p.; New Mexico Bureau of Mines and Mineral Resources Open-file Report 119, 161 p.

Allen, J. R., and Balk, R., 1954, Mineral resources of Fort Defiance and Tohatchi quadrangles, Arizona and New Mexico: New Mexico Bureau of Mines and Mineral Resources, Bulletin 36, 192 p.

Anderson, C. A., 1933, Tuscan formation California, with a discussion concerning the origin of volcanic breccias: University of California Publications in Geological Science, v. 23, p. 215-276.

Bates, R. L., and Jackson, J. A., 1980, Glossary of geology, (2nd edition): Falls Church, Virginia, American Geological Institute, 749 p.

Blakestad, R. B., Jr., 1978, Geology of the Kelly mining district, Socorro County, New Mexico: M.S. Thesis, University of Colorado, 174 p.; New Mexico Bureau of Mines and Mineral Resources Open-file Report 43, 139 p.

Bornhorst, T. J., 1976, Volcanic geology of the Crosby Mountains and vicinity, Catron County, New Mexico: M.S. Thesis, University of New Mexico, 113 p.

Bornhorst, T. J., Jones, D. P. Elston, W. E., Damon, P. E. and Shafiqullah, M., 1982, New radiometric ages on volcanic rocks from the Mogollon-Datil volcanic field, southwestern New Mexico: Isochron/West, no. 35, p. 13-15.

Bouthroyd, J. C., 1972, Coarse-grained sedimentation on a braided outwash fan, northeast Gulf of Alaska: Coastal Resource Division, University of South Carolina, Columbia, Technical Report no. 6, 127 p.

Bowring, S. A., 1980, The geology of the west-central Magdalena Mountains, Socorro County, New Mexico: M.S. thesis, New Mexico Institute of Mining and Technology, 127 p.; New Mexico Bureau of Mines and Mineral Resources Open-file Report 120, 135 p.

Brenchley, P. J., 1969, Origin of matrix in Ordovician greywackes, Berwyn Hills, North Wales: Journal of Sedimentary Petrology, v. 39, no. 4, p. 1297-1301.

Brown, D. M., 1972, Geology of the southern Bear Mountains, Socorro County, New Mexico: M.S. thesis, New Mexico Institute of Mining and Technology, 110 p.; New Mexico Bureau of Mines and Mineral Resources Open-file Report 52, 110 p.

Bruning, J. E., and Chapin, C. E., 1974, The Popotosa Formation- a Miocene record of Basin and Range deformation, Socorro County, New Mexico: Geological Society of America Abstracts with Programs, v. 6, no. 5, p. 430.

Callender, J. F., Seager, W. R., Swanberg, L. A., 1983, Late Tertiary and Quaternary tectonics and volcanism: Las Cruses, New Mexico Energry Institute, Geothermal Resources of New Mexico Scientific Map Series, 4 sheets, scale 1:500,000.

Cather, S. M., 1980, Petrology, diagenesis, and genetic stratigraphy of the Eocene Baca Formation, Alamo Navajo Reservation and vicinity, Socorro County, New Mexico, M.S. thesis: University of Texas (Austin), 243 p.; New Mexico Bureau of Mines and Mineral Resources Open-file Report 125, 263 p.

----, 1983, Lacustrine deposits of the Eocene Baca Formation, western Socorro County, New Mexico: New Mexico Geological Society Guidebook 34, p. 179-185.

Cather, S. M., and Johnson, B. D., 1984, Eocene tectonics and depositional setting of west-central New Mexico and eastern Arizona: New Mexico Bureau of Mines and Mineral Resources Circular 192, 33 p.

Chamberlin, R. M., 1974, Geology of the Council Rock district, Socorro County, New Mexico: M.S. thesis, New Mexico Institute of Mining and Technology, 134 p.; New Mexico Bureau of Mines and Mineral Resources Open-file Report 50, 143 p.

----, 1980, Cenozoic stratigraphy and structure of the Socorro Peak volcanic center, central New Mexico: D.Sc. dissertation, Colorado School of Mines, 495 p.; New Mexico Bureau of Mines and Mineral Resources Open-file Report 118, 532 p.

Chapin, C. E., 1971, K-Ar age of the La-Jara Peak Andesite and its possible significance to mineral exploration in the Magdalena Mining District, New Mexico: Isochron/West, no. 2, p. 43-44.

Chapin, C. E., and Seager, W. R., 1975, Evolution of the Rio Grande rift in the Socorro and Las Cruces areas: New Mexico Geological Society Guidebook 26, p. 279-321.

Chapin, C. E., and Deal, E. G., 1976, The A-L Peak Tuff, New Mexico- a composite ash-flow sheet: Geological Society of America Abstracts with Programs, v. 8, no. 5, p. 575.

Chapin, C. E., Chamberlin, R. N., Osburn, G. R., White, D. W., Sanford, A. R., 1978, Exploration framework of the Socorro geothermal area, New Mexico; in Chapin, C. E., and Elston, W. E., eds., Field guide to selected cauldrons and mining districts of the Datil-Mogollon volcanic field, New Mexico: New Mexico Geological Society Special Publication 7, p. 115-129.

Coffin, G. C., 1981, Geology of the northwestern Gallinas Mountains, Socorro County, New Mexico: M.S. thesis, New Mexico Institute of Mining and Technology, 202 p.; New Mexico Bureau of Mines and Mineral Resources Open-file Report 159, 214 p.

Deal, E. G., 1973, Geology of the northern part of the San Mateo Mountains, Socorro County, New Mexico - A study of a rhyolite ash-flow tuff cauldron and the role of laminar flow in ash-flow tuffs: Ph.D. dissertation, University of New Mexico, 136 p.

Deal, E. G., and Rhodes, R. C., 1976, Volcano-tectonic structures in the San Mateo Mountains, Socorro County, New Mexico, in Elston, W. E. and Northrop, S. A., eds., Cenozoic volcanism in southwestern New Mexico: New Mexico Geological Society Special Publication 5, p. 51-56.

Dickinson, W. R., 1970, Interpreting detrital modes of graywacke and arkose: Journal of sedimentary Petrology, v. 40, p. 695-707.

Dzulynski, St., Ksiazkiewilz, M., and Kuenen, P. H., 1959, Turbidites in flysch of the Polish Carpathian Mountains: Geologic Society of America Bulletin, v. 60, p. 1080-1118.

Eggleston, T. L., 1982, Geology of the central Chupadera Mountains, Socorro County, New Mexico: M.S. thesis New Mexico Institute of Mining and Technology, 161 p.; New Mexico Bureau of Mines and Mineral Resources Open-file Report 141, 162 p.

Enos, P., 1977, Flow regimes in debris flows: Sedimentology, v. 24, p. 133-142.

Ewart, A., 1982, The mineralogy and petrology of Tertiary-Recent orogenic volcanic rocks: with special reference to the andesitic-basaltic compositional range in Thorpe, R. G., ed., Andesites: John Wiley and Sons, New York, p. 39-81.

Farkas, S. E., 1969, Geology of the southern San Mateo Mountains, Socorro and Sierra Counties, New Mexico: Ph.D. dissertation, University of New Mexico, 137 p.

Fisher, R. V., 1971, Features of coarse-grained, high-concentration fluids and their deposits: Journal of Sedimentary Petrology, v. 41, no. 4, p. 916-927.

Fodor, R. V., 1976, Volcanic geology of the northern Black Range, New Mexico: in Elston, W. E., and Northrop, S. A., eds., Cenozoic volcanism in southwestern New Mexico: New Mexico Geological Society Special Publication 5, p. 68-70.

Folk, R. L., 1974, Petrology of sedimentary rocks: Hemphill Publishing Company, Austin, Texas, 182 p.

Galehouse, J. S., 1971, Point counting, in Carver, R. E., ed., Procedures in sedimentary petrology,: Wiley-Interscience, New York, p. 385-407.

Gile, L. H., Hawely, J. W., and Grossman, R. B., 1981, Soils and geomorphology in the Basin and Range areas of southern New Mexico- Guidebook to the desert project: New Mexico Bureau of Mines and Mineral Resources Memoir 39, 222 p.

Givens, D. B., 1957, Geology of the Dog Springs quadrangle, New Mexico: New Mexico Bureau of Mines and Mineral Resources Bulletin 58, 37 p.

Guilinger, D. R., 1982, Geology and uranium potential of the Tejana Mesa-Hubbell Draw Area, Catron County, New Mexico: M.S. thesis, New Mexico Institute of Mining and Technology, 129 p.; New Mexico Bureau of Mines and Mineral Resources Open-file Report 176, 129 p.

Hampton, M. A., 1972, The role of subaqueous debris flow in generating turbidity events: Journal of Sedimentary Petrology, v. 42, p. 775-793.

----, 1979, Buoyancy in debris flows: Journal of Sedimentary Petrology, v. 49, no. 3, p. 753-758.

Harrison, R. W., 1980, Geology of the northeastern Datil Mountains, Socorro and Catron Counties, New Mexico, M.S. thesis, New Mexico Institute of Mining and Technology, 137 p.; New Mexico Bureau of Mines and Mineral Resources Open-file Report 136, 146 p.

Hay, R. L., 1954, Structural relationships of tuff-breccia in the Absaroka Range, Wyoming: Geological Society of America Bulletin, v. 65, p. 605-620.

----, 1956, Pitchfork formation, detrital facies of early basic breccia, Absaroka Range, Wyoming: American Association of Petroleum Geologists Bulletin, v. 40, no. 8, p. 1863-1898.

Heinrich, E. W., 1965, Microscopic Indentification of Minerals: McGraw Hill, New York, 414 p.

Helwig, J., 1970, Slump folds and early structures, northeastern Newfoundland Appalachians: Journal of Geology, no. 78, p. 172-187.

Herrick, C. L., 1900, Report of a geological reconnaissance in western Socorro and Valencia counties, New Mexico: American Geologist, v. 25, no. 6, p. 331-346.

Hook, S. C., 1983, Stratigraphy, paleontology, depositional framework, and nomenclature of marine Upper Cretaceous rocks, Socorro County, New Mexico: New Mexico Geological Society Guidebook 34, p. 165-172.

Hook, S. C., Molenaar, C. M., and Cobban, W. A., 1983, Stratigraphy and revision of nomenclature of upper Cenomanian to Turonian (Upper Cretaceous) rocks of west-central New Mexico, in Contributions to mid-Cretaceous paleontology and stratigraphy of New Mexico - Part II, S.C. Hook, compiler - New Mexico Bureau of Mines and Mineral Resources Circular 185, p. 7-28.

Jackson, R. A., 1979, Geology of the Puertecito-La Cruz Peak area, Socorro County, New Mexico; in Chapin, C. E. and others, Coal, uranium, oil and gas potential of the Riley-Puertecito area, Socorro County, New Mexico: New Mexico Bureau of Mines and Mineral Resources Open-file Report 103, 38 p., 4 sheets.

Johansen, S., 1983, The thick-splay depositional style of the Crevasse Canyon Formation, Cretaceous of west-central New Mexico: New Mexcio Geological Society Guidebook 34, p. 173-178.

Johnson, A. M., 1970, Physical Processes in Geology: Freeman Cooper Company, San Francisco, 433-445 p.

Johnson, B. D., 1978, Genetic stratigraphy and provenance of the Baca Formation, New Mexico and the Eagar Formation, Arizona: M.A. thesis, University of Texas (Austin), 150 p.

Jones, O. T., 1936, On the sliding or slumping of submarine sediments in Denbighshire, North Wales, during the Ludlow Period (Abstract and discussion): Proceedings of the Geological Society of London, v. 1315, p. 110-115.

----, 1939, The geology of the Colwyn Bay district; a study of submarine slumping during the Salopian period: Quarterly Journal of the Geological Society of London, 95, p. 335-376.

Kedzie, L. L., 1984, High precision 40Ar/39Ar dating of major ash-flow tuff sheets, Socorro, New Mexico: M.S. thesis, New Mexico Institute of Mining and Technology, [in prep.].

Krewedl, D. A., 1974, Geology of the central Magdalena Mountains, Socorro County, New Mexico: Ph.D. dissertation, University of Arizona, 128 p.

Lajoie, J., 1972, Slump fold axis orientation, an indication of paleoslope?: Journal of Sedimentary Petrology, v. 42, p. 584-586.

Laroche, T. M., 1981, Geology of the Gallinas Peak area, Socorro County, New Mexico: M.S. thesis, New Mexico Institute of Mining and Technology, 145 p.; New Mexico Bureau of Mines and Mineral Resources Open-file Report 128, 154 p.

Laughlin, A. W., Aldrich, M. J., Vaniman, D. T., 1983, Tectonic implications of mid-Tertiary dikes in west-central New Mexico: Geology, v. 11, p. 45-48.

Lewis, K. B., 1971, Slumping on a continental slope inclined at 1 - 4 degrees: Sedimentology, v. 16, p. 97-110.

Lopez, D. A., 1975, Geology of the Datil area, Catron County, New Mexico: M.S. thesis, University of New Mexico, 72 p.

Lopez, D. A., and Bornhorst, T. J., 1979, Geologic map of the Datil area, Catron County, New Mexico: U.S. Geological Survey Miscellaneous Geologic Investigations Map I-1098, scale 1:50,000.

Lucas, S. G., 1983, The Baca Formation and the Eocene-Oligocene boundary in New Mexico: New Mexico Geological Society Guidebook 34, p. 187-192.

Macdonald, G. A., 1972, Volcanoes: Prentice-Hall Inc., Englewood Cliffs, New Jersey, p. 170-181.

Massingill, G. R., 1979, Geology of Riley-Puertecito area, southeastern margin of the Colorado Plateau, Socorro County, New Mexico: D.G.S. thesis, University of Texas (El Paso), 301 p.; New Mexico Bureau of Mines and Mineral Resources Open-file Report 107, 316 p.

Mayerson, D. L., 1979, Geology of the Corkscrew Canyon-Abbe Spring area, Socorro County, New Mexico: M.S. thesis, New Mexico Institute of Mining and Technology, 150 p.; New Mexico Bureau of Mines and Mineral Resources Open-file Report 113, 160 p.

McGowen, J. H., and Groat, C. G., 1971, Van Horn Sandstone, West Texas: an alluvial fan model for mineral exploration: Report of Investigations, no. 72, Bureau of Economic Geology, University of Texas, Austin 57 p.

McKee, E. D., and Weir, G. W., 1953, Terminology for stratification and cross-stratification in sedimentary rocks: Geological Society of America Bulletin, v. 65, p. 381-390.

Middleton, G. V., and Hampton, M. A., 1976, Subaqueous sediment transport and deposition by sediment gravity flows, in Stanley, D. J. and Swift, D. J. P., eds., Marine sediment transport and environmental management: John Wiley, New York, p. 197-218.

Moore, D. G., 1961, Submarine slumps: Journal of Sedimentary Petrology v. 31, p. 343-357.

Morgenstern, N. R., 1967, Submarine slumping and the initiation of turbidity currents, in Richards, A. F., ed.: Marine Geotechnique, University of Illinois Press, Urbana, p. 189-220.

Osburn, G. R., and Chapin, C. E., 1983, Nomenclature for Cenozoic rocks of northeastern Mogollon-Datil volcanic field, New Mexico: New Mexico Bureau of Mines and Mineral Resources Stratigraphic Chart 1, one sheet, 7 p.

Parsons, W. H., 1969, Criteria for the recognition of volcanic breccias: Review: Geological Society of America, Memoir 115, p. 263-304.

Petty, D. M., 1979, Geology of the southeastern Magdalena Mountains, Socorro County, New Mexico: M.S. thesis, New Mexico Institute of Mining and Technology, 103 pp; New Mexico Bureau of Mines and Mineral Resources Open-file Report 106, 174 p.

Pettijohn, F. J., Potter, P. E., and Siever, R. S., 1973, Sand and Sandstone: Springer-Verlag, New York, 618 p.

Postma, G., 1984, Slumps and their deposits in fan delta front and slope: Geology, v. 12, p. 27-30.

Potter, S. C., 1970, Geology of Baca Canyon, Socorro County, New Mexico: M.S. thesis, University of Arizona, 54 p.

Potter, P. E., and Pettijohn E. J., 1977, Paleocurrents and basin analysis (2nd ed.): Springer-Verlag, New York, 425 p.

Roberts, D. G., 1972, Slumping on the eastern margin of the Rockall Bank, North Atlantic Ocean: Marine Geology, v. 13, p. 225-237.

Robinson, B. R., 1981, Geology of the D Cross Mountain quadrangle, Socorro and Catron Counties, New Mexico: D.G.S. dissertation, University of Texas (El Paso), 212 p.

Rodine, J. D., and Johnson, A. M., 1976, The ability of debris, heavily freighted with coarse clastic materials to flow on gentle slopes: Sedimentology, v. 23, p. 213-234.

Rupke, N. A., 1976, Large-scale slumping in a flysch basin, southwestern Pyrenes: Journal of the Geological Society of London, v. 132, p. 121-130.

----, 1980, Deep clastic seas, in Reading, H. G., ed.: Sedimentary environments and facies: Elsevier, New York, p. 372-415.

Scholle, P. A., 1979, Constituents, textures, cements, and porosities of sandstones and associated rocks: American Association of Petroleum Geologists Memoir 28, 201 p.

Snyder, D. O., 1971, Stratigraphic analysis of the Baca Formation, west-central New Mexico: Ph.D. dissertation, University of New Mexico 158 p.

Spradlin, E. J., 1976, Stratigraphy of Tertiary volcanic rocks, Joyita Hills area, Socorro County, New Mexico: M.S. thesis, University of New Mexico, 160 p.

Stauffer, P. H., 1967, Grain-flow deposits and their implications, Santa Ynez Mountains, California: Journal of Sedimentary Petrology, v. 37, p. 487-508.

Stearns, C. E., 1962, Geology of the north half of the Pelona Quadrangle, Catron County, New Mexico: New Mexico Bureau of Mines and Mineral Resources Bulletin 78, 46 p.

Stone, B. D., 1976, Analysis of slump slip lines and deformation fabric in slumped Pleistocene lake beds: Journal of Sedimentary Petrology, v. 46, p. 313-325.

Surdam, R. C., and Boles, J. R., 1979, Diagenesis of volcanic sandstones: Society of Economic Paleontologists and Mineralogists Special Publication 26, p. 227-242.

Theakstone, W. J., 1976, Glacial lake sedimentation, Austerdalsisen, Norway: Sedimentology, v. 23, p. 671-688.

Tonking, W. H., 1957, Geology of the Puertecito quadrangle, Socorro County, New Mexico: New Mexico Bureau of Mines and Mineral Resources Bulletin 41, 67 p.

Weber, R. H., 1963, Cenozoic volcanic rocks of Socorro County: New Mexico Geological Society Guidebook 14, p. 132-143.

----, 1971, K-Ar ages of Tertiary igneous rocks in central and western New Mexico: Isochron/west, no. 1, p. 33-45.

Wentworth, C. K., 1922, A scale of grade and class terms for clastic sediments: Journal of Geology, v. 30, p. 377-392.

Wilkinson, W. H., Jr., 1976, Geology of the Tres Montosas-Cat Mountain area, Socorro County, New Mexico: M.S. thesis, New Mexico Institute of Mining and Technology, 158 p.; New Mexico Bureau of Mines and Mineral Resoures Open-file Report 39, 169 p.

Willard, M. E., 1959, Tertiary stratigraphy of northern Catron County, New Mexico: New Mexico Geological Society, Guidebook 10, p. 92-99.

Williams, H., Turner, F. J., and Gilbert, C. M., 1954, Petrography: An introduction to the study of rocks in thin sections: W.H. Freeman and Company, San Francisco, 406 p.

Wilpolt, R. H., McAlpin, A. J., Bates, R. L., and Vorbe, G., 1946 Geologic map and stratigraphic sections of Paleozoic rocks of the Joyita Hills, Los Pinos Mountains, and Northern Chupadera Mesa, Valencia, Torrance, and Socorro Counties, New Mexico: U.S. Geological Survey Oil and Gas Investigations, Preliminary Map 61, scale 1:62,500.

Wilson, M. D., and Sedora, S. S., 1979, An improved thin section stain for potash feldspar: Journal of Sedimentary Petrology, v 49, no. 2, p. 637-638.

Winchester, D. E., 1920, Geology of the Alamosa Creek Valley, Socorro County, New Mexico; with special reference to the occurrence of oil and gas: U.S. Geological Survey, Bulletin 716-A, p. 1-15.

Woodcock, N. H., 1976, Structural style in slump sheets: Ludlow series, Powys, Wales: Journal of the Geological Society of London, v. 132, p. 399-415.

Van der Plas, L., and Tobi, A. C., 1965, A chart for judging the reliability of point counting results: American Journal of Science, v. 263, p. 87-90.

This thesis is accepted on behalf of the faculty of the Institute by the following committee:

Adviser

12/7/84

Date

219
PLATE I

GEOLOGIC MAP AND SECTIONS OF THE NORTHEASTERN GALLINAS MOUNTAINS SOCORRO COUNTY, NEW MEXICO

by

Lee A. Brouillard

1984

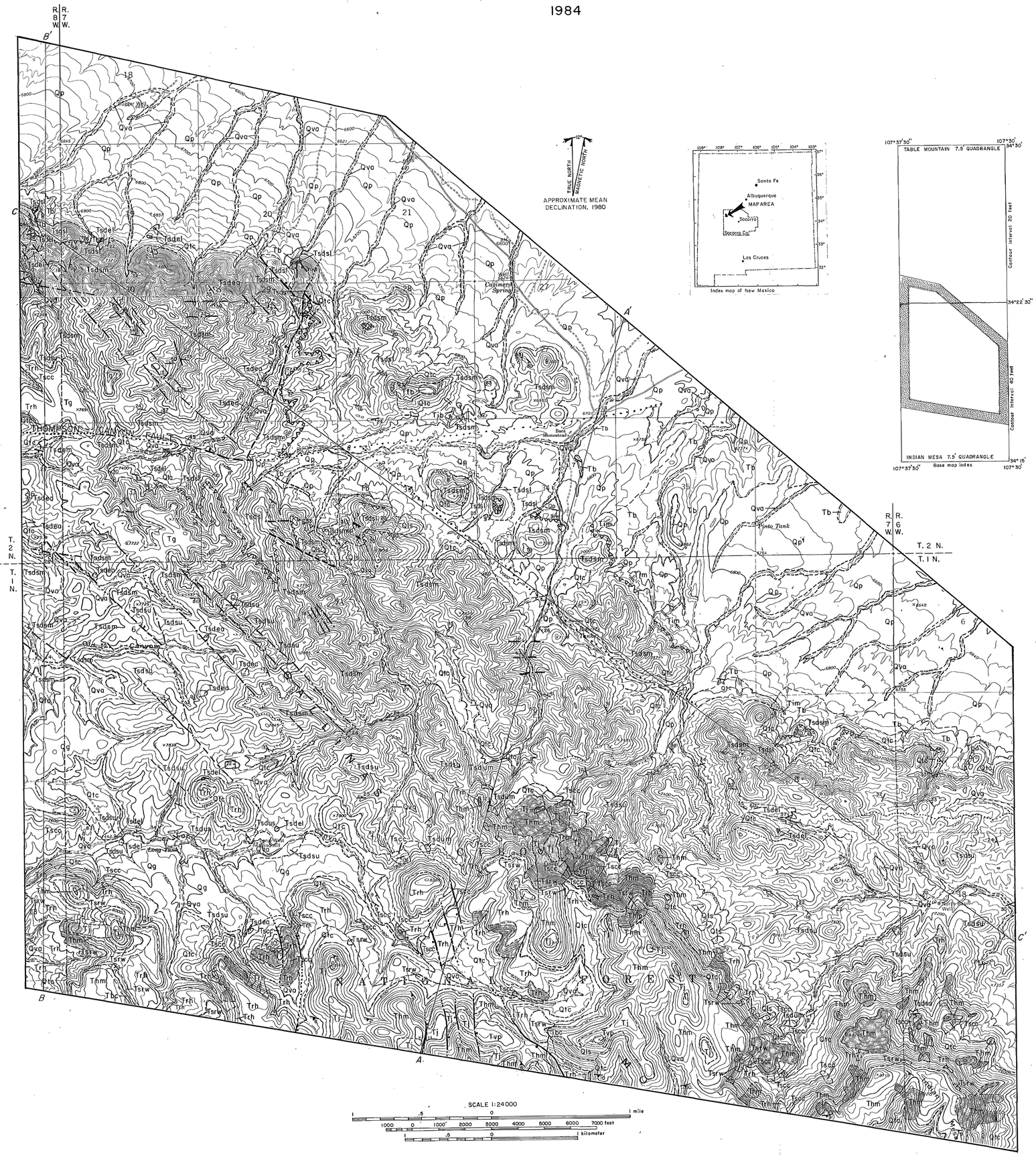

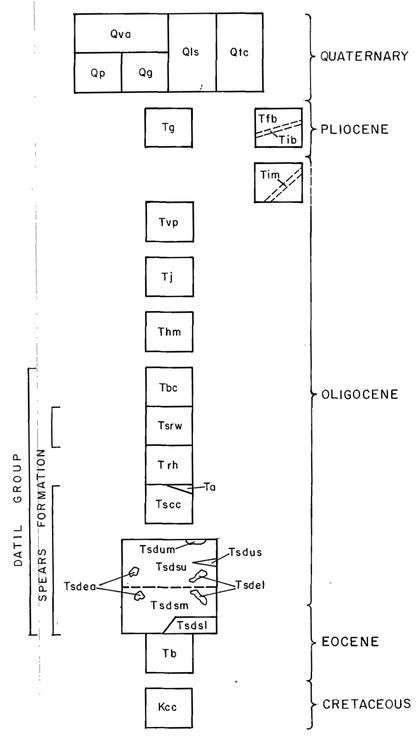

DESCRIPTION OF UNITS

Qva — **Valley alluvium**- unconsolidated to poorly lithified fluvial sand and gravel; includes older soil-stabilized alluvium and terrace deposits; found within canyons and associated with piedmont deposits.

Qtc — **Talus and colluvium**- unconsolidated or soil stabilized; talus and slope-wash deposits.

Qls / Thm — **Landslide deposits**- blocky deposits of cobble to boulder-sized debris and occasional slump blocks; stippled areas are landslides labeled in reference to the geologic formation from which the material originated.

Qg — **Gravels**- veneer of unconsolidated gravel consisting of clasts derived from adjacent highland areas. Deposits mantle an undulating to graded erosional surface in the Long Canyon area; 0-3 m thick.

Qp — **Upper piedmont slope deposits**- thin mantle of unconsolidated to poorly lithified alluvial-fan and colluvial gravel occurs on bedrock pediment. Extensively developed along the front of the northeastern Gallinas Mountains; 3-13.7 m thick.

Tg — **Highland gravels**- veneer of unconsolidated to poorly lithified gravel, which caps a moderately undulating erosion surface that slopes gently to the northwest; lies above the 7600 contour along the west-central border of map area; 0-15 m thick.

Tfb / Tib — **Basaltic flow and related intrusives**- microvesicular, microporphyritic to seriate texture, clinopyroxene-olivine basalt.

Tim — **Mafic intrusive**- pervasively altered and deeply weathered mafic dike(s); intrudes the Baca Formation along the mountain front-piedmont slope transition; 1.2-1.5 m in width.

Tvp — **Vicks Peak Tuff**- poorly to moderately welded, crystal-poor, quartz-poor, one-feldspar, rhyolite ash-flow tuff; multiple-flow, simple cooling unit; 0-27 m thick.

Tj — **La Jencia Tuff**- poorly to moderately welded, crystal-poor, quartz-poor, one-feldspar, rhyolite ash-flow tuff; multiple-flow, compound cooling unit; 0-43 m thick.

Thm — **Hells Mesa Tuff**- moderately to densely welded, crystal-rich, moderately quartz-rich, quartz-latite to rhyolite ash-flow tuff; multiple-flow, simple cooling unit; 12-153 m thick.

Tbc — **Blue Canyon Tuff**- poorly to moderately welded, crystal-rich, biotite-rich, quartz-poor, quartz-latite ash-flow tuff; 0-12 m thick.

Tsrw — **Rincon Windmill Member of the Spears Formation**- volcaniclastic sandstones and pebble to cobble conglomerates; 12-37 m thick.

Trh — **Rock House Canyon Tuff**- poorly to moderately welded, crystal-poor, moderately pumiceous, rhyolite ash-flow tuff; multiple flow, simple cooling unit; 60-72 m thick.

Ta — **Basaltic andesite flow**- clinopyroxene-olivine basaltic andesite; large (up to 6 cm), clear to chalky plagioclase laths occur as phenocrysts; occasional calcite amygdules; 0-12 m thick.

Tscc — **Chavez Canyon Member of the Spears Formation**- volcaniclastic sandstones and pebble to cobble conglomerates; minor debris-flow deposits near base; 24-249 m thick.

Dog Springs Member of the Spears Formation; 365-732 m thick.

Tsdsu — **upper Dog Springs Member**- debris-flow deposits; contain subrounded to rounded, dark, aphanitic, dacitic to andesitic clasts and lesser nonvolcanic material; 57-518 m thick.

Tsdus — **sandstone facies of the upper Dog Springs Member**- laterally discontinuous fluvial volcaniclastic sandstones and conglomerates.

Tsdum — **mudstone facies of the upper Dog Springs Member**- laterally discontinuous, laminated to thin-bedded claystones, siltstones, and mudstones; contains lesser, normally graded sandstones.

Tsdea — **exotic blocks of monolithologic volcanic breccia**- clast-dominated, intermediate-composition breccias.

Tsdel — **exotic blocks of Paleozoic limestone**- fossiliferous, micritic limestones.

Tsdsm — **middle Dog Springs Member**- debris-flow breccias; consist of dacitic to andesitic clasts set in fine-grained matrix of the same composition; occasionally contains nonvolcanic material; 76-524 m thick.

Tsdsl — **lower Dog Springs Member**- grain-flow deposits; consist of volcanic, lithic graywackes with occasional thin clay lenses; 0-167 m thick.

Tb — **Baca Formation**- redbed sequence of sandstone, mudstone, and minor conglomerate; 290 m exposed.

Kcc — **Crevasse Canyon Formation**- sandstones and black carbonaceous shales; a few thin coal beds. (shown in cross section only).

Pattern indicates rocks that typically show chaotic bedding (cross section only). Disturbed bedding is restricted to the Dog Springs Member of the Spears Formation.

SYMBOLS

Formation contact- dashed where approximate; dotted where gradational, as in the case of the middle-upper Dog Springs Member contact

Fault- dashed where approximate; dotted where covered or inferred; bar and ball on downthrown side

Facture zone

10 **Strike and dip of foliation**

5 **Strike and dip of beds**

Vertical beds

SLUMP STRUCTURES

Anticline showing direction of plunge

Syncline

Thrust or reverse fault- barbs on upper plate

Detachment surface- barbs on upper plate

Relative slip movement (cross-section view)- lateral slip movement, A = away, T = toward. Arrow indicates direction of dip-slip movement